

Mechanisms of Neurodegeneration
in Transgenic Models of
Huntington's Disease

Joana M. Amaral C. Gil

Coimbra, 2006

Department of Zoology
Faculty of Sciences and Technology
University of Coimbra

Thesis Cover:

Photomicrograph of a hippocampal section from a 12-week-old Huntington's Disease (HD) R6/2 mouse. The section was processed for the proliferating marker bromodeoxyuridine (BrdU; *red*) and the neuronal marker neuronal nuclei (NeuN; *green*) immunohistochemistry. As shown in *Chapters 5* and *6* of this Thesis, there is a significant reduction in the number of newly born neurons in the dentate gyrus (DG) of these mice.

*Dissertation submitted to the Faculty of Sciences
and Technology of the University of Coimbra in partial
fulfillment of the requirements for the Degree of Doctor of
Philosophy in Cell Biology.*

*Dissertação apresentada à Faculdade de Ciências
e Tecnologia da Universidade de Coimbra para obtenção
do Grau de Doutor em Biologia Celular.*

The most beautiful experience we can have is the mysterious. It is the fundamental emotion which stands at the cradle of true art and true science. Albert Einstein (1879 - 1955) physicist.

The possession of knowledge does not kill the sense of wonder and mystery. There is always more mystery. Anaïs Nin (1903 - 1977) writer.

*To My Parents
To Paul*

*Aos Meus Pais
Ao Paul*

Acknowledgments

When I started writing this Thesis a few months ago, I was craving for the moment when I could finally relax and write the *Acknowledgments*, since that would mean the end was close and the most difficult part of the process was over. But now that the moment finally arrived, I see myself stuck in this page with a very difficult task ahead of me. After all, it is not easy to summarize the past four years and acknowledge all the people that touched my life during this period in a couple of pages... But here it goes:

My Supervisors. I am deeply indebted to *Professor Ana Cristina Rego*, who opened the doors of Science for me almost seven years ago when I joined the Center for Neuroscience and Cell Biology of Coimbra, and with whom I learned the true meaning of hard work and dedication. Thank you for encouraging me to leave, and most of all, for always supporting and understanding my decisions, especially during the hardest moments of these last four years. I am also grateful to *Professor Patrik Brundin* for giving me the opportunity of becoming a member of his NESU Team at the Wallenberg Neuroscience Center in Lund, and for sharing his knowledge with me. Thank you also for organizing the Team Buildings (I have great memories of those days of true team spirit!), and yes, for all the monthly Lab Meetings (ShaSupps) and biweekly Journal Clubs! I did learn with the experience, and I am certainly more aware now of how fast I can speak sometimes. Finally, I also thank *Doctor Åsa Petersén* for introducing me to the field of Huntington's Disease and to *in vivo* work. I do need to acknowledge your encouragement and support when I first arrived in Lund, since not even in my wildest dreams I had imagine that I would actually become an *in vivo* scientist! Thank you also for establishing all the collaborations that allowed for the richness of many of these projects.

Funding. I thank the *Portuguese Foundation for Science and Technology (Fundação Portuguesa para a Ciência e a Tecnologia, FCT)*, for my Ph.D. fellowship (reference: SFRH/BD/6068/2001).

My Collaborators. I thank my collaborators for their valuable contribution and expertise. A special thanks goes to the technicians Birgit and Britt, for their competence, patience, and kindness. I am also thankful to Eva and Birgitta, for taking care of my paperwork, helping me each time I needed to find a new home, and organizing the NESU Team Building events.

My Colleagues & Friends from Lund, Sweden. My best memories from the three and a half years I spent in Lund are from the moments I shared with my peers. With all the parties, movie sessions, Saturday lunches, late dinners in the lab, and endless conversations about life, love, and science, I made true friends that became my family in Lund. I specially would like to thank: *Manolo*, for your definition of friendship in my last day in Lund, for being tough with me when I needed, and of course, for your Italian tiramisu; *Laurent (Lolo)*, for your friendship and enthusiasm, for all the dinners, fish soups, and French crepes, for showing up late at night when we were neighbors for endless hours of conversation, and for a great trip to L.A.; *Emma Lane (Em)*, for being there and listening to me, and for a great vacation in Portugal; *Jorien (Jo)*, for becoming my office-mate, for inspiring me with our talks about dreams and trips, and for sharing with me and Diogo the funniest canoe experience I'll ever have; *Jenny Papalex*i, for your brightness, for always believing that things will turn all right in the end, and for cooking with me a Greek dinner; *Jelena*, for being such a nice person and good friend, for creating the "Healthy Team" and all the gym and sauna sessions; *Tomas (Ex.-Dr. Olsson)* for having such a good spirit and all the laughs, and for going shopping with me and Laurent in L.A.; *Ruben*, for being such a nice person and for teaching us all a little bit about birds; *Natalija*, for your kindness, support, and for always helping me; *Sergey*, for all the movie sessions, for your Russian sense of humor, and for putting up with three Portuguese and/or three women in the office; *Jia-Yi*, for being always so kind and patient; *Bilal*, for interesting conversations about Science and life; *Kathy*, *Anna Persson*, *Caroline*, *Hinfan* and *Hannah*, the students who joined the lab for some months and with whom I shared good music and good laughs.

And last but not the least, the "Portuguese Colony": *Catarina (Cáti)* and *Diogo (Diogão)* for being my office mates and co-creators of the NESU aquarium, for all the jokes, laughs, and tears we shared, and for coming to Sweden to learn how to speak proper Brazilian; *Sofia (Sôfi)*, for being the sweetest flat-mate I could ever wished for and making sure that I would always have soup to eat, for always being there for me, and for being such a beautiful person; and from the Kemicentrum, *Cecília*, for your courage and happiness; and *Mónica (Jóvem)* for your strength, for being such a great friend, for giving me shelter when I most needed, and for always finding the best bargains.

My Colleagues & Friends from Portugal. The true friendship is the one that survives time and distance, and so I thank to all my Portuguese friends for having kept in regular contact with me during my years in Sweden and making me feel closer to home. I specially thank *Ana Sofia* and *Miguel Mano* for always visiting me wherever I end-up; *Paulo Pinheiro*, *João Frade*, and *Nuno Penacho*

for having such a good spirit and for great trips to Turkey and Greece; *David* and *Pedro Coxito*, for always keeping in touch and for visiting me in Lund; *Nuno Raimundo*, for always making me laugh, for coming to Lund twice, and for turning the “The Girl from Ipanema” one of my favorite songs; *Teresa Oliveira*, for your friendship and help, and for always taking care of my stuff in Coimbra; *Inês (Nê)*, for actually coming to the lab in Lund and working with me (in the same desk!) for a couple of months, and for all the stressful and happy moments we shared during the long nights of experiments; *Liliana (Lila)*, for being such a great friend throughout all these years and for making me believe in the future; and *Carla (Carlinha)*, for coming to work at the WNC for some months, for all we lived and shared, and for being always there for me.

My Family. It is impossible to express with words how grateful I am to my *Parents* for their love and support throughout the journey of my Ph.D. Thank you for always supporting my decisions, giving me strength and courage when I felt weak, celebrating my achievements, and most of all, for always being so close to me, even when we have an entire ocean between us! I also want to thank my brother *Tó*, my sister *Rita*, and my brother-in-law *Tiago*, for having such a good spirit and visiting me in Sweden when I had no electricity and a bit of a plumbing problem (now I am waiting for you in Canada!). And finally, I thank my aunts and uncles for their support, and my grandparents *Fernando*, *Angélica*, and *Lizete* (to whom unfortunately I won’t have the opportunity to personally thank) for their love and for being an example in my life.

My Love. *Paul*, thank you for the endless hours you spent proofreading this Thesis, for everything I learned from you about science, music, and life, and most importantly, for your love and for sharing your life with me.

***This Thesis is dedicated to my Parents and to Paul.
Esta Tese é dedicada aos meus Pais e ao Paul.***

Table of Contents

Abbreviations List	1
SUMMARY (English)	5
RESUMO (Portuguese)	7
Chapter 1. GENERAL INTRODUCTION.....: Huntington’s Disease and in vivo Transgenic Models Used to Study this Neurodegenerative Disorder	9
1.1. POLYGLUTAMINE DISEASES.....	11
1.2. HUNTINGTON’S DISEASE.....	13
1.2.1. <i>Clinical Manifestation</i>	13
1.2.2. <i>Neuropathology</i>	15
1.2.3. <i>Genetics</i>	17
1.3. HUNTINGTIN	18
1.3.1. <i>Proposed Functions of Wild-Type Huntingtin</i>	19
1.3.2. <i>Aggregation of Mutant Huntingtin</i>	21
1.3.3. <i>Mutant Huntingtin & Intracellular Dysfunction</i>	22
1.3.3.1. <i>Activation of Proteases</i>	23
1.3.3.2. <i>Protein Misfolding and Inhibition of Protein Degradation</i>	24
1.3.3.3. <i>Transcription Dysregulation</i>	25
1.3.3.4. <i>Disruption of Axonal Transport</i>	25
1.3.3.5. <i>Synaptic Dysfunction</i>	26
1.4. MECHANISMS OF DEGENERATION	27
1.4.1. <i>Corticostriatal Dysfunction & Excitotoxicity</i>	28
1.4.2. <i>Nigrostriatal Dysfunction & Dopamine Toxicity</i>	29
1.4.3. <i>Metabolic Dysfunction & Oxidative Stress</i>	29
1.4.4. <i>Cell Death – Apoptosis & Autophagy</i>	30
1.5. RODENT MODELS OF HUNTINGTON’S DISEASE.....	32
1.5.1. <i>Knock-in Mice</i>	33
1.5.2. <i>Transgenic Mice – Full-Length Models</i>	34
1.5.3. <i>Transgenic Mice – Truncated Models</i>	35
1.5.4. <i>Transgenic Rats</i>	35
1.6. THE R6 TRANSGENIC HUNTINGTON’S DISEASE MICE	36
1.6.1. <i>Characterization of R6 Mice</i>	37
1.6.1.1. <i>Generation</i>	37
1.6.1.2. <i>Neuropathology</i>	37
1.6.1.3. <i>Behavior</i>	39
1.6.1.4. <i>Pathology outside the Central Nervous System</i>	40
1.6.2. <i>Dysfunction in R6 Mice</i>	42
1.6.2.1. <i>Transcriptional Dysregulation</i>	42
1.6.2.2. <i>Dysfunction of the Corticostriatal Pathway</i>	43
1.6.2.3. <i>Changes in Signalling Pathways and Intracellular Homeostasis</i>	44

Table of
Contents

1.6.2.4. Mitochondrial Dysfunction and Oxidative Stress.....	45
1.6.3. <i>Therapeutic Strategies</i>	46
1.7. OBJECTIVES	47
Chapter 2 NORMAL SENSITIVITY TO EXCITOTOXICITY IN A TRANSGENIC HUNTINGTON'S DISEASE RAT	49
2.1. SUMMARY	51
2.2. INTRODUCTION	52
2.3. MATERIALS AND METHODS	53
2.3.1. <i>Transgenic Animals</i>	53
2.3.2. <i>Surgery</i>	54
2.3.3. <i>Tissue Processing and Histology</i>	54
2.3.4. <i>Stereological Techniques</i>	55
2.3.5. <i>Statistical Analysis</i>	55
2.4. RESULTS	55
2.5. DISCUSSION	58
Chapter 3 .. IMPAIRED DOPAMINERGIC NEUROTRANSMISSION IN R6/1 TRANSGENIC HUNTINGTON'S DISEASE MICE.....	61
3.1. SUMMARY	63
3.2. INTRODUCTION	64
3.3. MATERIALS AND METHODS	65
3.3.1. <i>Transgenic Animals</i>	65
3.3.2. <i>In vivo Microdialysis</i>	65
3.3.3. <i>Determination of the Dialysate DA, DOPAC & HVA Levels</i>	66
3.3.4. <i>Analysis of Whole Tissue Striatal DA Levels</i>	66
3.3.5. <i>Evaluation of Microdialysis Probe Placement</i>	66
3.3.6. <i>Statistical Analysis</i>	67
3.4. RESULTS	67
3.4.1. <i>Whole Tissue Striatal DA Levels in R6/1 Mice</i>	67
3.4.2. <i>Dialysate DA Striatal Levels in R6/1 Mice</i>	67
3.4.3. <i>Dialysate Basal Levels of DA Metabolites in R6/1 Mice</i>	68
3.5. DISCUSSION	69
Chapter 4 DYSFUNCTION OF THE LATERAL HYPOTHALAMUS IN HUNTINGTON'S DISEASE.....	73
4.1. SUMMARY	75
4.2. INTRODUCTION	76
4.3. MATERIALS AND METHODS	78
4.3.1. <i>Transgenic Animals</i>	78
4.3.2. <i>Human HD Brains</i>	79
4.3.3. <i>Tissue Processing and Histology</i>	79
4.3.4. <i>Stereological Techniques and Cell Quantification</i>	80
4.3.5. <i>Radioimmunoassay</i>	82

4.3.6. Electron Microscopy.....	82
4.3.7. Scoring of Narcoleptic-Like Episodes.....	82
4.3.8. EEG and EMG Recordings.....	83
4.3.9. Statistical Analysis.....	83
4.4. RESULTS.....	83
4.4.1. Orexin Loss in R6/2 Mice	83
4.4.2. Narcoleptic-Like Episodes in R6/2 Mice.....	87
4.4.3. Orexin Cell Loss in HD Brains	89
4.4.4. Loss of MCH-Containing Neurons in R6/2 Mice.....	90
4.5. DISCUSSION.....	92
Chapter 5..... ASIALOERYTHROPOETIN IS NOT EFFECTIVE IN THE R6/2 LINE OF HUNTINGTON'S DISEASE MICE	95
5.1. SUMMARY	97
5.2. INTRODUCTION	98
5.3. MATERIALS AND METHODS	100
5.3.1. Transgenic Animals	100
5.3.2. Administration of AsialoEPO and Body Weight Measurements	101
5.3.3. Behavioral Testing.....	101
5.3.3.1. Rotarod.....	101
5.3.3.2. Paw Claspings.....	101
5.3.3.3. Motor Activity in an Open Field	102
5.3.4. Administration of BrdU and Tissue Processing.....	102
5.3.5. Immunohistochemistry.....	102
5.3.6. Stereological Techniques and Cell Quantification.....	103
5.3.7. Statistical Analysis.....	104
5.4. RESULTS.....	105
5.4.1. AsialoEPO Does Not Reverse Motor Impairments in R6/2 Mice.....	105
5.4.2. No Effect of AsialoEPO on Body Weight.....	106
5.4.3. AsialoEPO Treatment Does Not Reverse Striatal Neuropathology in R6/2 Mice.....	106
5.4.4. AsialoEPO Administration Had No Effect on the Reduced BrdU Labeling in the R6/2 Mouse Dentate Gyrus.....	107
5.5. DISCUSSION.....	109
Chapter 6..... REDUCED HIPPOCAMPAL NEUROGENESIS IN R6/2 TRANSGENIC HUNTINGTON'S DISEASE MICE	113
6.1. SUMMARY	115
6.2. INTRODUCTION	116
6.3. MATERIALS AND METHODS	116
6.3.1. Transgenic Animals	116
6.3.2. Administration of BrdU and Tissue Processing.....	117
6.3.3. Immunohistochemistry.....	117
6.3.4. Stereological Techniques and Cell Quantification.....	118

Table of Contents

6.3.5. <i>Statistical Analysis</i>	119
6.4. RESULTS	119
6.4.1. <i>R6/2 Mice Exhibit Decreased Hippocampal Cell Proliferation With the Progression of the Disease</i>	119
6.4.2. <i>Decreased Hippocampal Neurogenesis at Both Early and at End Stage of Disease in R6/2 Mice</i>	122
6.4.3. <i>R6/2 Mice Exhibit Normal Proliferation in the SVZ</i>	124
6.5. DISCUSSION	126
Chapter 7. FINAL CONCLUSIONS & FUTURE DIRECTIONS	133
7.1. FINAL CONCLUSIONS.....	135
7.2. FUTURE DIRECTIONS	137
REFERENCES	139

Abbreviations List

ACTH, adreno-corticotrophic hormone
AD, Alzheimer's disease
AMPA, α -amino-3-hydroxy-5-methylisoxazole-4-propionate
ANOVA, analysis of variance
AsialoEPO, asialoerythropoietin
BDNF, brain-derived neurotrophic factor
BrdU, bromodeoxyuridine
BSA, bovine serum albumine
CAG, cytosine-adenine-guanine
cAMP, cyclic-adenosine monophosphate
CBP, CREB-binding protein
c-IAP2, cellular inhibitor of apoptosis proteins-2
CMV, cytomegalovirus
CNS, central nervous system
CRE, cAMP response element
CREB, CRE binding protein
CSF, cerebrospinal fluid
DA, dopamine
DAB, 3,3-diaminobenzidine
DARPP-32, DA and cAMP regulated phosphoprotein of a molecular weight of 32 kDa
DAT, DA transporter
DG, dentate gyrus
DOPAC, 3,4-dihydrophenylacetic acid
DRPLA, DentatoRubral and PallidoLuysian Atrophy
EEG, electroencephalogram
EMG, electromyography
EPO, erythropoietin
ER, endoplasmic reticulum
FGF2, fibroblast growth factor 2
FJ, Fluoro-Jade
GABA, γ -aminobutyric acid
GAD, glutamic acid decarboxylase
GAPDH, glyceraldehyde-3-phosphate dehydrogenase
GFAP, glial fibrillary acidic protein
GLT 1, glutamate transporter 1
GnRH, gonadotrophin releasing hormone
G protein, GTP-binding protein
HAP1, huntingtin-associated protein 1
HD, Huntington's Disease
HEAT, huntingtin, elongation factor 3, protein phosphatase 2A, target of rapamycin 1
HIP1, huntingtin interacting protein 1

Abbreviations

HIP2, huntingtin interacting protein 2
HIPPI, HIP1-protein interactor
HO[•], hydroxyl radical
H₂O₂, hydrogen peroxide
HPLC, high performance liquid chromatography
HSPs, heat shock proteins
5-HT, 5-hydroxytryptamine
HVA, homovanillic acid
IEG, immediate early gene
IGF1, insulin growth factor 1
iNOS, inducible isoform of nitric oxide synthase
InsP3R1, inositol (1,4,5)-triphosphate receptor type 1
i.p., intraperitoneal
IT15, Interesting Transcript 15
Jak2, Janus kinase 2
KA, kainate
MCH, melanin-concentrating hormone
MCHR1, MCH-receptor 1
MCHR2, MCH-receptor 2
mGluR5, metabotropic glutamate receptor type 5
MLK2, mixed-lineage kinase 2
mTOR, mammalian target of rapamycin
NDS, normal donkey serum
NeuN, neuronal nuclei
NFκB, nuclear factor-κB
NHS, normal horse serum
NIIs, neuronal intranuclear inclusions
NMDA, *N*-methyl-D-aspartate
nNOS, neuronal isoform of nitric oxide synthase
NO[•], nitric oxide
3-NP, 3-nitropropionic acid
NRSEs, neuron-restrictive silencer elements
NRSF, neuron-restrictive silencer factor
NSF, N-ethylmaleimide-sensitive factor
NSS, normal swine serum
O₂^{•-}, superoxide
OB, olfactory bulb
6-OHDA, 6-hydroxydopamine
OX1R, orexin receptor 1
OX2R, orexin receptor 2
PBS, phosphate buffered saline
PC, posterior commissure
PCNA, proliferating cell nuclear antigen
PCR, polymerase chain reaction

PD, Parkinson's disease
PET, positron emission tomography
PFA, paraformaldehyde
PSD95, postsynaptic density 95
QA, quinolinic acid
REM, rapid eye movement
REST, repressor-element-1 transcription factor
RIA, radioimmunoassay
RMS, rostral migratory stream
ROS, reactive oxygen species
SBMA, Spinal and Bulbar Muscular Atrophy (also called Kennedy Disease)
SCA, Spino-Cerebellar Ataxia
SCO, subcommisural organ
S.E.M., standard error of the mean
SGZ, subgranular zone
SH3, Src homology-3
SNARE, soluble NSF attachment protein receptor
SOD, superoxide dismutase
Sp1, specific protein-1
SVZ, subventricular zone
TAF_{II}130, TBP associated factor
TATA, thymine-adenine-thymine-adenine
TBP, TATA-binding protein
TdT, terminal deoxynucleotidyl transferase
TH, tyrosine hydroxylase
TUNEL, TdT-mediated dUTP nick-end labeling
3V, third ventricle
WT, wild-type
XIAP, X-linked inhibitor of apoptosis proteins
YAC, yeast artificial chromosome

Summary

Huntington's disease (HD) is a devastating neurodegenerative disorder caused by an expanded CAG repeat in the *IT15* gene, which encodes for huntingtin. The disease is classically characterized by accumulation of huntingtin in neuronal intranuclear inclusions, a progressive degeneration of neurons in the striatum and the cerebral cortex, which leads to progressive motor and cognitive deterioration, and inevitably death. Since the discovery of the mutation responsible for HD, several transgenic rodent models have been generated. The most widely studied are the R6 lines that express exon 1 of the *IT15* gene with 115 (R6/1) or 145 (R6/2) CAG repeats. The work presented in this thesis further characterizes these transgenic HD rodent models (particularly the R6 mice) and describes, for the first time, a number of novel histological and functional changes in HD.

The first part of this thesis evaluates changes in neurotransmitter systems, at the level of glutamate receptor stimulation (*Chapter 2*) and dopamine (DA) release (*Chapter 3*). More precisely, the work presented in *Chapter 2* demonstrates that, unlike R6 mice that are known to be resistant to excitotoxic insults, a newly generated HD transgenic rat (which expresses 22% of the *IT15* gene with 51 CAG repeats) is not resistant to this damage. These results, together with previous research, suggest that the response of transgenic HD rodent models to excitotoxicity is dependent on the length of the transgene expressed. On the other hand, *Chapter 3* describes an impairment in the release of DA in R6/1 mice, as determined by *in vivo* microdialysis upon membrane depolarization-induced exocytosis and DA transporter-mediated efflux. In support of this result, a reduction in whole striatal DA levels and basal levels of DA metabolites were also observed. These results suggest a dysfunction of the dopaminergic nigrostriatal pathway in HD.

The second part of this thesis explores the involvement of nonstriatal brain regions, namely the lateral hypothalamus (*Chapter 4*) and the dentate gyrus (DG) of the hippocampus (*Chapters 5 and 6*), in the neuropathology of the R6/2 HD mouse.

Chapter 4 describes, for the first time, loss of specific neuronal populations in the lateral hypothalamus of R6/2 mice. Two major neuronal populations were affected: orexin-containing neurons (which regulate the sleep/wakefulness cycle) and melanin-concentrating hormone-containing neurons (which play a role in maintaining energy homeostasis). Importantly, the progressive loss of orexin neurons was accompanied by the development of narcoleptic-like symptoms in R6/2 mice, which closely resemble the deficits reported in *orexin* knockout mice

by other researchers. In conjunction with the loss of these neurons we also observed decreased levels of orexin in the cerebrospinal fluid of end-stage R6/2 mice. Interestingly, we also found loss of orexin neurons in samples of the lateral hypothalamus of HD patients. Overall, these results clearly implicate the lateral hypothalamus in the pathology of HD.

Finally, *Chapters 5* and *6* describe, for the first time, a dysfunction in yet another nonstriatal brain region, the DG of the hippocampus, in R6/2 mice. The DG constitutes one of the regions in the adult mammalian brain where neurogenesis (i.e., generation of new neurons) occurs. R6/2 mice show a progressive decrease in the number of proliferating cells and neurons in the DG when compared to wild-type littermate controls. Moreover, this decrease can be detected as early as 2 weeks of age, when the R6/2 mice do not show any clear behavioral symptoms. Finally, treating the R6/2 mice with asialoerythropoietin (an erythropoietin analogue) did not reverse the decreased rate of neurogenesis nor had any effect on the neuropathology or the development of motor symptoms.

Overall, the results presented in this thesis provide new evidence that corroborates the implication of excitotoxicity and dopaminergic dysfunction in the HD striatum. It also demonstrates pathological changes and morphological dysfunction in nonstriatal structures, such as the lateral hypothalamus and the DG of the hippocampus. Moreover, this data further contributes to our understanding of the transgenic rodent models used in HD research by expanding our knowledge of their neuropathology. We speculate that this work may be instrumental in the design and screening of new therapies to treat this devastating neurodegenerative disorder.

Resumo

A doença de Huntington (HD, do inglês ‘Huntington’s disease’) é uma doença neurodegenerativa causada pela expansão de repetições do trinucleotídeo CAG no gene *IT15* que codifica a proteína huntingtina. Esta doença é classicamente caracterizada pela formação de inclusões nucleares de huntingtina em células neuronais e pela progressiva degenerescência dos neurónios do estriado e do córtex cerebral. Clinicamente, a HD manifesta-se pela deterioração progressiva das capacidades motoras e cognitivas, resultando na morte do paciente. Desde a descoberta da mutação responsável pela HD, vários modelos transgênicos têm vindo a ser gerados em rato e ratinho, entre os quais se destacam as linhas R6 que expressam o exon 1 do gene *IT15* com 115 (linha R6/1) ou 145 (linha R6/2) repetições do trinucleotídeo CAG. O trabalho apresentado nesta tese caracteriza alguns destes modelos transgênicos (em particular os ratinhos R6) e descreve, pela primeira vez, alterações morfológicas e funcionais que poderão contribuir para a patologia da HD.

Na primeira parte desta tese são avaliadas as alterações nos sistemas de neurotransmissão, em particular a activação de receptores de glutamato (*Capítulo 2*) e a libertação de dopamina (DA) (*Capítulo 3*). Deste modo, o trabalho apresentado no *Capítulo 2* demonstra que o modelo transgénico para a HD que foi recentemente gerado em rato (e que expressa 22% do gene *IT15* com 51 repetições do trinucleotídeo CAG) não apresenta alterações na susceptibilidade dos neurónios do estriado a lesões excitotóxicas. Estes resultados, juntamente com estudos anteriores, sugerem que a resposta dos vários modelos transgênicos para a HD a insultos excitotóxicos é dependente do tamanho do transgene. Por outro lado, no *Capítulo 3* são apresentadas novas evidências que suportam uma desregulação na libertação de DA em ratinhos R6/1. A libertação deste neurotransmissor foi detectada por microdiálise *in vivo* após exocitose induzida por despolarização da membrana plasmática e após indução da libertação de DA através do seu transportador membranar. Para além disso, um decréscimo dos níveis totais de DA no estriado e dos níveis basais dos metabolitos de DA foram observados em ratinhos R6/1. Estes resultados confirmam o envolvimento de uma disfunção da via dopaminérgica nigro-estriatal na patologia da HD.

A segunda parte desta tese explora o envolvimento de algumas regiões cerebrais não estriatais, o hipotálamo lateral (*Capítulo 4*) e o giro dentado (DG, do inglês ‘dentate gyrus’) do hipocampo (*Capítulos 5 e 6*), na neuropatologia do ratinho R6/2.

O *Capítulo 4* descreve, pela primeira vez, a perda de populações neuronais no hipotálamo lateral de ratinhos R6/2. Os neurónios afectados contêm orexina (um peptídeo que regula o ciclo diurno/nocturno) ou a hormona concentradora da melanina, que desempenha um papel importante na manutenção da homeostase energética. A perda progressiva dos neurónios que contêm orexina é acompanhada pelo desenvolvimento de sintomas do tipo narcoléptico nos ratinhos R6/2, semelhantes aos sintomas descritos em ratinhos que não expressam o gene da *orexina*. Para além disso, os níveis deste peptídeo no líquido cefalorraquidiano de ratinhos R6/2 também se encontram reduzidos, e a perda de neurónios que contêm orexina também foi detectada em cérebros de doentes com HD. Estes resultados reforçam a importância do hipotálamo lateral na patologia da HD.

Finalmente, os *Capítulos 5 e 6* descrevem, pela primeira vez, a disfunção de outra região cerebral não estriatal, o DG do hipocampo, no ratinho R6/2. O DG constitui uma das regiões no cérebro adulto de mamíferos onde ocorre a formação de novos neurónios, um processo designado por neurogénese. Os ratinhos R6/2 apresentam um decréscimo progressivo no número de células proliferativas e de novos neurónios nesta região cerebral, quando comparados com ratinhos controlo da mesma idade. Para além disso, este decréscimo pode ser detectado às duas semanas de idade, uma altura em que os ratinhos transgénicos ainda não apresentam quaisquer sintomas. Por fim, o tratamento de ratinhos R6/2 com asialo-eritropoietina (um análogo da eritropoietina) não teve qualquer efeito na redução da proliferação celular observada no hipocampo destes animais, bem como na neuropatologia e no desenvolvimento dos sintomas motores.

Conjuntamente, os resultados apresentados nesta tese corroboram o envolvimento da excitotoxicidade e da disfunção dopaminérgica na HD, e demonstram, ao nível morfológico e funcional, o envolvimento de estruturas cerebrais não estriatais na patologia da HD. Para além disso, estes resultados contribuem para uma melhor caracterização dos modelos transgénicos mais usados na investigação da HD e descrevem novos aspectos da sua neuropatologia, possibilitando o desenvolvimento de novas terapias para esta doença neurodegenerativa.

Chapter 1

General Introduction

Huntington's Disease and *in vivo* Transgenic Models Used to Study this Neurodegenerative Disorder

Chapter partially based on the following reviews:

Gil J, and Rego AC (2006): "Mechanisms of neurodegeneration in Huntington's disease", (*Manuscript in preparation*).

Petersén Å, **Gil J**, and Brundin P (2006): "Revolutionizing Huntington's disease research: the R6 transgenic mice", (*Manuscript in preparation for Brain Res Rev*).

1.1. Polyglutamine Diseases

The expression of unstable trinucleotide repeats is known to be the underlying cause of several neurological disorders. Nine of these diseases are caused by the expansion of cytosine-adenine-guanine (CAG) repeats (which code for the amino acid glutamine) on specific genes, leading to the expression of a glutamine tract in the respective proteins. Hence, these disorders are referred as polyglutamine diseases (for review see Gusella and MacDonald, 2000; Zoghbi and Orr, 2000; Ross, 2002; Gatchel and Zoghbi, 2005).

The polyglutamine diseases include Spinal and Bulbar Muscular Atrophy (SBMA; also called Kennedy Disease), DentatoRubral and PallidoLusian Atrophy (DRPLA), Spino-Cerebellar Ataxia (SCA) types 1, 2, 3 (also called Machado-Joseph Disease), 6, 7, and 17, and Huntington's Disease (HD), the most common of these neurodegenerative disorders. In all 9 diseases, the first symptoms normally appear in midlife. They then progress over time and are caused by dysfunction and eventual loss of specific neuronal populations. Death of affected individuals occurs 10 to 20 years after the appearance of the first symptoms. With the exception of SBMA (which has a X-linked recessive pattern of inheritance), polyglutamine expansion diseases are dominantly inherited.

Interestingly, the age of onset and the severity of the disease are inversely correlated with the number of CAG repeats. Each disorder shows a characteristic threshold for the length of the glutamine tract (**Table I**), below which symptoms are not manifested and above which a progressive decrease in the age of onset is observed. Excessively large expansions result in severe juvenile-onset cases, characterized by widespread neurodegeneration and cell death. However, the age of onset and progression of polyglutamine diseases may be determined by factors other than the CAG expansion, since for a given CAG repeat there is a great variation in the age of onset.

The CAG repeats show both somatic and germline instability, causing intergenerational instability (i.e., variation of the number of repeats from generation to generation). This is frequently observed in paternal transmissions and may result in anticipation of the disease characterized by earlier age of onset, increase in the severity of the symptoms and faster progression of the disease in the next generation (for review see Gusella and MacDonald, 2000; Zoghbi and Orr, 2000; Gatchel and Zoghbi, 2005). Interestingly, for most polyglutamine diseases (including HD) alleles with CAG repeats within the upper limit of the normal range are less stable during transmission through the germline than shorter alleles. Therefore, these are believed to constitute the allele pool from which the pathologic mutations are generated. As a result, there

is a positive correlation between the frequency of “long normal alleles” and the disease prevalence in any given population (for review see Ho *et al.*, 2001).

Table I – Features of the various polyglutamine neurodegenerative diseases.

Polyglutamine Disease	Mutated Protein	Expanded CAG Repeat	Affected Brain Regions	Main Clinical Symptoms
<i>SBMA (Kennedy Disease)</i>	Androgen Receptor	38-62	Anterior horn and bulbar neurons, dorsal root ganglia	Motor weakness, swallowing difficulty, hypogonadism
<i>DRPLA</i>	Atrophin-1	49-88	Cerebellum, cerebral cortex, basal ganglia, Luys body	Ataxia, epilepsy, choreoathetosis, dementia
<i>SCA-1</i>	Ataxin-1	40-82	Cerebellar Purkinje cells, dentate nucleus, brain stem	Ataxia, slurred speech, spasticity, cognitive impairment
<i>SCA-2</i>	Ataxin-2	32-200	Cerebellar Purkinje cells, fronto-temporal lobes, brain stem	Ataxia, decreased reflexes, polyneuropathy, motor neuropathy
<i>SCA-3 (Machado-Joseph Disease)</i>	Ataxin-3	61-84	Cerebellar dentate neurons, basal ganglia, brain stem, spinal cord	Ataxia, parkinsonism, severe spasticity
<i>SCA-6</i>	α 1A-voltage-dependent Ca^{2+} channel	20-29	Cerebellar Purkinje cells, dentate nucleus, inferior olive	Ataxia, dysarthria, nystagmus, tremor
<i>SCA-7</i>	Ataxin-7	37-306	Cerebellum, brain stem, macula, visual cortex	Ataxia, retinal degeneration
<i>SCA-17</i>	TATA-binding protein (TBP)	47-63	Cerebellum, caudate nucleus, putamen, thalamus, frontal and temporal cortex	Ataxia, behavioural changes or psychosis, intellectual deterioration, seizures
<i>HD</i>	Huntingtin	35-121	Striatum (caudate nucleus and putamen), cerebral cortex, hypothalamus	Movement abnormalities, chorea, dystonia, cognitive decline, dementia

(Adapted from Gusella and MacDonald, 2000; Zoghbi and Orr, 2000; Gatchel and Zoghbi, 2005).

The genes carrying the expanded CAG repeat that are responsible for these 9 disorders share no homology except for the CAG repeat itself. As a consequence, the proteins that they code for are unrelated to each other (**Table I**). Therefore, it has been suggested that the expanded polyglutamine track on each of these unrelated proteins is directly responsible for the neurodegeneration seen in polyglutamine expansion disorders. On the other hand, the affected proteins have been suggested to play an indirect modulatory role on some of the disease-specific characteristics, such as which specific brain regions become affected, the number of CAG repeats necessary for the manifestation of disease

symptoms, and the rate of disease progression (for review see Gusella and MacDonald, 2000; Ross, 2002).

Another interesting feature common to most polyglutamine diseases (SBMA, DRPLA, SCA-1, -3, -7, -17, and HD) is the localization of the respective mutant proteins into ubiquitinated neuronal inclusions. These inclusions are thought to result from the accumulation of misfolded mutant proteins that are not degraded by the proteasome despite the presence of ubiquitin residues, which are known to target proteins for proteasomal degradation. In addition, these inclusions may also contain several different intracellular molecules with which the mutant proteins establish aberrant interactions. Therefore, protein aggregation appears to be a critical event in most polyglutamine diseases (for review see Zoghbi and Orr, 2000; Gatchel and Zoghbi, 2005).

1.2. Huntington's Disease

HD is the most common and well studied polyglutamine neurodegenerative disorder. It has a prevalence of 3 to 10 affected subjects per 100,000 individuals in Western Europe and North America (for review see Vonsattel and DiFiglia, 1998; Ho *et al.*, 2001).

The disorder was first described in the 19th century by George Huntington, who identified both its clinical features and pattern of familial transmission. However, it was not until 1993 that a multicenter consortium, organized by the Hereditary Disease Foundation, discovered the actual HD gene mutation. This is an unstable expansion of CAG repeats within the coding region of the "Interesting Transcript 15" (*IT15*) gene, which is located on the short arm of chromosome 4 (4p63) and encodes huntingtin, a protein of yet unknown function. The mutation results in a stretch of glutamine residues located in the NH₂-terminal of huntingtin (The Huntington's Disease Collaborative Research Group, 1993). Although the abnormal protein is ubiquitous expressed throughout the organism, cell degeneration appears to be restricted to the brain (for review see Vonsattel and DiFiglia, 1998).

1.2.1. Clinical Manifestation

Mutant huntingtin is expressed throughout life. However, in most cases the onset of the disease occurs in midlife, between the ages of 35 and 50 years. When intergenerational instability and anticipation occur, the first symptoms can appear during early childhood, leading to rare and more severe infantile or juvenile cases. The disease progresses over time and is invariably fatal 15 to 20

years after the onset of the first symptoms. In juvenile cases the progression is faster, leading to death 7 to 10 years after the onset of symptoms (for review see Ho *et al.*, 2001).

Classically described as Huntington's *Chorea* (the Greek word for dance), the first signs of the disease are subtle: clumsiness, difficulties with smooth eye pursuit, and slight uncontrolled and awkward movements. These motor disturbances, with the loss of voluntary movement coordination, progress slowly. The involuntary movements of the proximal and distal muscles become more severe and the patients gradually lose their capacity to move and eventually communicate. In late stages of the disease, the chorea tends to be replaced by bradykinesia and rigidity, where death soon follows due to heart failure or aspiration pneumonia. In juvenile patients the symptomatology is considerably different, being characterized by bradykinesia, tremors, rigidity and dystonia, where the chorea may be completely absent. Affected children may also suffer epileptic seizures (for review see Vonsattel and DiFiglia, 1998; Gusella, 2001; Ho *et al.*, 2001; Petersén and Brundin, 2002).

The majority of patients also suffer from inexplicable muscle wasting and weight loss, despite constant caloric intake (Sanberg *et al.*, 1981; Kirkwood *et al.*, 2001; Djousse *et al.*, 2002). The cause of these peripheral symptoms is still unclear. A number of endocrine abnormalities have also been reported in HD patients, including increased levels of corticosteroids (Heuser *et al.*, 1991; Leblhuber *et al.*, 1995; Björkqvist *et al.*, 2006a) and reduced levels of testosterone (Markianos *et al.*, 2005). Furthermore, 10-25% of HD patients exhibit diabetes mellitus (Farrer *et al.*, 1985).

The cognitive capacities are also severely affected during the course of HD, which can be classified as subcortical dementia. The slowing of intellectual processes is the first sign of cognitive impairment in HD patients. Chronic depression sometimes occurs years before the onset of motor symptoms. Cognitive impairments progress over time and late-stage HD patients show profound dementia. Manic-depressive behaviour and personality changes (irritability, apathy, and sexual disturbances) are often part of the psychiatric syndrome (for review see Vonsattel and DiFiglia, 1998; Gusella, 2001; Ho *et al.*, 2001; Petersén and Brundin, 2002).

Based on the above features, the criteria used for the diagnostic of HD include: **(1)** a family history of HD; **(2)** progressive motor disability with chorea or rigidity with no other cause; and **(3)** psychiatric disturbances with progressive dementia with no other cause (for review see Vonsattel and DiFiglia, 1998). Currently, all individuals showing these symptoms are submitted to genetic testing in order to screen for the HD mutation and confirm the diagnosis.

1.2.2. Neuropathology

The pathological hallmark of HD is the gradual atrophy of the striatum (caudate nucleus and putamen), which can be observed in 95% of all HD cases (Figure 1.1).

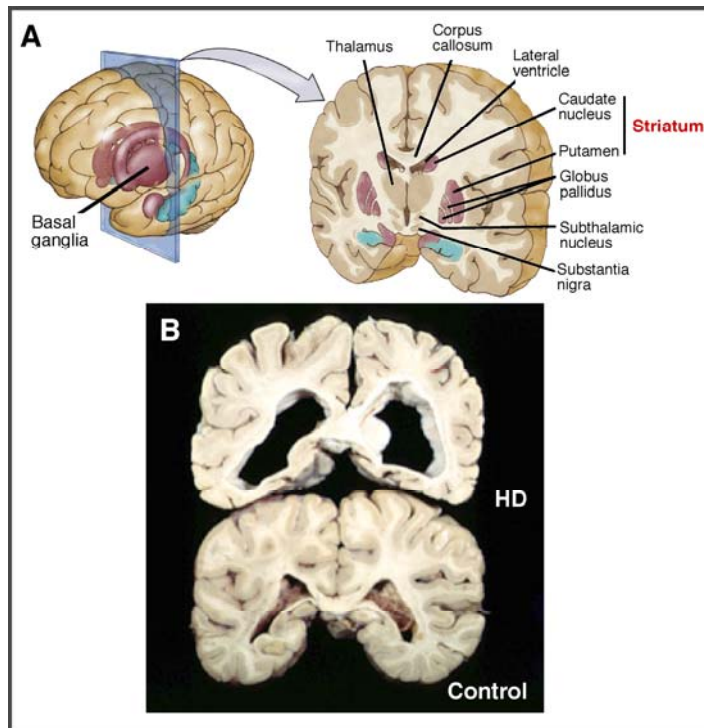


Figure 1.1. – (A) A schematic representation of the human basal ganglia from a three-dimensional and coronal perspectives. The basal ganglia includes the striatum, which comprises the caudate nucleus and putamen. Adapted from Kolb and Whishaw, 2006. (B) Macroscopic photographs of HD and normal control brains in coronal view. Note that the striatum is severely atrophied in the HD brain. Adapted from the web-page of the Harvard Center for Neurodegeneration & Repair: <http://www.hcnr.med.harvard.edu/visitorInfo/huntingtons.php>

The most commonly used grading system to assess the severity of HD degeneration was developed by Vonsattel and colleagues (1985). It is based on the pattern of striatal degeneration in *post mortem* tissue and classifies HD cases into five different severity grades (0 to 4): *Grade 0*, which comprises 1% of all HD brains, superficially appears indistinguishable from normal brains after gross

examination. However, with histological examination, a 30-40% neuronal loss can be detected in the head of the caudate nucleus. *Grade 1* occurs in 4% of all HD brains and comprises atrophy in the tail, and in some cases the body of the caudate nucleus. Neuronal loss and astrogliosis are evident in the head (50% loss), tail, and to a less extent, in the body of the caudate nucleus. *Grade 2* comprises 16% of the cases, with gross striatal atrophy that is more pronounced than that detected in grade 1 brains. *Grade 3* comprises 54% of all HD brains, with severe gross striatal atrophy. *Grade 4* includes 25% of all HD cases, with severe atrophy of the striatum and up to 95% neuronal loss (Vonsattel *et al.*, 1985).

Interestingly, the degree of striatal atrophy also correlates with the degeneration of other nonstriatal brain structures. For instance, in *grades 1* and *2* nonstriatal structures are generally spared or only show a slight atrophy; whereas, in *grades 3* and *4* the cerebral cortex (particularly layers III, V, and VI), globus pallidus, thalamus, subthalamic nucleus, substantia nigra, white matter, and cerebellum can be markedly affected (for review see Vonsattel and DiFiglia, 1998). Recent studies have also indicated that the hypothalamus can be significantly atrophied in HD patients (Kassubek *et al.*, 2004), which is in agreement with previous findings of loss of somatostatin-positive neurons in the lateral tuberal nucleus of the hypothalamus (Kremer *et al.*, 1990, 1991). Because of the generalized cerebral atrophy observed with the most severe cases, the overall brain weight can decrease by up to 40% (**Figure 1.1**; for review see Gusella, 2001).

Within the striatum, the most afflicted neuronal populations are the medium-sized projection spiny neurons, which correspond to 80% of the striatal neuronal population. These neurons use the inhibitory transmitter γ -aminobutyric acid (GABA), and either enkephalin, dynorphin, or substance P as co-transmitters. These neurons are in part regulated by the dopaminergic inputs emanating from the substantia nigra in the brain stem, and project back to the substantia nigra and to the globus pallidus. Since these medium-sized spiny neurons exert an inhibitory effect, it is believed that the loss of their inhibitory input is the underlying cause of the uncontrolled movements characteristic of HD (for review see Gusella, 2001).

Interestingly, different degrees of degeneration can be observed within the striatal spiny neuronal population, with enkephalin-containing neurons being more susceptible than substance P-containing neurons. Conversely, medium-sized aspiny interneurons (containing somatostatin, neuropeptide Y, or NADPH-diaphorase), cholinergic interneurons, and parvalbumin-containing GABAergic neurons are relatively spared in HD brains. Since striatal neurons receive glutamatergic input from the cerebral cortex, it has been suggested that the

degree of degeneration of the various striatal populations results from their glutamate receptor composition, which in turn can modulate their susceptibility to glutamate stimulation. Thus, the most vulnerable spiny neurons are those that express ionotropic *N*-methyl-D-aspartate (NMDA) receptors predominantly formed by NR1 and NR2B subunits; whereas, the less vulnerable spiny neurons express mainly the NR2D subunit (see *section 1.4.1*). However, the spiny neurons also demonstrate increased vulnerability in late stages of the disease (for review see Vonsattel and DiFiglia, 1998; Davies and Ramsden, 2001).

Eliminado: become vulnerable

Eliminado: to degeneration

HD is also characterized by the presence of neuronal intranuclear inclusions (NIIs) (DiFiglia *et al.*, 1997a) and protein aggregates in dystrophic neurites (Sapp *et al.*, 1999) in striatal and cortical neurons, which is a feature of several other polyglutamine diseases (*section 1.1*). These inclusions are present in 1 to 5% of all striatal neurons and in 3 to 6% of all cortical neurons (DiFiglia *et al.*, 1997a). Interestingly, the frequency of neurons bearing NIIs is drastically increased in juvenile cases of HD, reaching a frequency of 38 to 52% in the cerebral cortex (DiFiglia *et al.*, 1997a).

Eliminado: -

Eliminado: -

Eliminado: -

NIIs appear before the loss in brain weight, which in turn, is known to precede the loss of body weight and the onset of neurological symptoms (for review see Vonsattel and DiFiglia, 1998). These events suggest that the abnormal accumulation of mutated protein is one of the initial pathologic events during the development of HD. Moreover, the number of cortical inclusions correlates well with the length of the CAG repeat expansion and the age of disease onset (Becher *et al.*, 1998), further indicating that the development of NIIs is a good predictor of the disease stage.

Eliminado: ing

Eliminado: first

Eliminado: stage

1.2.3. Genetics

As mentioned above (*section 1.2*), the mutation responsible for HD constitutes a stretch of uninterrupted CAG trinucleotide repeats located near the 5'-end in exon 1 of the *IT15* gene coding sequence, which comprises 67 exons. Consequently, the mutated protein (huntingtin) bears a tract of consecutive glutamine residues in its NH₂-terminal, 17 amino acids downstream from the initiator methionine (The Huntington's Disease Collaborative Research Group, 1993).

Eliminado: the

Eliminado: Therefore

The disease is inherited in an autosomal dominant manner. The normal and mutant alleles are transmitted from generation to generation in a Mendelian fashion. The mutant allele is unstable during meiosis, changing in length in the majority of intergenerational transmissions, with either slight increases of 1 to 4 units or decreases of 1 to 2 units. In rare occasions, larger size increases occur in parental transmissions, which reflects a particularly high mutation rate during

Eliminado: mendelian

Eliminado: ,

Eliminado: and t

Eliminado: -

Eliminado: -

Eliminado: reflecting

spermatogenesis (The Huntington's Disease Collaborative Research Group, 1993; for review see Gusella, 2001).

The number of CAG repeats (i.e., glutamine residues) is the primary and major determinant of disease severity, accounting for about 60% of the variance in the age of onset of the first symptoms. The remaining variance is attributable to other genetic features and environmental factors. Normally, asymptomatic individuals have less than 35 CAG repeats; whereas, HD is manifested when the number of repeats exceeds this threshold. Alleles with 35 to 39 repeats are associated with later onset of the disease, although incomplete penetrance has been observed in some individuals who have shown no symptoms or neuropathological signs. Alleles of 40 to 50 units give rise to the most common adult-onset form of the disease; whereas, the longest repeats (normally associated with high allele instability during parental transmission) are responsible for the severe juvenile and infantile cases (The Huntington's Disease Collaborative Research Group, 1993; for review see Gusella, 2001).

Importantly, there is a positive correlation between the number of CAG repeats and the Vonsattel grades of neuropathological severity (*section 1.2.2*), with greater CAG repeat lengths being associated with greater degrees of cell death in the striatum and higher Vonsattel grades (for review see Vonsattel and DiFiglia, 1998).

1.3. Huntingtin

Huntingtin is a protein composed by more than 3100 amino acids and with a molecular mass of approximately 349 kDa, depending on the exact number of glutamine residues. A polymorphic proline-rich segment follows the polyglutamine tail (The Huntington's Disease Collaborative Research Group, 1993). Huntingtin does not show structural homology with any other known protein.

The wild-type protein is widely expressed throughout the body, in both neuronal and non-neuronal cells, raising the question of how and why the disease mutation results in a selective neuronal loss. As mentioned above (*section 1.2.2*), in the HD brain, particularly in the two most affected regions, the striatum and cerebral cortex, an altered intracellular localization and perinuclear accumulation of mutant huntingtin is observed, with the formation of NIIs (DiFiglia *et al.*, 1997a) and aggregates in dystrophic neurites (Sapp *et al.*, 1999). However, the neurons bearing inclusions do not correspond to the most vulnerable ones. Indeed, the interneurons that are spared during the course of the disease are the ones that display the highest frequency of aggregates

- Eliminado: ,
- Eliminado: with t
- Eliminado: reminder being
- Eliminado: , as well as
- Eliminado: -
- Eliminado: usually cause the disease late in life
- Eliminado: n
- Eliminado: of the disease; a
- Eliminado: -
- Eliminado: ;

(Kuemmerle *et al.*, 1999), raising the question of whether inclusions are toxic, protective, or just an epiphenomenon of the disease mechanism.

1.3.1. Proposed Functions of Wild-Type Huntingtin

Pioneer studies have clearly shown that wild-type huntingtin is essential for normal embryonic development, since engineered knockout mutations that disrupt exon 4 (Duyao *et al.*, 1995), exon 5 (Nasir *et al.*, 1995), or the promoter (Zeithlin *et al.*, 1995) of the mouse HD gene homolog *Hdh* leading to its complete inactivation, result in embryonic lethality. Interestingly, the HD mutation does not seem to abrogate the developmental functions of huntingtin, since HD patients appear to develop normally and the symptoms only start to manifest several years after birth. Nevertheless, normal huntingtin appears to be required not only during embryogenesis but also throughout life, since conditional knockout mice in which the *Hdh* gene is inactivated during adulthood are sterile and develop a progressive neuronal degenerative phenotype (Dragatsis *et al.*, 2000).

Eliminado: ed

Eliminado: apparently

Eliminado: just

Eliminado: was turned off

Within the cell, wild-type huntingtin is mainly localized in the cytoplasm associated with organelles such as mitochondria, the Golgi apparatus, the endoplasmic reticulum (ER), synaptic vesicles, and several components of the cytoskeleton. Wild-type huntingtin is also present inside the nucleus, although to a lesser extent (for review see Young, 2003; Landles and Bates, 2004).

Eliminado: and

Eliminado: as well as with

Yeast two-hybrid screenings, western-blotting, and immunoprecipitation studies have shown that wild-type huntingtin binds to several proteins. The latest review that was published on this subject listed 27 huntingtin-interacting proteins (Li and Li, 2004), and the list is continuously growing. Relevant examples include: (1) *Huntingtin-Associated Protein 1 (HAP1)*, a novel protein with at least two isoforms (HAP1-A and HAP1-B) that is expressed in several tissues including the brain. HAP1 interacts with the p150 subunit of dynactin, thus being involved in intracellular transport; (2) *Huntingtin Interacting Protein 1 (HIP1)*, a protein implicated in cytoskeleton assembly as well as in endocytosis that binds to α -adaptin and clathrin; (3) *Huntingtin Interacting Protein 2 (HIP2)*, an ubiquitin-conjugating enzyme that catalyzes the covalent attachment of ubiquitin units to intracellular proteins, tagging them for degradation by the proteasome; (4) *Glyceraldehyde-3-Phosphate Dehydrogenase (GAPDH)*, a glycolytic enzyme; and (5) *Microtubules and β -Tubulin*, components of the cytoskeleton (for review see Gusella and MacDonald, 1998; Walling *et al.*, 1998; Li and Li, 2004).

In some cases, a functional relationship between wild-type huntingtin and its interacting proteins has also been established, as illustrated with the following

Eliminado: was

examples. (1) *Postsynaptic Density 95 (PSD95)*, is a protein located in the postsynaptic membrane that is involved in the anchoring of NMDA and kainate (KA) receptors to the membrane. Wild-type huntingtin was shown to regulate these receptors through the binding of its Src homology-3 (SH3) sequence (proline-x-x-proline) to PSD95 (Sun *et al.*, 2001). (2) *Repressor-Element-1 Transcription Factor (REST)* / *Neuron-Restrictive Silencer Factor (NRSF)* is a transcriptional factor complex that binds to neuron-restrictive silencer elements (NRSEs) present in certain neuronal gene promoters, such as the *Brain Derived Neurotrophic Factor (BDNF)* promoter, inhibiting their expression. Wild-type huntingtin promotes BDNF expression by interacting with REST/NRSF in the cytoplasm and thus preventing this complex to translocate into the nucleus (Zuccato *et al.*, 2003). (3) *Vesicular transport of BDNF along the microtubules* is also promoted by wild-type huntingtin and involves HAP1 and the p150 subunit of dynactin (Gauthier *et al.*, 2004). (4) *HAP1 and Mixed-Lineage Kinase 2 (MLK2) stimulate and modulate* the activity of the helix-loop-helix transcription factor *NeuroD* (Marcora *et al.*, 2003), which is crucial for the development of the dentate gyrus (DG) of the hippocampus (Liu *et al.*, 2000), and for the morphogenesis of pancreatic islets (Huang *et al.*, 2002). Interaction of wild-type huntingtin with both HAP1 and MLK2 was shown to promote the expression of this transcription factor (Marcora *et al.*, 2003). (5) *HIP1* interaction with wild-type huntingtin prevents its binding to the HIP1-protein interactor (HIPPI) and the consequent activation of caspase-8 by this protein complex (Gervais *et al.*, 2002).

The anti-apoptotic function of wild-type huntingtin has also been corroborated with several *in vitro* studies. These have demonstrated that expression of the full-length protein protected conditionally immortalized striatal-derived cells from a variety of apoptotic stimuli. Wild-type huntingtin appeared to act downstream of mitochondrial cytochrome c release, preventing the formation of a functional apoptosome complex and the consequent activation of caspase-9 (Rigamonti *et al.*, 2001) and caspase-3 (Rigamonti *et al.*, 2000).

Interestingly, huntingtin sequence has 10 HEAT (Huntingtin, Elongation Factor 3, Protein Phosphatase 2A, Target Of Rapamycin 1) repeats, which are conserved repeating segments of approximately 40 amino acids that form 2 hydrophobic α -helices (Andrade and Bork, 1995). The function of these motives is still unclear, although they are found in a variety of proteins that are involved in intracellular transport and chromosomal segregation (Neuwald and Hirano, 2000).

Overall, these studies indicate that wild-type huntingtin may exert a variety of intracellular functions such as: (1) protein trafficking; (2) vesicle transport and anchoring to the cytoskeleton; (3) clathrin-mediated endocytosis; (4)

Eliminado: :

Eliminado: ,

Eliminado: and

Eliminado:);

Eliminado: -

Eliminado: -

Eliminado:);

Eliminado:);

Eliminado: and stimulate

Eliminado: a functional hippocampal

Eliminado:);

Eliminado: An

Eliminado: was

Eliminado: ,

Eliminado: which

Eliminado: showed that

postsynaptic signaling; (5) transcriptional regulation; (6) and anti-apoptotic function (Figure 1.2). Thus, wild-type huntingtin is believed to have a pro-survival role inside the cell (for review see Gusella and MacDonald, 1998; Walling *et al.*, 1998; Landles and Bates, 2004; Li and Li, 2004).

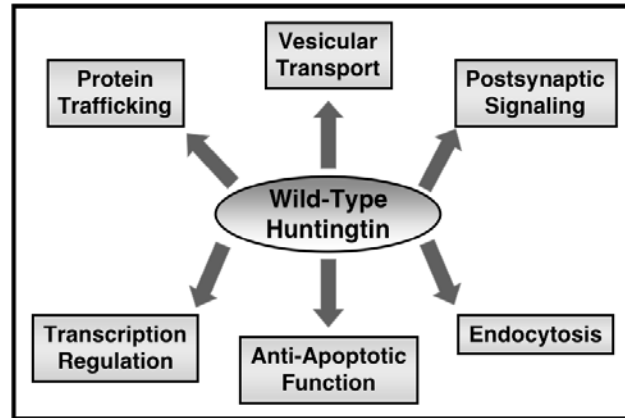


Figure 1.2. – Proposed functions of wild-type huntingtin. Based on the identification of several huntingtin-interacting proteins, it is believed that wild-type huntingtin may exert various intracellular functions that contribute to cell survival.

1.3.2. Aggregation of Mutant Huntingtin

Two non-mutually exclusive mechanisms have been suggested to explain the formation of aggregates of mutant huntingtin:

1) *The Polar Zipper Model.* According to this theory, the normal tertiary protein conformation is destabilized by the presence of the expanded polyglutamine tract, leading to the establishment of abnormal protein-protein interactions with other polyglutamine-bearing proteins (including molecules of mutant and wild-type huntingtin). This results in the formation of insoluble β -pleated sheets that form polar zipper structures via hydrogen bonding (Perutz *et al.*, 1994; Stott *et al.*, 1995).

2) *The Transglutaminase Model.* Transglutaminases are enzymes that are involved in the cross-linking of glutamine residues and, thus may also participate in the formation of aggregates. Indeed, *in vitro* studies have shown that huntingtin is a transglutaminase substrate, and that the transglutaminase-mediated cross-linking increases with the length of the polyglutamine stretch (Kahlem *et al.*, 1998). Hence, the expanded polyglutamine tract caused by the disease mutation could result in an increased transglutaminase-mediated cross-linking

Eliminado: through

Eliminado: ,

Eliminado: therefore,

Eliminado: be involved

Eliminado: mutant huntingtin

Eliminado: ,

with other molecules of mutant and wild-type huntingtin, as well as other polyglutamine-containing proteins, leading to the precipitation and intraneuronal accumulation of protein complexes. In support of this model, transglutaminase activity was shown to be increased in HD brains (Karpuj *et al.*, 1999).

Once formed, these aggregates of mutant huntingtin are transported by the microtubule organization center, or centrosome, to a perinuclear localization (Waelter *et al.*, 2001; Hoffner *et al.*, 2002).

Because the formation of mutant huntingtin aggregates is regarded as a hallmark of HD, many hypothesize that aggregation of mutant huntingtin is the trigger point that eventually leads to cell demise in HD. Indeed, several proteins have been shown to abnormally interact and be recruited into the aggregates of mutant huntingtin, causing a severe dysregulation of several key intracellular pathways (see *section 1.3.3*). Nevertheless, mutant huntingtin inclusions may only represent a side effect of the ongoing cell dysfunction, or may even exert a protective role during the early stages of the disease. Indeed, it is possible that the inclusions represent a means for the cell to sequester the toxic N-terminal fragments and oligomers of mutant huntingtin as well as other misfolded proteins, which in the soluble form could cause a more rapid and severe damage (for review see Ciechanover and Brundin, 2003; Gunawardena and Goldstein, 2005).

Eliminado: of the

Eliminado: and its intraneuronal accumulation.

Eliminado: was

Eliminado: reported to be

Eliminado: The

Eliminado: and several lines of evidence led to the hypothesis

Eliminado: exercise

Eliminado: much

Eliminado: and faster

1.3.3. Mutant Huntingtin & Intracellular Dysfunction

The expanded polyglutamine is believed to confer a new function to huntingtin that is toxic to the cell (*toxic gain of function*). Indeed, the mutant protein (in either its soluble or insoluble/aggregate form) has been shown to disrupt several intracellular pathways by abnormally interacting and/or sequestering key components of these multiple pathways into the aggregates (**Figure 1.3**). On the other hand, several lines of evidence also suggest that a *loss of function of wild-type huntingtin* (due to its decreased expression and/or sequestration into the aggregates by interacting with the mutant protein) also contributes to the disruption of intracellular homeostasis, culminating in neuronal dysfunction and death (**Figure 1.3**).

Eliminado: to huntingtin

Eliminado: disturb

The contribution of both the toxic gain of function of mutant huntingtin and the loss of function of wild-type huntingtin for the dysregulation of relevant intracellular pathways that ultimately lead to cell loss in HD is summarized in **Figure 1.3** and through the following sections.

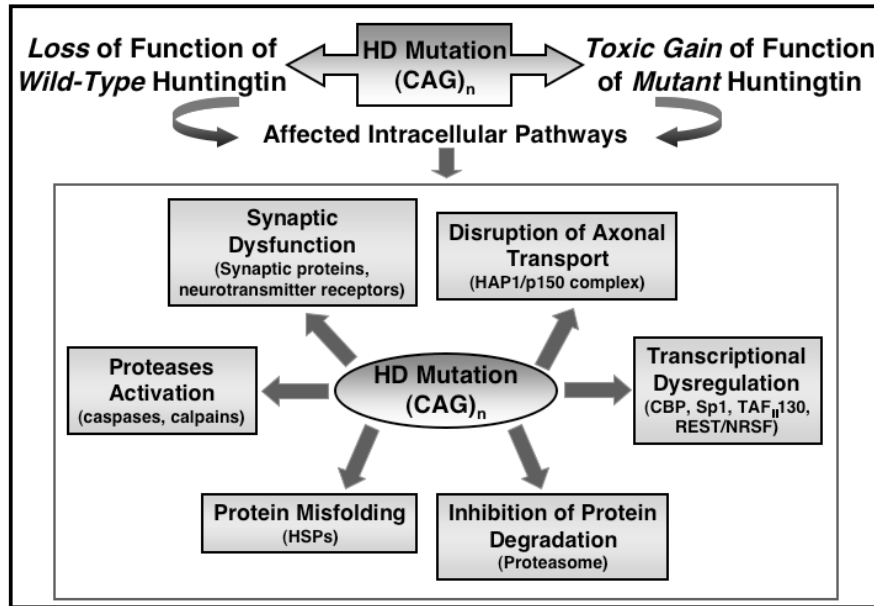


Figure 1.3. – Both the loss of function of wild-type huntingtin and the toxic gain of function of mutant huntingtin contribute to the dysregulation of relevant intracellular pathways. These include: (1) activation of proteases such as calpains and caspases; (2) protein misfolding and inhibition of protein degradation (through the interaction with heat shock proteins and the proteasome); (3) transcriptional dysregulation (via abnormal interaction with numerous transcription factors); (4) disruption of axonal transport; and (5) synaptic dysfunction (by interfering with the expression and/or function of several synaptic proteins and neurotransmitter receptors).

1.3.3.1. Activation of Proteases

Protease cleavage sites for caspase-3 (Goldberg *et al.*, 1996; Kim *et al.*, 2001; Sun *et al.*, 2002) and calpain (Kim *et al.*, 2001; Gafni and Ellerby, 2002; Sun *et al.*, 2002) have been identified within the first 550 amino acids of huntingtin, and proteolysis has been shown to increase in the presence of longer polyglutamine tails (Gafni and Ellerby, 2002; Sun *et al.*, 2002). Caspase-3 and calpain-mediated sequential proteolysis of mutant huntingtin was suggested to produce N-terminal fragments that are more toxic and prone to aggregate (Kim *et al.*, 2001) and that diffuse passively into the nucleus due to its smaller size (Gafni and Ellerby, 2002; Sun *et al.*, 2002). Moreover, these fragments can in turn recruit more proteases into the aggregates, favoring their subsequent

- Eliminado: was
- Eliminado: be
- Eliminado: d
- Eliminado: than full-length huntingtin
- Eliminado: can
- Eliminado: It is suggested that

activation. This creates a positive feedback loop that results in further aggregation and proteolytic cleavage that may ultimately contribute to cell death.

Eliminado: s

Furthermore, the expanded polyglutamine also reduces the binding of huntingtin to HIP1 (*section 1.3.1*), which is then free to associate with HIPPI and induce the activation of caspase-8, an initiator caspase that triggers the apoptotic cascade (Gervais *et al.*, 2002).

Finally, a very recent study has shown that yeast artificial chromosome (YAC) mice (see *section 1.5.2*) expressing a full-length mutant huntingtin construct that is resistant to cleavage by caspase-6, do not develop striatal neurodegeneration (Graham *et al.*, 2006). These results strongly suggest that proteolysis of mutant huntingtin by caspase-6 is an important event in HD.

1.3.3.2. Protein Misfolding and Inhibition of Protein Degradation

Heat shock proteins (HSPs) like HSP40 and HSP70, which are chaperones involved in the refolding of misfolded proteins, are also sequestered into aggregates of mutant huntingtin *in vitro* (Wytenbach *et al.*, 2000). Since the abnormally long polyglutamine tract is likely to result in an overall misfolding of huntingtin, the interaction of HSPs with mutant huntingtin may represent an attempt of the cell to refold the mutant protein. However, by being sequestered into the aggregates, these chaperones will be prevented from exerting their normal protective functions and, over the years, this is likely to lead to an intracellular accumulation of misfolded proteins (for review see Ho *et al.*, 2001).

Furthermore, several components of the proteasome (the major intracellular system for degradation of misfolded and abnormal proteins), such as its regulatory and catalytic subunits and ubiquitin conjugation enzymes, are also sequestered into these aggregates *in vitro* (Wytenbach *et al.*, 2000). Again, the presence of ubiquitin residues in mutant huntingtin aggregates may be the result of an unsuccessful attempt of the cell to tag the mutated protein for degradation by the proteasome. Alternatively, the HD mutation may actually render the protein resistant to proteasomal degradation. Indeed, the mutant protein with its expanded polyglutamine tail may physically block the proteasome, preventing the entrance of further substrates into the proteasome complex. Yet another explanation is that the proteasome degradation system may become overloaded with an increasing number of misfolded and mutated proteins in the cell. As a consequence, the neurons may be progressively depleted of functional proteasomes, which will lead to a progressive accumulation of misfolded and abnormal proteins, further increasing the rate of protein aggregation (for review see Ho *et al.*, 2001; Berke and Paulson, 2003; Ciechanover and Brundin, 2003).

1.3.3.3. *Transcription Dysregulation*

Mutant huntingtin may also establish abnormal protein-protein interactions with several nuclear proteins and transcription factors, recruiting them into the aggregates and inhibiting their transcriptional activity. Examples include tyrimidine-adenine-tyrimidine-adenine (TATA)-binding protein (TBP), CREB [cyclic-adenosine monophosphate (cAMP) response element (CRE) binding protein]-binding protein (CBP), specific protein-1 (Sp1), and the TBP associated factor (TAF_{II}130); all of which interact with mutant huntingtin through the expanded polyglutamine tail. Other nuclear proteins, such as the pro-apoptotic transcription factor p53, also interact with mutant huntingtin via its SH3 sequences, which are distal from the polyglutamine tract (for review see Tobin and Signer, 2000; Sugars and Rubinsztein, 2003; Landles and Bates, 2004).

On the other hand, mutant huntingtin may also lose the ability to bind and interact with other transcription factors regulated by wild-type huntingtin, as is the case of the NRSE-binding transcription factors (*section 1.3.1*). In this particular case, the failure of mutant huntingtin to interact with REST/NRSF in the cytoplasm leads to its nuclear accumulation, where it binds to NRSE sequences and promotes histone deacetylation, leading to the remodeling of the chromatin into a closed structure. As a result, there is a suppression of NRSE-containing genes, including BDNF (Zuccato *et al.*, 2003). This is one case where the loss of the normal huntingtin function can have profound effects, leading to decreased levels of BDNF, an important survival factor for striatal neurons.

1.3.3.4. *Disruption of Axonal Transport*

The formation of neuropil aggregates of mutant huntingtin has led to the hypothesis that axonal transport may be impaired in HD. Indeed, as stated above (*section 1.3.1*), it is believed that normal huntingtin can play a role during axonal transport, perhaps via association with HAP1, promoting both retrograde and anterograde transport. The expanded polyglutamine tract may inhibit this function, compromising the bidirectional transport of different cargoes along the axons, further implicating the loss of wild-type huntingtin function in HD (for review see Gunawardena and Goldstein, 2005). In fact, it was recently shown that mutant huntingtin is responsible for altering the wild-type huntingtin/HAP1/p150 complex (*section 1.3.1*), causing an impaired association between motor proteins and microtubules, and attenuating BDNF transport, which results in loss of neurotrophic support (Gauthier *et al.*, 2004).

Alternatively, aggregates may physically block transport within narrow axonal terminals (for review see Gunawardena and Goldstein, 2005). In fact, dystrophic striatal and corticostriatal neurites in HD brains exhibit several

characteristics of blocked axons, such as accumulation of vesicles and organelles in swollen axonal projections and multiple huntingtin aggregates (DiFiglia *et al.*, 1997a; Sapp *et al.*, 1999). Interestingly, the appearance of striatal axonal inclusions are better correlated with striatal neuronal loss than the formation of NIIs (for review see Gunawardena and Goldstein, 2005).

1.3.3.5. Synaptic Dysfunction

A direct consequence of impaired axonal transport (*section 1.3.3.4*) is disruption of neuronal synaptic transmission. Specifically, this may occur by the depletion of synaptic vesicles and proteins involved in vesicle recycling and receptor endocytosis from the nerve terminals.

Moreover, a number of studies suggest that mutant huntingtin can lead to synaptic dysfunction by altering the availability of various synaptic proteins (for review see Li JY *et al.*, 2003; Smith *et al.*, 2005). Examples include a progressive depletion of complexin II, a protein that regulates the fusion of synaptic vesicles with the presynaptic plasma membrane (Morton and Edwardson, 2001; Morton *et al.*, 2001), a decrease of the SNARE (soluble N-ethylmaleimide-sensitive factor [NSF] attachment protein receptor) protein synaptobrevin-2, and the G protein rabphilin 3A in the HD striatum (Morton *et al.*, 2001). A depletion of PACSIN1/syndapin (a neurospecific phosphoprotein involved in receptor recycling) from synapses, due to its interaction with the mutant huntingtin SH3 domains, has also been demonstrated (Modregger *et al.*, 2002).

These effects may result from a direct abnormal interaction between the mutant protein and some of the synaptic proteins (e.g., PACSIN1), which may lead to their sequestration into huntingtin inclusions. Alternatively, they may represent a consequence of the altered gene transcription (*section 1.3.3.3*), which may cause the down-regulation of some of these synaptic proteins. Moreover, wild-type huntingtin interacts with various vesicle proteins that are important for endocytosis (*section 1.3.1*). These interactions may be impaired in the presence of the mutation thus compromising the synaptic process, which emphasizes the importance of the loss of wild-type huntingtin function (for review see Li JY *et al.*, 2003).

Furthermore, mutant huntingtin can also induce synaptic dysfunction at the postsynaptic level by disrupting the expression and activity of several postsynaptic neurotransmitter receptors (for review see Li JY *et al.*, 2003; Smith *et al.*, 2005). Indeed, by interfering with Sp1-mediated transcription, mutant huntingtin can induce the down-regulation of D1, D2 and D3 dopamine (DA) receptors (Dunah *et al.*, 2002). On the other hand, the expanded polyglutamine

interferes with the ability of huntingtin to bind to PSD95 and regulate the function of NMDA and KA receptors (*section 1.3.1*; Sun *et al.*, 2001). Mutant huntingtin may also interfere with the recycling of membrane receptors through the interaction with several proteins that normally regulate this process (Modregger *et al.*, 2002), further contributing to postsynaptic dysfunction.

1.4. Mechanisms of Degeneration

Over the course of HD, the intracellular dysfunction induced by mutant huntingtin (*section 1.3.3*) progressively leads to the degeneration of important neuronal pathways and cell loss in the striatum, select layers of the cerebral cortex, and other brain regions (*section 1.2.2*).

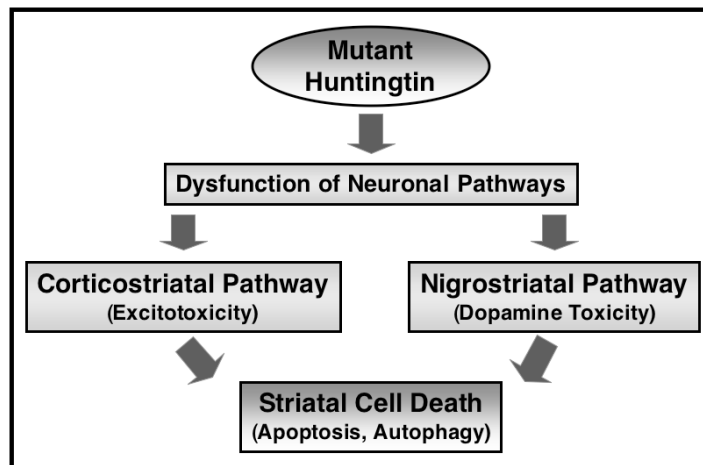


Figure 1.4. – Intracellular dysfunction induced by mutant huntingtin progressively causes the degeneration of relevant neuronal pathways. A dysfunction of corticostriatal and nigrostriatal pathways can have deleterious consequences in the striatum. In particular, excitotoxicity and dysregulation of DA neurotransmission can promote a cascade of events that ultimately contributes to the loss of striatal neurons.

Although not necessarily a direct result of the mutant protein, various mechanisms such as glutamate-induced excitotoxicity, DA-mediated toxicity, metabolic impairment, mitochondrial dysfunction, oxidative stress, apoptosis, and autophagy have been implicated in the pathology of HD. Many of these mechanisms may slowly develop over time, becoming increasingly pronounced

by the late stages of the disease. Moreover, they are not mutually exclusive and are likely to occur in parallel and promote each other, ultimately culminating in neuronal loss (**Figure 1.4**).

1.4.1. Corticostriatal Dysfunction & Excitotoxicity

The striatum receives excitatory glutamatergic inputs from the entire cerebral cortex. Striatal neurons display selective vulnerability with HD and this may be due to the vast glutamatergic inputs they receive and/or the particular types of glutamate receptors expressed in these cells (*section 1.2.2*). Indeed, striatal interneurons, which are less affected in HD, have fewer excitatory inputs than striatal projection neurons. Moreover, most medium spiny GABAergic projection neurons express high levels of the NMDA receptor NR2B subunit (*section 1.2.2*), which increases the receptor channel permeability and determines its sensitivity to glycine, the Mg^{2+} -blockage, and the channel deactivation time. Correspondingly, the spared interneurons express much lower levels of this subunit, which probably confers them a higher threshold for activation (for review see Sieradzan and Mann, 2001). Furthermore, the metabotropic glutamate receptor type 5 (mGluR5) is greatly expressed in the postsynaptic membranes of striatal projection neurons. The activation of these facilitatory receptors enhances the responses of NMDA receptors to glutamate activation, contributing to excitotoxicity (for review see Vonsattel and DiFiglia, 1998).

Therefore, dysfunctional cortical glutamatergic neurons may cause a sustained glutamate stimulation of the vulnerable striatal neuronal populations. Under conditions of chronic excitotoxicity, the intracellular Ca^{2+} concentration increases and can have deleterious consequences including mitochondrial dysfunction, activation of the Ca^{2+} -dependent neuronal isoform of nitric oxide synthase (nNOS), generation of nitric oxide (NO^{\bullet}) and other reactive oxygen species (ROS), and activation of Ca^{2+} -dependent proteases such as calpains. Importantly, mutant huntingtin can also sensitize the inositol (1,4,5)-triphosphate receptor type 1 (InsP3R1) located in the membrane of the ER, promoting a further increase in intracellular Ca^{2+} (Tang *et al.*, 2003). Collectively, these events can contribute to the progressive neurodegeneration observed in the HD striatum.

In further support of the excitotoxic hypothesis of HD neurodegeneration, intra-striatal injections of the NMDA agonist quinolinic acid (QA) induce a selective neuronal loss both in rats (Beal *et al.*, 1986, 1991) and in primates (Ferrante *et al.*, 1993) that resembles human HD.

1.4.2. Nigrostriatal Dysfunction & Dopamine Toxicity

The striatum also receives dopaminergic input from the substantia nigra, which implicates this pathway in the selective striatal degeneration observed with HD (for review see Petersén and Brundin, 2002). In support, several studies have shown degeneration of nigrostriatal projections (Ferrante and Kowall, 1987; Ginovart *et al.*, 1997; Bohnen *et al.*, 2000; Suzuki *et al.*, 2001) and atrophy of dopaminergic neurons in the substantia nigra in HD brains (Oyanagi *et al.*, 1989; Yohrling *et al.*, 2003). Aggregates of mutant huntingtin were also found in this brain region (Gutekunst *et al.*, 1999). Furthermore, a marked loss of tyrosine hydroxylase (TH; the rate-limiting enzyme for DA biosynthesis) (Yohrling *et al.*, 2003) and down-regulation of the DA transporter (DAT) and the DA D1 and D2 receptors occur in HD brains (Augood *et al.*, 1997; Ginovart *et al.*, 1997), probably due to altered gene transcription induced by mutant huntingtin (*section 1.3.3.5*). Overall, these results suggest that both a presynaptic and a postsynaptic impairment may contribute to a dysfunctional nigrostriatal pathway.

The nigrostriatal dysfunction may be involved in causing the motor and cognitive deficits observed with HD. In support, loss of both pre- and postsynaptic markers of DA neurotransmission is positively correlated with cognitive performance in asymptomatic and symptomatic HD patients (for review see Bäckman and Farde, 2001). Furthermore, as mentioned above (*section 1.2.1*), late stages of the disease are normally characterized by bradykinesia and rigidity, symptoms that may be directly caused by the progressive loss of DA receptors in the striatum.

Importantly, DA itself can be a source of ROS and a trigger of oxidative stress. Under normal conditions, the enzyme monoamino oxidase converts DA into 3,4-dihydrophenylacetic acid (DOPAC) and hydrogen peroxide (H₂O₂). However, DA can also undergo a nonenzymatic process of auto-oxidation producing DA quinones and H₂O₂, and a DA semiquinone and superoxide (O₂^{•-}). H₂O₂ and O₂^{•-} can be further oxidized in the presence of transition metal ions, producing the extremely reactive hydroxyl radical (HO[•]) (for review see Sulzer and Zecca, 2000).

1.4.3. Metabolic Dysfunction & Oxidative Stress

Studies in HD patients and HD postmortem tissue have shown: (1) a significant reduction in aconitase activity in the caudate, putamen and cerebral cortex (Tabrizi *et al.*, 1999); (2) a significant decrease in the activities of mitochondrial complexes II-III and IV in the caudate and putamen (Gu *et al.*, 1996; Browne *et al.*, 1997) and of mitochondrial complex I in the muscle

(Arenas *et al.*, 1998). Contradictory results have also been published regarding the activity of mitochondrial complex I in HD platelets, with an initial study showing a striking reduction of the activity of this complex (Parker *et al.*, 1990), and a subsequent study reporting no deficiencies in platelet mitochondrial function (Gu *et al.*, 1996); (3) increased lactate concentrations in the cerebral cortex (Jenkins *et al.*, 1993); (4) an increase in the lactate/pyruvate ratio in the cerebrospinal fluid (CSF) (Koroshetz *et al.*, 1997); (5) a reduced phosphocreatine/inorganic phosphate ratio in skeletal muscle (Lodi *et al.*, 2000); and (6) a decreased resting membrane potential as well as a reduced threshold for Ca^{2+} -induced depolarization in mitochondria from HD lymphoblasts (Panov *et al.*, 2002).

Taken together, these reports implicate mitochondrial dysfunction and metabolic impairment in HD pathology (for review see Sawa, 2001). Whether these energy deficits occur early on during the disease progress is still uncertain (for review see Davies and Ramsden, 2001; Petersén and Brundin, 2002). Nevertheless, systemic administration of the toxin 3-nitropropionic acid (3-NP; an irreversible inhibitor of mitochondrial complex II) causes striatal neurodegeneration in rats and primates. Intra-striatal injection of this toxin or malonate (a reversible mitochondrial complex II inhibitor) also leads to striatal neuronal loss (for review see Brouillet *et al.*, 1999), further implicating mitochondrial dysfunction in HD.

Importantly, mitochondrial dysfunction is also the major contributor to oxidative stress that along with the excitotoxic activation of nNOS (*section 1.4.1*) and the metabolism of DA (*section 1.4.2*), can lead to a toxic increase in the levels of ROS. Susceptible neurons, as in the case of HD, may not be able to handle increased ROS production. High ROS levels may promote intracellular cascades of oxidative stress by oxidizing proteins and DNA, and triggering lipid peroxidation. Therefore, it is reasonable to speculate that oxidative stress might play a crucial role in the neurodegenerative process of HD. However, no alterations in the levels of lipid peroxides and no signs of major oxidative damage to DNA and proteins have been detected in the caudate nucleus, putamen, and frontal cortex of HD patients (Alam *et al.*, 2000), casting doubt upon the oxidative stress hypothesis.

1.4.4. Cell Death – Apoptosis & Autophagy

As stated above, mutant huntingtin is a substrate for several caspases and calpains, which are believed to mediate the formation of the toxic N-terminal fragments. Moreover, sequestration of pro-caspases into the aggregates is thought to promote their activation, thus promoting an intracellular cascade of

proteolytic events (*section 1.3.3.1*). Furthermore, calpain (Gafni and Ellerby, 2002), caspases 1 (Ona *et al.*, 1999), and caspase-8 (Sanchez *et al.*, 1999) activity is increased in HD brains. These findings have led to the hypothesis that an apoptotic mechanism is responsible for HD neuronal loss. Indeed, early studies had identified apoptotic-like cells in the HD striatum with terminal deoxynucleotidyl transferase (TdT)-mediated dUTP nick-end labeling (TUNEL) (Dragunow *et al.*, 1995; Portera-Cailliau *et al.*, 1995; Thomas *et al.*, 1995; Butterworth *et al.*, 1998). However, no DNA laddering was observed after DNA electrophoresis, suggesting that the characteristic DNA fragmentation pattern of apoptosis does not occur (Dragunow *et al.*, 1995; Portera-Cailliau *et al.*, 1995). Furthermore, the detection of activated astrocytes in HD brains suggests inflammation (Hedreen and Folstein, 1995), which is generally absent in apoptotic conditions. Therefore, the evidence for a pure apoptotic process contributing to HD cell death is not convincing. Nevertheless, the activation of certain apoptotic pathways is likely to contribute to some degree to HD pathology (for review see Hickey and Chesselet, 2003a).

Some evidence suggest that autophagy, a process by which lysosomes degrade cytoplasmic proteins and organelles, may mediate cell loss in HD. In support, HD brains display endosomal/lysosomal organelles, multivesicular bodies, and lipofuscin accumulation reminiscent of autophagy (for review see Petersén and Brundin, 2002). Furthermore, a positive correlation has been found between the number of autophagic vacuoles and the length of the polyglutamine expansion in HD lymphoblasts (Nagata *et al.*, 2004). Moreover, several studies have also shown that expression of mutant huntingtin induces endosomal/lysosomal activity (Kegel *et al.*, 2000) and sequestration of the mammalian target of rapamycin (mTOR, a protein kinase involved in the regulation of autophagy) into the aggregates of mutant huntingtin with subsequent inhibition of its kinase activity (Ravikumar *et al.*, 2004). These events lead to autophagy, which in turn may promote huntingtin degradation and the clearance of aggregates (Ravikumar *et al.*, 2002, 2004; Quin *et al.*, 2003).

This process may represent an initial attempt of the HD cell to eliminate the mutant protein that over the course of the disease becomes overloaded, insufficient and dysfunctional, eventually resulting in cell degradation. Indeed, the lysosomal proteases cathepsins D, B and L were recently shown to promote the generation and accumulation of mutant huntingtin fragments (Kim *et al.*, 2006). Furthermore, sequestration of Beclin 1 (a protein essential for autophagy) into NIIs might reduce the autophagic clearance of mutant huntingtin (Shibata *et al.*, 2006).

1.5. Rodent Models of Huntington's Disease

Our understanding of HD pathogenesis, as well as the ability to develop novel therapies, depend on the availability of suitable models of the disease. Although *in vitro* cellular models are important for providing valuable insights into the molecular mechanisms of the disease, they cannot replace the need for *in vivo* models.

Table II – Characteristics of the most used HD animal models.

Transgenic Model	Promotor	CAG Repeats	Expression Level	Background Strain	Age of Death	Abnormal Behavior	Neuropathology
Knock-in Mice							
Hdh 94	<i>Hdh</i>	94	100%	129Sv x C57BL/6J	Normal life span	Hyperkinesia followed by hypokinesia	NIIs; cell dysfunction; no cell loss or gliosis
HdH 150	<i>Hdh</i>	150	n.d.	129/Ola x C57BL/6J	> 12 months	Motor deficits	NIIs; no cell loss; gliosis
YAC Transgenic Mice							
YAC 72	<i>IT15</i>	72	30-50%	FVB/N	> 12 months	Hyperkinesia followed by hypokinesia	Selective striatal cell death; no NIIs
YAC 128	<i>IT15</i>	128	75%	FVB/N	< 12 months (males)	Hyperkinesia followed by hypokinesia; cognitive deficits	NIIs; Selective striatal and cortical cell death and atrophy
Truncated Transgenic Mice							
R6/1	<i>IT15</i>	Approx. 115	31%	CBA x C57BL/6J	32-40 weeks	Behavioral and motor deficits	NIIs; limited cell loss; brain atrophy; cell dysfunction
R6/2	<i>IT15</i>	Approx. 145	75%	CBA x C57BL/6J	10-16 weeks	Rapid deterioration of cognitive and motor functions	NIIs; limited cell loss; brain atrophy; cell dysfunction
N171-82Q	<i>Mouse prion protein</i>	82	10-20%	C3H/HEJ x C57BL/6J	24-30 weeks	Motor deficits	NIIs; striatal neuronal degeneration
HD94-Tet Regulated	<i>CMV</i> ; Tetracycline-responsive operator	94	n.d.	CBA x C57BL/6J	Early death	Motor deficits reversed by transgene inhibition	NIIs and striatal atrophy reversed by transgene inhibition
Transgenic Rats							
HD Tg Rat	<i>Hdh</i>	51	22%	Sprague Dawley	24 months	Cognitive deficits and progressive motor dysfunction	NIIs; specific striatal cell loss and atrophy; cell dysfunction

(Adapted from Menalled and Chesselet, 2002; Hickey and Chesselet, 2003b).
n.d., not determined.

In vivo non-mammalian HD models, such as those generated in *Drosophila melanogaster*, have proven to be valuable in studying important intracellular pathways involved in the disease process (e.g., aggregation, transcriptional regulation, proteasome-mediated protein degradation, etc.). These models are also useful for rapidly screening potential beneficial pharmacologic compounds (e.g., inhibitors of aggregation, and drugs that target cellular stress responses) (for review see Marsh *et al.*, 2003). However, modeling HD in rodent models is useful for understanding the relation between neuronal dysfunction and/or death and the development of abnormal behaviours. Moreover, rodent models also provide excellent tools to further test the efficiency of new therapies and compounds, including those originally screened with the simpler *Drosophila* models (for review see Beal and Ferrante, 2004; Hersch and Ferrante, 2004; Li JY *et al.*, 2005).

There are several rodent models available for the study of HD. These models primarily differ in the size of the expressed huntingtin fragment, the number of CAG repeats, the promoter driving the transgene and consequently the expression of the mutant protein, the background strain, etc. As a consequence, each model exhibits unique phenotypes (for review see Menalled and Chesselet, 2002; Hickey and Chesselet, 2003b). A summary of the most common used HD rodent models is presented in **Table II**.

1.5.1. Knock-in Mice

Knock-in mice were engineered by inserting elongated polyglutamine tracts into the mouse *Hdh* gene. Thus, the mutated gene is expressed under its natural promoter, in the appropriate genomic context of the *Hdh* gene, and the offspring are both heterozygous and homozygous for the mutation (for review see Menalled and Chesselet, 2002; Hickey and Chesselet, 2003b). In theory, these mice represent the most faithful reproduction of the human genetic condition, though no major behavioral deficits were observed in the initial reports (Shelbourne *et al.*, 1999). Follow-up studies have subsequently shown that homozygous knock-in mice develop behavioral abnormalities at a very early stage, prior to any neuropathological change. Their abnormal behavior is characterized by a biphasic activity pattern (an initial marked increase in rearing followed by a period of hypoactivity) that resembles the progression of motor symptoms in HD patients (for review see Hickey and Chesselet, 2003b; Levine *et al.*, 2004).

Importantly, microaggregates of the mutant protein can be detected in the brains of four different HD knock-in models at an early disease stage (2-6 months of age). However, NIIs are only present at later stages (10-18 months).

Furthermore, the degree of neuropathology is positively correlated with the number of CAG repeats. Mice carrying 94 CAG repeats (Hdh94) show aggregates and NIIs exclusively in the striatum; whereas, mice with 150 CAG repeats (Hdh150) show a more widespread distribution of aggregates throughout the brain. Interestingly, in most knock-in models, cell loss and gliosis are generally absent (for review see Menalled and Chesselet, 2002; Hickey and Chesselet, 2003b; Levine *et al.*, 2004).

Overall, the phenotype of HD knock-in mice supports the idea that neuronal dysfunction precedes cell death in HD, and might be the primary cause of the early functional abnormalities.

1.5.2. Transgenic Mice – Full-Length Models

Various transgenic mouse models have been generated using the full-length human *IT15* gene with different CAG lengths as the transgene.

Transgenic mice expressing the full-length *IT15* gene with either 48 or 89 CAG repeats under the control of the cytomegalovirus (*CMV*) promoter develop progressive motor impairments, which are accompanied by striatal neuronal loss as determined with TUNEL staining. However, NIIs are nearly absent in these transgenic mice (Reddy *et al.*, 1998).

YAC mice expressing the full-length *IT15* gene with 72 (Hodgson *et al.*, 1999) or 128 (Slow *et al.*, 2003) CAG repeats display a selective degeneration of striatal medium spiny neurons. Moreover, small nuclear aggregates of the mutant protein can be observed in YAC brains. Behaviourally, YAC mice also exhibit biphasic motor impairments with an initial period of hyperactivity followed by a hypoactive phase. (Hodgson *et al.*, 1999; Slow *et al.*, 2003).

The YAC128 mice have been well characterized and a positive correlation between the onset of motor deficits and the extent of striatal cell loss had been documented (Slow *et al.*, 2003). At 12 months of age, these mice show a significant atrophy of the striatum, globus pallidus and cortex with relative sparing of the hippocampus and cerebellum. Similarly, neuronal loss at this age is present in the striatum and cortex, the two brain regions most affected in HD patients, but not in the hippocampus. Moreover, nuclear accumulation of mutant huntingtin can be observed in the striatum as early as 2 months of age, coinciding with the onset of behavioral symptoms (Van Raamsdonk *et al.*, 2005a). Recent studies have also indicated that YAC128 transgenic HD mice develop mild cognitive deficits, which precede the onset of motor abnormalities and progressively deteriorate with age (Van Raamsdonk *et al.*, 2005b).

1.5.3. Transgenic Mice – Truncated Models

To address the question of CAG repeat stability in the mouse genome, Mangiarini and colleagues (1996) created transgenic mice with truncated fragments of the *IT15* gene. They were surprised to find that these fragments were sufficient to generate a neurological phenotype similar to the human condition. These transgenic HD mouse models were referred to as the R6 lines (Mangiarini *et al.*, 1996) and are represented in the majority of the studies in this thesis. As such, a thorough and extensive description of these models is presented in *section 1.6*.

Other truncated transgenic mouse models exist that express a cDNA encoding an N-terminal fragment of huntingtin with 171 amino acids bearing either 18 (N171-18Q), 44 (N171-44Q), or 82 (N171-82Q) glutamine residues (Schilling *et al.*, 1999). N171-82Q mice express relatively low steady-state levels of the transgene and show loss of body weight, behavioural abnormalities (loss of coordination, tremors, hypokinesia and abnormal gait), accumulate NIIs and neuritic aggregates of mutant huntingtin, and die prematurely (Schilling *et al.*, 1999).

Another valuable transgenic mouse model is the conditional model generated by Yamamoto and colleagues (Yamamoto *et al.*, 2000). This HD mouse was engineered such that the expression of mutant huntingtin fragments is controlled by the tetracycline responsive system, allowing the gene to be turned off by oral administration of tetracycline derivatives. When the transgene expression was activated from birth (i.e., in the absence of any treatment), the mice progressively developed motor dysfunctions, neuronal inclusions both in the striatum and cortex, loss of striatal volume, and astrocytosis. Surprisingly, inhibition of transgene expression in symptomatic mice by antibiotic treatment ameliorated the behavioral deficits and abolished the inclusions (Yamamoto *et al.*, 2000). These exciting findings suggest that the impact of the mutant protein can be arrested and even reversed, which can have tremendous implications for the development of therapies for HD.

1.5.4. Transgenic Rats

Recently, von Hörsten and collaborators developed the first transgenic rat model of not just HD but of any neurodegenerative disorder (von Hörsten *et al.*, 2003). This transgenic rat model expresses a 1962 bp *IT15* cDNA fragment carrying 51 CAG repeats under the control of the endogenous rat *Hdh* promoter. These HD rats develop an adult-onset neurological phenotype characterized by reduced anxiety, cognitive impairment, and a progressive motor dysfunction. At the neuropathological level, the brains of these rats exhibit NIIs, striatal

shrinkage, and neuronal loss (von Hörsten *et al.*, 2003; Kantor *et al.*, 2006). Reduced brain glucose metabolism was also detected by high-resolution positron emission tomography (PET). In the late stage of the disease, the rats suffer from a rapid loss of body weight associated with a severe muscular atrophy, which invariably leads to death at around 24 months (von Hörsten *et al.*, 2003). Both hetero- and homozygous animals also show decreases of the densities of several neurotransmitter receptors, including cholinergic muscarinic 1, 5-hydroxytryptamine (5-HT), A2A adenosine, D1 and D2 DA, and GABA(A) receptors (Bauer *et al.*, 2005).

These transgenic rats may represent an accurate model of HD since they: **(1)** express a HD allele that is associated with the development of adult-onset HD (von Hörsten *et al.*, 2003); **(2)** develop a striatum-restricted pathology (von Hörsten *et al.*, 2003; Kantor *et al.*, 2006); and **(3)** present a slow disease progression with deterioration of their motor performance and development of chorea-like symptoms (Cao *et al.*, 2006). These HD transgenic rats are further characterized in *Chapter 2* of this thesis.

1.6. The R6 Transgenic Huntington's Disease Mice

Undoubtedly, the HD models that have been most extensively studied are the R6 transgenic mouse lines produced in 1996 by Gillian Bates and colleagues (**Figure 1.5**; Mangiarini *et al.*, 1996). Currently there are about 270 publications describing the phenotype or the testing of novel treatments in these transgenic mice models.

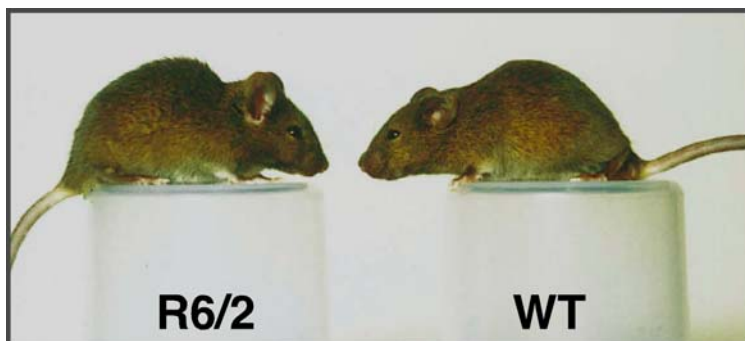


Figure 1.5. – A transgenic R6/2 mouse and a wild-type littermate control. Note that at 12 weeks of age, the R6/2 mouse is significantly smaller than its wild-type littermate control. Adapted from Mangiarini *et al.*, 1996.

1.6.1. Characterization of R6 Mice

1.6.1.1. Generation

The R6 transgenic mice were generated by microinjection of a segment of the 5'-end of the *IT15* gene, obtained from a single HD patient, into a single CBAXC57BL/J6 mouse embryo (Mangiarini *et al.*, 1996). The transgene contained around 1 kb of the 5'-untranslated region, the exon 1 with around 130 CAG repeats, and the first 262 bp of intron 1. Five lines with different CAG repeat lengths were originally generated: R6/0 (142 CAG repeats, showing no expression of the transgene), R6/1 (116 CAG repeats), R6/2 (144 CAG repeats), R6/5 (128-156 CAG repeats) and the control line HDex 6 (18 CAG repeats). The R6/1 and R6/2 lines have been the most commonly studied. Exon 1 of the *IT15* gene constitutes around 3% of the entire gene and is expressed under the human *IT15* promoter in most tissues. Expression levels of the transgene are approximately 31% and 75% of the endogenous huntingtin level in the R6/1 and R6/2 models, respectively (**Table II**). Intergenerational instability has been found in the R6 lines, which is associated with paternal transmission (Mangiarini *et al.*, 1997). No repeat instability was found in the R6/0 line, indicating that this effect is related to transcription (Mangiarini *et al.*, 1997). Most R6/1 and R6/2 females are infertile (Mangiarini *et al.*, 1996; Papalexi *et al.*, 2005), and males are used to breed the colonies. R6/2 males are ideally bred to first generation hybrids of CBAXC57BL/J6, a strategy that stabilizes the contribution of the two strain backgrounds across generations. This minimizes the risk of introducing new modifier genes that may differ between strains (Hockly *et al.*, 2003; for review see Menalled and Chesselet, 2002).

1.6.1.2. Neuropathology

In R6/2 mice there is reduced neuronal loss in the striatum. To date, only one study reporting a 25% decrease in the total number of striatal cells in 12-week-old transgenic mice (Stack *et al.*, 2005) has been published. On the other hand, “dark cell degeneration” has been described in a small number of neurons in 12 (Stack *et al.*, 2005) and 14-week-old mice (i.e., at a very late stage in the development of the disease) (Iannicola *et al.*, 2000; Turmaine *et al.*, 2000; Yu *et al.*, 2003). This “dark cell degeneration”, detected by toluidine blue- or osmium-stained tissue by electron microscopy, is characterized by condensation but no fragmentation of both the cytoplasm and nucleus with ultrastructural preservation of intracellular organelles. Cells with these features are found in the anterior cingulate cortex, the dorsal striatum, the hippocampus, and in the Purkinje cell layer of the cerebellum of R6/2 mice. Similar features have been

described in HD patients. The mechanism of cell death is thought to be neither classically apoptotic nor necrotic, and autophagy may be involved (Iannicola *et al.*, 2000; Turmaine *et al.*, 2000). Necrotic cell death markers are not evident and no substantial increase in striatal glial fibrillary acidic protein (GFAP)-positive cells has been found in R6/1 or R6/2 mice (Hansson *et al.*, 1999; Yu *et al.*, 2003). Nevertheless, a more pronounced age-related decline in the number of microglia in the R6/2 brains has been detected (Ma *et al.*, 2003).

Other HD neuropathological features are evident in R6 mice, such as the nuclear accumulation of truncated mutant huntingtin in ubiquitinated aggregates. The appearance of NIIs is an early event that can be detected in the striatum, cortex, and hippocampus of R6/2 mice as early as postnatal day 1 (Stack *et al.*, 2005). Between 3.5 to 4.5 weeks of age, NIIs are clearly evident in select neuronal populations in the CA1 region of the hippocampus, the periventricular nucleus of the hypothalamus (Morton *et al.*, 2000), all layers of the cerebral cortex, and in 50% of the striatal neurons (Davies *et al.*, 1997; Meade *et al.*, 2002). By 3.5 weeks these NIIs are already ubiquitin-positive (Meade *et al.*, 2002). Between 3 and 9 weeks of age, the number of neurons with inclusions and the inclusion size increase in all brain regions, and by 10 weeks of age, more than 80% of all neurons in the brain contain NIIs (Morton *et al.*, 2000; Meade *et al.*, 2002). The nuclear changes progress over time, and by 10 to 12 weeks invaginations of the nuclear membrane and an increase in the nuclear pore density occurs. It is important to note that NIIs are neuronal specific, since they have never been observed in glial cells (Davies *et al.*, 1997).

Not all neuronal populations acquire the same proportions of NIIs. In the striatum, the frequency of NIIs is lower in choline acetyltransferase-, nNOS- or calretinin-containing interneurons (around 10-20%) than in calbindin-positive projection neurons and parvalbumin-positive interneurons (around 90%) (Kosinski *et al.*, 1999; Meade *et al.*, 2002). In the cortex, essentially all pyramidal neurons of layers II-III and V-VI and all granule cells of layer IV develop NIIs by 9 weeks. However, some populations of cortical neurons (e.g., somatostatinergic and calbindinergic interneurons) develop NIIs more slowly and to a lesser extent (Meade *et al.*, 2002). Neurons in the DG show NIIs significantly later than neurons in the CA1 and CA3 regions (Morton *et al.*, 2000; Hansson *et al.*, 2001b). Only around 30% of the dopaminergic neurons in the substantia nigra contain NIIs (Petersén *et al.*, 2002b).

Aggregates of truncated mutant huntingtin have also been detected in neuronal processes (dendrites and axons) in R6 mice (Li H *et al.*, 1999). These neuropil aggregates are smaller than NIIs, do not appear to contain ubiquitin, and co-localize with synaptic vesicles. Their formation highly correlates with the development of neurological symptoms in R6 mice (Li H *et al.*, 1999), further

implicating an impaired axonal transport (*section 1.3.3.4*) and synaptic transmission (*section 1.3.3.5*) in HD neuropathology.

Although there is no extensive neuronal loss in R6/2 mice, their brains weights decrease about 20% by the age of 12 weeks (Davies *et al.*, 1997). The total striatal volume is reduced by 17% in 18-week-old R6/1 mice, with no corresponding cell loss, reactive astrocytosis or TUNEL-positive apoptotic neurons in the striatum (Hansson *et al.*, 1999). Interestingly, the nigrostriatal (Petersén *et al.*, 2002b) and corticostriatal (Puschban *et al.*, unpublished observations) connections appear to be anatomically preserved. However, dopaminergic neurons of the substantia nigra of R6/1 mice show a 15% reduction in cross sectional area at the age of 16 weeks (Petersén *et al.*, 2002b). In addition, the medium-sized striatal projection neurons display around 20% loss of soma area, as well as a decrease in their dendritic arborization and spine density (Klapstein *et al.*, 2001), indicating that cell atrophy is responsible for the decreased brain weight observed in these mice.

1.6.1.3. Behavior

At birth, R6 mice are indistinguishable from their wild-type littermates. The first motor symptoms appear at 4 weeks of age in both R6/2 (Luesse *et al.*, 2001) and R6/1 (Bolivar *et al.*, 2004) lines, which are manifested as hyperactivity in the open field test. At 3.5 weeks of age R6/2 mice demonstrate a visual-spatial learning impairment and a memory deficit in the Morris water maze test that progress up to 7 weeks of age (Lione *et al.*, 1999; Murphy *et al.*, 2000), although cognition is difficult to properly assess when motor dysfunction is apparent and progressively deteriorates with age (Luesse *et al.*, 2001). By 6 to 8 weeks of age R6 mice become hypoactive as assessed with the open field test (Carter *et al.*, 1999; Luesse *et al.*, 2001; Bolivar *et al.*, 2003, 2004). This hypoactivity is associated with a decline in motor coordination, as assessed by performance on a rotarod, and is detected by 5 to 6 weeks of age in R6/2 (Hockly *et al.*, 2003) and at 8 weeks in R6/1 mice (Hansson *et al.*, 2001b). The decline in rotarod performance in R6/1 mice is clearly correlated to an increased numbers of striatal neurons exhibiting NIIs (Hansson *et al.*, 2001b). By 8 weeks of age, the R6/2 mice begin to exhibit other behavioral abnormalities, such as stereotypical hindlimb grooming, tremor, paw claspings when suspended by the tail (**Figure 1.6**), dyskinesia and irregular gait. Handling or noise-induced convulsions may also appear at this time (Mangiarini *et al.*, 1996; Gil *et al.*, unpublished observations). Moreover, deterioration of the sleep-wake cycle and of the circadian rhythms of R6/2 mice is apparent at around 14 weeks of age (Morton *et al.*, 2005).



Figure 1.6. – A 12-week-old R6/2 mouse adopting the feet-clasping posture. When suspended by the tail, a symptomatic R6/2 mouse will press both its front and hind limbs against the stomach. A normal mouse will hold its hind limbs outward in order to steady itself. Adapted from Mangiarini *et al.*, 1996.

Depending on the colony, death occurs at around 13 to 16 weeks of age in R6/2 mice (Carter *et al.*, 1999), with the actual cause of premature death unknown. Undoubtedly, from a pathophysiological point of view and because the survival of R6/2 mice is often used as an outcome parameter when testing novel treatments, it would be extremely valuable to identify factors that are responsible for death. In some cases, it is clear that R6/2 mice succumb during a generalized convulsion (Mangiarini *et al.*, 1996; Gil *et al.*, unpublished observations). Interestingly, there is a marked difference in the R6/2 line lifespan (from 12 to 17 weeks of age) depending on the location of the colony. These differences are likely due to different procedures regarding breeding and animal welfare conditions. For example, variations in the number of mice per cage, enriched versus impoverished environment, accessibility to food and water at a symptomatic stage and background noise level (prone to elicit epileptic seizures) (Gil *et al.*, unpublished observations) may play a role in the survival of the mice (for a detailed discussion see Hockly *et al.*, 2003).

1.6.1.4. Pathology outside the Central Nervous System

Notably, huntingtin inclusions are found in islets of Langerhans, fibers of skeletal and cardiac muscle, in the medulla and reticular layer of the adrenal glands cortex, in kidney tubular/interstitial/glomerular cells, neuronal ganglion cells of the myenteric plexus of the stomach wall, and in the Meissners plexus of

the duodenum of 6-week-old R6/2 mice (Sathasivam *et al.*, 1999). The mice also display NIIs in the retina that result in severe vision deficiencies by the age of 10 weeks in R6/2 and at 32 weeks in R6/1 mice (Helmlinger *et al.*, 2002). These tissues show a variety of other pathological changes but, similar to what happens in the central nervous system (CNS), it is not clear whether the inclusions are the cause, a consequence, or simply an epiphenomenon of these abnormal alterations (Sathasivam *et al.*, 1999).

Many of these tissues that exhibit mutant huntingtin inclusions also display a generalized atrophy. Thus, the liver, heart and kidney begin to atrophy in R6/2 mice at 6 to 8 weeks of age and shrink to around 50% of normal sizes in late stages.

At 4 weeks of age, testis size is decreased. This atrophy is gradual and continues throughout the life span of the mice (Sathasivam *et al.*, 1999; Papalexi *et al.*, 2005). The testicular atrophy is probably related to the sterility observed in 50% of all R6/2 males and with the complete loss of fertility of all R6/2 males at 8 weeks of age. This phenomenon may be caused by the reduction in gonadotrophin releasing hormone (GnRH)-expressing neurons in the hypothalamus of R6/2 mice and the consequent impairment of gonadotropic hormones (Papalexi *et al.*, 2005).

All skeletal muscle tissue begins to atrophy in R6/2 mice at 6 weeks of age (Sathasivam *et al.*, 1999). Furthermore, age-dependent denervation-like abnormalities occur, and morphological alterations of neuromuscular junctions are observed in R6/2 skeletal muscles (Ribchester *et al.*, 2004). Interestingly, these skeletal muscle abnormalities are accompanied by a progressive loss of the regenerative capacity of motor neurons in R6/2 mice (Ribchester *et al.*, 2004). Moreover, dysregulation of gene expression is also detected in the R6/2 skeletal muscle, with an increased expression of ubiquitin-conjugating enzymes and DNA repair enzymes, which may be involved in a stress response to the toxic polyglutamines (Luthi-Carter *et al.*, 2002).

The weight loss typically seen in HD patients is reproduced in the R6 mice. The R6/2 mice begin to lose body weight at around 9 to 10 weeks of age (Hockly *et al.*, 2003). Despite an increased accumulation of body fat and increased levels of leptin, a regulator of the fat metabolism (Fain *et al.*, 2001), these mice still lose weight (**Figure 1.5**).

Diabetes has been reported in some colonies of R6/2 mice (Hurlbert *et al.*, 1999; Luesse *et al.*, 2001). However, no differences in survival, weight loss, motor coordination or activity occur between R6/2 mice with manifest or latent diabetes (Luesse *et al.*, 2001). R6/2 mice of 12 weeks of age have dramatic reductions of glucagon in α -cells and of insulin in β -cells in the pancreas (Hurlbert *et al.*, 1999). The accumulation of intranuclear inclusions in pancreatic

R6/2 islets correlates with impaired expression of transcriptional regulatory proteins essential for insulin gene expression and progressive reductions in insulin mRNA levels (Andreassen *et al.*, 2002). Recently it has been shown that β -cell mass fails to increase normally with age in these mice (Björkqvist *et al.*, 2005). Although no abnormal cell death has been detected, cell replication is dramatically decreased in R6/2 islets. Also, despite an unaltered electrical activity, exocytosis is virtually abolished in β -cells, which may be due to a massive reduction in the number of insulin containing secretory vesicles (Björkqvist *et al.*, 2005).

Interestingly, many of these peripheral alterations, such as muscular atrophy, abdominal fat accumulation, insulin resistance, and reduced bone mineral density, are reminiscent of Cushing disease symptoms, which are caused by progressive alterations in the hypothalamic-pituitary-adrenal axis that lead to increased glucocorticoid levels (Björkqvist *et al.*, 2006a). Indeed, we recently discovered that R6/2 mice show a hypertrophy of the adrenal cortex and a progressive increase in serum and urine corticosterone levels. In addition, the intermediate pituitary lobe was markedly enlarged and circulating adrenocorticotrophic hormone (ACTH) was increased. Moreover, R6/2 mice demonstrate a 50% reduction in the expression of pituitary DA D2 receptors. Since DA transmission inhibits ACTH expression, this reduction in pituitary DA receptors may explain the observed increase in ACTH levels, and consequently, the increased production of glucocorticoids (Björkqvist *et al.*, 2006a).

To conclude, many non-CNS tissues are indeed affected in R6 mice and in certain cases dysfunction seems to occur independently of the presence of huntingtin inclusions.

1.6.2. Dysfunction in R6 Mice

1.6.2.1. Transcriptional Dysregulation

Several changes in gene expression in the brains of R6/2 mice have been reported (Luthi-Carter *et al.*, 2000, 2002, 2003; Zucker *et al.*, 2005). In the R6/2 striatum, 70 mRNAs out of 600 were differentially expressed at 6 weeks of age. The major alterations included a down-regulation of striatal genes involved in cAMP and retinoid signaling pathways, and up-regulation of genes indicative of stress and inflammation, including DNA repair enzymes (Luthi-Carter *et al.*, 2000). Similar alterations in gene expression have also been detected in the cerebral cortex, the cerebellum, and in muscle tissue, suggesting a lack of regional selectivity for this transcriptional dysregulation (Luthi-Carter *et al.*, 2002).

In an attempt to further characterize the striatal transcriptional dysregulation observed in the R6/2 striatum, a recent study demonstrated that both medium spiny projection neurons and nNOS-containing interneurons exhibit altered patterns of gene expression (Zucker *et al.*, 2005). Within the nNOS-positive interneurons, mRNAs for nNOS, the NMDA receptor subunit NR2D, PSD95, and HAP1 were altered. This raises the possibility that these proteins confer protection against neurodegeneration in this interneuronal population (Zucker *et al.*, 2005).

Interestingly, transgenic HD mouse models that express either the full-length huntingtin (Hodgson *et al.*, 1999) or one third of the protein (Laforet *et al.*, 2001) exhibit fewer transcriptional changes, and a slightly different transcriptional pattern as compared to R6 mice (Chan *et al.*, 2002). The high number of gene expression changes in the R6 model suggests that short N-terminal fragments of mutant huntingtin are particularly potent in eliciting transcriptional dysregulation (Chan *et al.*, 2002). Furthermore, although emerging evidence suggests that protein context is crucial for determining toxicity of polyglutamine expansions (for review see La Spada and Taylor, 2003), at least some of the transcriptional changes appear independent of the specific protein bearing the glutamine expansion, as similar changes have been found in transgenic mouse models for other CAG triplet repeat disorders (Luthi-Carter *et al.*, 2002).

1.6.2.2. Dysfunction of the Corticostriatal Pathway

The glutamatergic corticostriatal pathway has also been examined in the R6 mice. However, contradictory results have been reported. Although whole tissue levels of glutamate are not altered in 12-week-old R6/2 mice (Reynolds *et al.*, 1999), microdialysis studies reveal reduced basal extracellular levels of glutamate and an increased release with KCl stimulation in R6/1 mice at 16 weeks of age (Nicniocaill *et al.*, 2001). However, in another microdialysis study extracellular glutamate levels were found to be unchanged in R6/2 mice (Behrens *et al.*, 2002). Nevertheless, a partial inhibition of the glutamate transporter 1 (GLT 1) caused an age-dependent increase in extracellular glutamate levels in R6/2 mice, consistent with the idea of a dysfunctional glutamate transport capacity. This finding is consistent with the age-dependent down-regulation of GLT-1 mRNA and protein levels, which lead to a reduced function of the transporter (Lievens *et al.*, 2001; Behrens *et al.*, 2002). In these studies, a reduction in glutamate synthetase expression was also reported to occur in R6/2 mice, suggesting a perturbation of the glutamate-glutamine cycle (Lievens *et al.*, 2001; Behrens *et al.*, 2002).

Electrophysiological studies have also revealed a progressive decline in excitatory post-synaptic current frequency, which is specific to glutamatergic input, in R6/2 mice (Cepeda *et al.*, 2003). These studies point to synaptic loss at the corticostriatal connections. However, isolated large-amplitude synaptic events from the cortex were found to occur frequently in 6-week-old R6/2 mice, which could account for the generalized convulsions observed in these mice (Cepeda *et al.*, 2003). Interestingly, although GABA and glutamic acid decarboxylase (GAD) 67 mRNA levels are normal in the striatum of R6/2 mice, GAD67 expression is significantly reduced in the frontal and parietal cortex (Gourfinkel-An *et al.*, 2003), which could lower the threshold for triggering seizures.

1.6.2.3. Changes in Signalling Pathways and Intracellular Homeostasis

At the single cell level, R6/2 striatal neurons demonstrate greater depolarized resting membrane potentials than wild-type neurons (Levine *et al.*, 1999). Moreover, in striatal slices from 8-week-old R6/2 mice, a 5-fold increase in intracellular Ca^{2+} concentration was detected, indicating a fundamental alteration in Ca^{2+} homeostasis. Interestingly, intracellular Ca^{2+} dysfunction is supported by the observation that R6/2 striatal neurons can tolerate a dramatic overload of cytoplasmic Ca^{2+} , induced by application of QA, which would normally lead to Ca^{2+} deregulation and cell death. The mechanism behind this Ca^{2+} tolerance is unknown but it may be related to either the capacity of these cells to remove intracellular Ca^{2+} , to sequester it into internal organelles, and/or buffer it in the cytoplasm (Hansson *et al.*, 2001b).

Several lines of evidence suggest that a lack of trophic support can contribute to striatal neurodegeneration in HD. Indeed, normal huntingtin directly regulates the expression of BDNF (section 1.3.1; Zuccato *et al.*, 2003), which appears to be reduced in the presence of mutant huntingtin (section 1.3.3.3; Zuccato *et al.*, 2001). By breeding R6/1 mice with BDNF^{+/-} mice, and consequently disrupting the expression of BDNF, Canals and co-workers (2004) reported that a decrease in BDNF promotes the onset of motor symptoms, which happens to correlate with the loss of DARPP-32 (DA and cAMP regulated phosphoprotein of a molecular weight of 32 kDa)-positive striatal neurons in these mice. Interestingly, this accelerated neuronal dysfunction could be reverted by the exogenous administration of BDNF (Canals *et al.*, 2004). R6/1-BDNF^{+/-} double mutant mice also exhibit increased aggregates in the substantia nigra pars compacta, a decrease in retrograde labeling of dopaminergic neurons, a reduction in striatal DA content, and a reduced expression of DA receptors (Pineda *et al.*, 2005). Finally, these double mutant mice exhibited lower

locomotor activity in response to amphetamine, further implicating BDNF in the motor disturbances associated with the dysfunction of the dopaminergic system (Pineda *et al.*, 2005).

1.6.2.4. Mitochondrial Dysfunction and Oxidative Stress

A number of studies suggest that mitochondrial dysfunction and oxidative stress also play a role in R6 neuropathology. The evidence is outlined below.

1) Increased concentrations of 8-hydroxy-2-deoxyguanosine, a marker for oxidative damage to DNA, have been found in the striatum of 12- to 14-week-old R6/2 mice (Bogdanov *et al.*, 2001).

2) At the same age, there is a reduction in aconitase and mitochondrial complex IV activity in the striatum. There is also a decrease in complex IV activity in the cerebral cortex (Tabrizi *et al.*, 2000).

3) Up-regulation of caspases 1 and 3 (Chen *et al.*, 2000) and activated caspase-9 and -3 (Kiechle *et al.*, 2002) have been found in end stage R6 mice. In addition, a progressive increase in the cytoplasmic levels of cytochrome c occurs, suggesting the involvement of the mitochondrial apoptotic pathway.

4) Increased immunolabelling for the inducible isoform of nitric oxide synthase (iNOS) and 3-nitrotyrosine was observed in R6/2 brains, which can be interpreted as a sign of increased NO[•] production and subsequent NO[•]-mediated oxidative stress (Tabrizi *et al.*, 2000). Interestingly, in R6/1 mice, the NOS activity is increased at 19 weeks and then reduced at 32 weeks (Perez-Severiano *et al.*, 2002);

5) A biphasic change in the expression and activity of nNOS was also found in the striatum and cerebellum of R6/2 (Deckel *et al.*, 2001) and R6/1 mice (Deckel *et al.*, 2002b). Initially the expression and activity of this enzyme increases but then decreases as the disease state progresses. Furthermore, the decreased expression and activation of nNOS in the late stages of the disease correlate with body weight loss, abnormal clasping, and decreased performance on the rotarod task. Moreover, a biphasic change in the expression of the Ca²⁺-calmodulin-dependent proteins calmodulin kinases II and IV (both of which are regulators of nNOS transcription and activation) has been proposed to underlie the alterations in nNOS expression and activity (Deckel *et al.*, 2001, 2002a, 2002b).

6) Total superoxide dismutase (SOD) and Cu/Zn-SOD activity is increased in the striatum of young R6/1 mice and decreased in 35-week-old R6/1 mice (Santamaria *et al.*, 2001). These authors suggest that the initially elevated enzymatic activity represents a compensatory mechanism against oxidative stress, which eventually breaks down in older mice (Santamaria *et al.*, 2001);

7) Ascorbate (vitamin C), an extracellular non-enzymatic antioxidant, is reduced during periods of behavioral activity in R6/2 mice at 6 weeks, suggesting an impaired release of this vitamin and contributing to insufficient antioxidant protection (Rebec *et al.*, 2002).

Hence, R6 mice demonstrate increased markers for oxidative stress along with a compromised antioxidant capacity. With this in mind, it is important to point out that treating R6 mice with several antioxidant drugs (e.g., α -lipoic acid, ascorbate, co-enzyme Q₁₀) can, to some extent, ameliorate the neuropathology and extend the survival of these mice (for review see Beal and Ferrante, 2004; Hersch and Ferrante, 2004; Li JY *et al.*, 2005). However, these treatments only prolong the survival of R6 mice by 10 to 15%, which suggests that oxidative stress is not the major mediator in the disease process and/or that the treatments do not completely eliminate the production of free radicals.

1.6.3. Therapeutic Strategies

It is more likely that a combination of multiple factors is responsible for the severe pathology observed in R6/2 mice (*section 1.6.2*). As such, multiple approaches have been suggested to treat and reverse HD pathology in this model (for review see Beal and Ferrante, 2004; Hersch and Ferrante, 2004; Li JY *et al.*, 2005). These approaches can be classified according to their mode of action: (1) inhibition of histone deacetylation and methylation; (2) inhibition of protein misfolding and oligomerization; (3) transglutaminase inhibition; (4) caspase inhibition; (5) inhibition of excitotoxicity; (6) energy supplementation and rescue of metabolic impairment; (7) use of antioxidants; (8) genetic manipulations; (9) transplantation; and (10) environmental enrichment. Many of these treatment approaches have been found to exert ameliorative effects on the behavior and neuropathology of these transgenic mice and to increase their survival by up to 32% (for review see Li JY *et al.*, 2005), demonstrating that the R6 mouse models are in principle amenable to therapy. Nevertheless, their accelerated progression of the disorder is not mimicked in the human condition, which may potentially reduce the ability to detect subtle improvements with a specific treatment.

Furthermore, many studies with animal models are plagued by inconsistent experimental protocols (especially with behavioral tests) and inappropriate statistical analysis. Hockly and co-workers (2003) have shown that rotarod performance and weight loss produce quantitative, reliable and reproducible data that can be easily analyzed by standard parametric statistical methods and accurately predict the progressive nature of the disease in R6 mice (Hockly *et al.*, 2003). However, one need to keep in mind that measuring behavioural

deficits such as rotarod performance may be influenced by other variables than pure motor functions. For example, in the case of R6 mice, muscle weakness, metabolic disruption, and hypothalamic dysfunction (see *Chapter 4*; Petersén *et al.*, 2005) can influence rotarod performance. Moreover, although it has been reported that R6 mice can die suddenly during a convulsive attack (Mangiarini *et al.*, 1996; Gil *et al.*, unpublished observations), the actual cause of death of these mice is still unknown, which should be considered when analysing survival data.

1.7. Objectives

As described above, HD is a multifactorial neurodegenerative disorder, characterized by a variety of symptoms that range from motor deficits, profound cognitive dysfunction, loss of body weight, to endocrine changes (*section 1.2.1*). However, much of the research has primarily focused on striatal degeneration, which mainly accounts for the motor impairment; whereas, other brain regions have received little attention. Moreover, even the striatal degeneration may result or be augmented by the impairment of other brain structures that directly or indirectly interact with the striatum (*sections 1.4.1* and *1.4.2*).

Therefore, the two major themes that underly the work in this thesis are:

- 1) To further elucidate the contribution of nonstriatal structures that directly interact with the striatum (i.e., the cortex and the substantia nigra) on striatal neurodegeneration;
- 2) To explore the pathological changes of other nonstriatal brain regions (i.e., hypothalamus and hippocampus) that can contribute to other symptomologies of HD (peripheral and cognitive deficits).

Bearing these two themes in mind, the specific objectives of this thesis are as follows:

- 1) To evaluate the striatal response to an excitotoxic insult that mimicks an excessive activation of the glutamatergic corticostriatal pathway in the newly generated rat model (*Chapter 2*).
- 2) To further characterize the impairment of the dopaminergic nigrostriatal pathway in the R6/1 mouse, by using *in vivo* microdialysis (*Chapter 3*).
- 3) To determine whether the lateral hypothalamus, a structure involved in the regulation of several endocrine functions, is affected by HD pathology in both R6/2 mice and human HD brains (*Chapter 4*).
- 4) To study the contribution of the DG of the hippocampus, a structure important for cognitive functioning, on the generation of new neurons and in HD pathology in R6/2 mice (*Chapter 5* and *6*).

- 5) To assess the effects of a novel neuroprotective compound (asialoerythropoietin; asialoEPO) on motor function, striatal neuropathology and hippocampal cell proliferation in R6/2 mice (*Chapter 5*).

Chapter 2

Normal Sensitivity to Excitotoxicity in a Transgenic Huntington's Disease Rat

Chapter based on the following publication:

Winkler C, **Gil J**, Araújo IM, Rieß O, Skripuletz T, von Hörsten S, and Petersén Å (2006): "*Normal sensitivity to excitotoxicity in a transgenic Huntington's disease Rat*". Brain Res. Bull. **69**:306-310.

2.1. Summary

Excitotoxic cell damage by excessive stimulation of glutamate receptors has been hypothesized to contribute to the pathogenesis of HD. Transgenic mouse models of HD have shown variable sensitivity to excitotoxicity. The models differ in the genetic background, the type and length of the promoter driving the transgene expression, the CAG repeat length and/or the *IT15* gene construct length. Furthermore, one has to differentiate whether transgenic or knock-in models have been used. All these factors may be crucial determinants in the responsiveness to an excitotoxic insult. Here, we explored the responsiveness to excitotoxic damage using a transgenic HD rat model carrying 22% of the *IT15* gene, which is driven by the rat *Hdh* promoter and harbors 51 CAG repeats. Transgenic HD rats received unilateral intrastriatal injections of the glutamate analogue quinolinic acid at 3 and 18 months of age. Lesion size was assessed 7 days later using the degenerative stain Fluoro-Jade (FJ) and by counting surviving neurons that were immunolabeled with neuronal nuclei marker (NeuN). No difference in susceptibility to excitotoxicity was found between the HD rats and controls. Our study supports the mouse data that shows unaltered susceptibility to excitotoxicity with the expression of around 25% of the full *IT15* gene. We conclude that differences in sensitivity to excitotoxicity between genetic animal models of HD may relate to the length of the expressed *IT15* gene.

2.2. Introduction

With the generation of the R6 mouse lines a unique opportunity was established to assess the influence of expanded polyglutamine tracts on the susceptibility of striatal neurons to excitotoxicity. Unexpectedly, R6 mice were found to be practically resistant to damage induced by intrastriatal injection of QA, an NMDA receptor agonist that normally causes excitotoxic degeneration (Hansson *et al.*, 1999). It was found that the resistance to QA developed gradually as the mice aged. Thus, at 3 weeks of age R6/1 mice displayed similar vulnerability to QA as wild-type control mice; whereas, 8- to 13-week-old R6/1 began to demonstrate resistance that was fully developed by 18 to 36 weeks of age. R6/2 mice, which have a longer CAG repeat, developed complete resistance to QA as early as 6 weeks of age (Hansson *et al.*, 2001b). This resistance was also observed after intrastriatal injections of NMDA (Hansson *et al.*, 2001b), DA, 6-hydroxydopamine (6-OHDA) (Petersén *et al.*, 2001), and malonate (Hansson *et al.*, 2001a; Petersén *et al.*, 2002b). Moreover, the resistance to QA was not limited to the striatum, as the hippocampus, in particular the CA1 region and to a lesser extent the DG, also demonstrate resistance to damage (Hansson *et al.*, 2001b). Striatal and hippocampal resistance to excitotoxic damage also occurs following systemic injections of KA (Morton and Leavens, 2000) and 3-NP (Hickey and Morton, 2000). It was also shown that R6/2 mice are partially resistant to hippocampal damage induced by a period of global cerebral ischemia (Schiefer *et al.*, 2002). The glutamate agonist α -amino-3-hydroxy-5-methylisoxazole-4-propionate (AMPA) was the only toxin which R6 mice have been found not to be resistant to (Hansson *et al.*, 2001b).

Although the mechanism responsible for the observed resistance of R6 mice to these different toxins is not fully understood, it does not appear to be the result of a reduction in the number of NMDA receptors or a decreased receptor-mediated influx of Ca^{2+} (Hansson *et al.*, 2001b). It is possible that a reduction of the excitatory input to the striatum observed in older R6 mice (Cepeda *et al.*, 2001, 2003) can contribute to this resistance. Alternatively, the resistance phenomenon may be similar to pre-conditioning, as observed with ischemia, where permanent exposure to low levels of excitotoxicity and to changes in intracellular Ca^{2+} homeostasis (*section 1.4.1*) allows neurons to adapt to an even greater excitotoxic insult and sudden increase in intracellular Ca^{2+} concentration. On the other hand, the lack of resistance to AMPA-induced insults may be related with the fact that activation of these receptors is normally associated with an excessive influx of Na^+ and consequent cell swelling. Therefore, it is reasonable to speculate that R6 mice have a better capacity to handle the

NMDA-induced Ca^{2+} overload than the AMPA-mediated Na^+ influx (Hansson *et al.*, 2001b).

The work pioneered in the R6 mice has led others to study the phenomena in other HD mouse models, where at least 6 different genetic animal models of HD have so far been evaluated. Using a similar methodology of intrastriatal QA injections, the results have been mixed (Zeron *et al.*, 2002; Jarabek *et al.*, 2004; Slow *et al.*, 2005). It appears that differences in the genetic background of the particular mouse strain, the promoter driving the transgene construct, the length of the *IT15* gene, and the number of CAG repeats may explain these conflicting results (Petersén *et al.*, 2002a).

In order to further evaluate the role of glutamate-mediated excitotoxicity in HD striatal degeneration, we examined the response of the recently generated HD transgenic rat to intrastriatal QA injections. This transgenic rat model carries a truncated huntingtin cDNA fragment with 51 CAG repeats under the control of the native rat *Hdh* promoter that corresponds to 22% of the full-length *IT15* gene (section 1.5.4; von Hörsten *et al.*, 2003). Since previous studies in the R6 and the YAC mouse models have shown that excitotoxic susceptibility may develop over time (Hansson *et al.*, 2001b; Zeron *et al.*, 2002), we used both young and aged HD transgenic rats (3 and 18 months of age, respectively), and examined their responsiveness to intrastriatal injections of QA using a similar procedure to the one employed in the previous mouse studies.

2.3. Materials and Methods

2.3.1. Transgenic Animals

Transgenic HD rats with 51 CAG repeats (section 1.5.4; von Hörsten *et al.*, 2003), and their wild-type littermates were used in this study. The transgenic HD rat expresses a cDNA (position 324–2321) corresponding to 22% of the full-length *IT15* gene under the control of the 886 bp rat *Hdh* promoter. The HD rat background strain is Sprague–Dawley strain derived. F10 rats were used for these experiments. Rats were housed under a 12 hours light/dark cycle with food and water *ad libitum*. Two time points were chosen, either 3 ($n = 8$ for wild-type rats; $n = 10$ for transgenic HD rats) or 18 ($n = 6$ for wild-type rats; $n = 9$ for transgenic HD rats) months of age. Previous research has shown that at 3 months of age these HD rats display signs of reduced anxiety, and at 9 to 18 months start exhibiting motor dysfunction and cognitive impairments (von Hörsten *et al.*, 2003; Nguyen *et al.*, 2006). All research and animal care procedures were

approved by the District Government, Hanover, Germany, and performed according to international guidelines for the use of laboratory animals.

2.3.2. Surgery

QA (Sigma, Steinheim, Germany) was dissolved in 0.1 M phosphate buffered saline (PBS, pH 7.4). Under isoflurane anesthesia, the rats received a single unilateral intraatrial injection of 80 nmol of QA in 1 μ l at the following stereotactic coordinates using a 5 μ l Hamilton syringe: 1.2 mm rostral to bregma, 2.7 mm right of the midline, and 4.5 mm ventral to the dural surface, with the incision bar set at zero. The injection rate was 0.2 μ l/minute, and the cannula remained in place for an additional 3 minutes before being slowly retracted.

2.3.3. Tissue Processing and Histology

Rats were perfused with 4% paraformaldehyde (PFA) 7 days after the surgery. The brains were postfixed overnight in the same solution and dehydrated in 20% sucrose/0.1 M PBS. Serial coronal sections were cut on a freezing sliding microtome at 30 μ m thickness and collected in PBS. Tissue from wild-type and transgenic rats was processed in parallel for immunohistochemistry to control for staining intensity.

One series of rat brain sections was processed for Nissl stain (cresyl violet; ICN Biomedicals Inc., Aurora, OH, USA). Briefly, free-floating rat brain sections were mounted onto gelatin-coated slides and immersed in cresyl violet for 1 – 2 minutes (until the nuclei were clearly visible). After being immersed in a series of ethanol solutions of increasing concentrations (70%, 95% and 100%), the mounted sections were finally immersed in xylene and coverslipped with DPX mounting medium (BDH Laboratory Supplies, Poole, UK). Another series of sections were processed for FJ (Histo-Chem, Jefferson, AR, USA), which is thought to stain for degenerating neurons (Schmued *et al.*, 1997), as previously described (Hansson *et al.*, 1999). Briefly, free-floating rat brain sections were mounted onto gelatin-coated slides and immersed in a series of ethanol solutions of decreasing concentrations (100% and 70%). The mounted sections were then incubated in 0.06% potassium permanganate (in distilled water) for 15 minutes and finally in FJ solution (0.001% FJ + 0.1% acetic acid in distilled water) for 30 minutes in the dark. After rinsing and drying (at 60°C for 15 minutes), the mounted sections were immersed in xylene and coverslipped with DPX mounting medium.

A further series of brain sections was processed immunohistochemically for

the neuron-specific marker NeuN (Chemicon, Temecula, CA, USA). Briefly, free-floating sections were quenched (to block the endogenous peroxidases) in 3% H₂O₂/10% methanol in 0.1 M PBS for 15 minutes. After rinsing in 0.1 M PBS, sections were incubated in a blocking solution containing 5% normal horse serum (NHS) and 0.25% Triton X-100 in 0.1 M PBS. They were then incubated for 48 hours at 4°C with a primary mouse monoclonal anti-NeuN antibody (diluted 1:1000) in blocking solution. After rinsing, sections were incubated for 1 hour at room temperature with the secondary antibody biotinylated horse anti-mouse IgG (diluted 1:200; Dakopatts, Copenhagen, Denmark) followed by a final rinse. The bound antibodies were then visualized with an avidin–biotin–peroxidase complex system (Vectastain ABC Elite Kit; Vector Laboratories, Burlingame, CA, USA) using 3,3-diaminobenzidine (DAB) as the chromogen.

2.3.4. Stereological Techniques

All morphological analyses were performed on blind-coded slides, using a 10x objective fitted on an Olympus BH2 microscope, a X-Y-Z step motor stage run by an IBM PC computer, a CCD-IRIS color video camera, and the CAST-GRID software (Olympus Denmark A/S, Albertslund, Denmark).

The striatal lesion area (defined by the presence of FJ-labeled cells or the lack of NeuN positive cells) was delineated in sections processed for either FJ-staining or NeuN immunohistochemistry (distance between the sections: 210 µm). The total striatal area at the non-injected side was delineated in 5 NeuN labeled sections (the level of these sections began 2 sections anterior to the appearance of the anterior commissure). The striatal lesion volume and the total striatal volume were calculated, taking into account the frequency of sections (1:8) and their thickness (30 µm), according to the Cavalieri principle (Gundersen *et al.*, 1988).

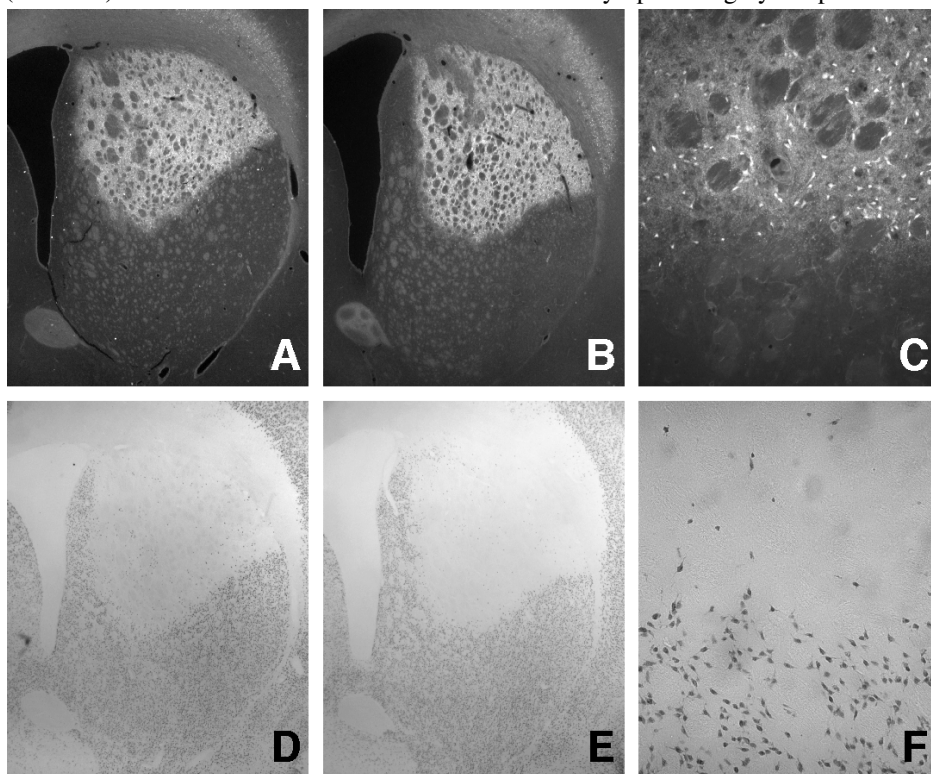
2.3.5. Statistical Analysis

For group comparisons, data were subjected to a 2-factor analysis of variance (ANOVA) using the Statview 5.4 Package (Abacus Concepts, Berkeley, CA, USA). Data are presented as means ± standard error of the mean (S.E.M.). Statistical significance was set at $p < 0.05$.

2.4. Results

The volume of the striatal lesion induced by the unilateral injection of QA in transgenic and wild-type rats of 3 and 18 months of age was analyzed 7 days post-surgery in sections stained for FJ (**Figures 2.1.A–C**) or processed for NeuN immunohistochemistry (**Figures 2.1.D–F**).

Figure 2.1. - *Striatal QA-induced lesions assessed with FJ staining and NeuN immunohistochemistry.* Rats were subjected to an intrastriatal injection of 1 μ l of QA (80 nmol) and the lesion volumes were assessed 7 days post surgery. Representative



photographs showing QA-induced striatal lesions in a 18 month-old wild-type (**A**) and a HD transgenic (**B**) rats using FJ-staining. Higher magnification of FJ staining in a wild-type rat (**C**). Representative photographs showing the adjacent sections processed for NeuN immunohistochemistry in a 18 month-old wild-type (**D**) and a HD transgenic (**E**) rats. Higher magnification of NeuN immunohistochemistry in a wild-type rat (**F**). Scale bar = 1 mm (**A**) and = 140 μ m (**C**).

Regions positive for FJ were immunonegative for NeuN, indicating loss of neurons. Within the FJ-positive areas vast numbers of degenerating cells exhibiting dense nuclei were observed, as confirmed with the cresyl violet stain

(data not shown). In wild-type controls the striatal lesion volume amounted to approximately 43% of the total striatal volume, making it reasonable to detect subtle changes in the sensitivity to QA of the transgenic HD rats. However, there was no significant difference between the FJ-stained lesion volumes between groups (2-factor ANOVA; $p = 0.91$, $F(1, 29) = 0.01$), although a small difference between all rats of 3 and 18 months of age was detected (2-factor ANOVA; $p = 0.02$, $F(1, 29) = 5.73$) with no interaction between genotype and age (2-factor ANOVA; $p = 0.43$, $F(1, 29) = 0.63$) (**Figures 2.1.A–C and 2.2.A**).

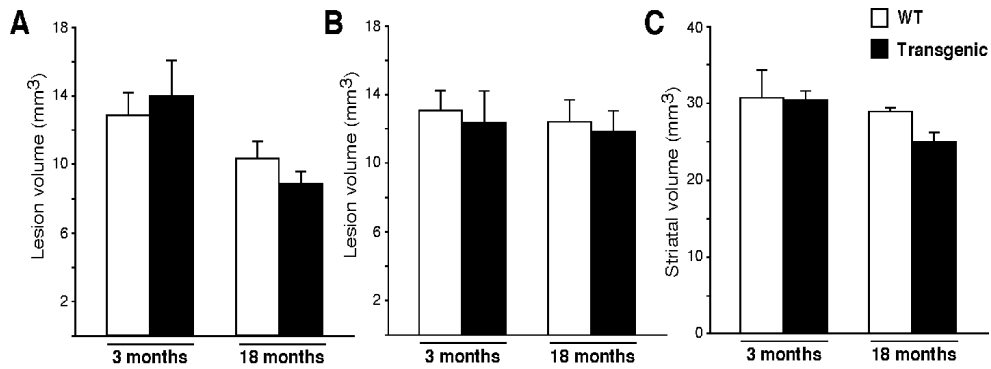


Figure 2.2. - *No resistance to excitotoxic damage in HD rats.* The striatal lesion volume following an injection of 80 nmol QA did not differ between 3 and 18 month-old transgenic HD rats, or their wild-type littermates. The lesion volumes were assessed in sections stained with FJ (**A**) and processed for NeuN immunohistochemistry (**B**). There was no difference in the total striatal volumes between the genotypes of the different ages as assessed in sections processed for NeuN immunohistochemistry (**C**). Values represent means \pm S.E.M.

Correspondingly, no differences in lesion volumes were detected with NeuN processed sections between genotypes (2-factor ANOVA; $p = 0.75$, $F(1, 29) = 0.10$), age groups (2-factor ANOVA; $p = 0.62$, $F(1, 29) = 0.25$), or any interaction between genotype and age (2-factor ANOVA; $p = 0.93$, $F(1, 29) = 0.01$) (**Figures 2.1.D–F and 2.2.B**).

After discovering no major differences in cell loss, we decided to examine whether the striatum had atrophied prior to the lesion by measuring total striatal volume at the non-injected side with NeuN immunohistochemistry (**Figure 2.2C**). A 2-factor ANOVA revealed no differences in the total striatal volume between genotypes ($p = 0.25$, $F(1, 29) = 1.37$), age groups ($p = 0.06$, $F(1, 29) = 3.75$), or any interaction between genotype and age ($p = 0.45$, $F(1, 29) = 0.59$).

2.5. Discussion

In HD, there is a selective neuronal loss in the cerebral cortex and striatum, despite ubiquitous expression of the mutant huntingtin in all cells (*section 1.2.2*; for review see Vonsattel and DiFiglia, 1998). Interestingly, these afflicted regions are all densely innervated by glutamatergic input. Furthermore, intra-striatal injections of glutamate analogues both in rats (Beal *et al.*, 1986, 1991) and in primates (Ferrante *et al.*, 1993) give rise to an HD-like neuropathology. These factors have led to the hypothesis that excitotoxicity plays a role in HD (*section 1.4.1*).

In this study, neither young nor old transgenic HD rats (von Hörsten *et al.*, 2003) displayed altered sensitivity to excitotoxicity.

Results ranging from reduced to increased sensitivity to excitotoxicity have been found in the various rodent models for HD. Although the animals vary in many parameters such as strain, transgene construct, promoter, CAG repeat length, and expression levels, most probably the length of the expressed *IT15* gene is crucial in determining the response to excitotoxicity.

The HD rat expresses 22% of the full-length *IT15* gene and displayed no altered susceptibility to excitotoxicity. This result is in agreement with a previous study that shows a maintained excitotoxic response in transgenic mice expressing around 30% of the full *IT15* gene, independent of CAG repeat length and age of the mice (Petersén *et al.*, 2002a).

On the other hand, R6 mice express around 3% of the *IT15* gene, with 117–150 CAG repeats, and do demonstrate a profound resistance to excitotoxic insults (Hansson *et al.*, 1999, 2001b). Similarly, other mouse models that also express only a small percentage of the full *IT15* gene, such as the N171-82Q mouse (Jarabek *et al.*, 2004) and the recently generated “shortstop” mouse expressing around 120 CAG repeats (Slow *et al.*, 2005), demonstrate resistance to QA insults. A decrease in several proteins involved in the signaling pathways triggered by the activation of NMDA and DA D1 receptors (such as PSD95, nNOS, and the DA D1 receptor) has been suggested to account for the reduced sensitivity to an excitotoxic insult in N171-82Q mice (Jarabek *et al.*, 2004).

In contrast, in YAC72 (Zeron *et al.*, 2002) and YAC128 (Graham *et al.*, 2005) mice, which express the full-length *IT15* gene, a greater sensitivity to excitotoxicity has been reported. Interestingly, YAC mice expressing full-length mutant huntingtin resistant to proteolysis mediated by caspase-6 are protected against excitotoxicity induced by QA (Graham *et al.*, 2006). This result suggests

that caspase-6-induced cleavage of full-length mutant huntingtin selectively mediates susceptibility to excitotoxic stress in YAC mice.

To conclude, the data from these studies in HD mouse models, together with our results in the HD rat, suggest that the length of the expressed *IT15* transgene should be considered when studying cellular responses to neurotoxins.

Importantly, the diversity of results that have been obtained with intrastriatal injections of excitotoxins, ranging from resistance to enhanced susceptibility, makes it difficult to conclude on the actual impact of excitotoxic insults on HD striatal neurodegeneration. Moreover, in the human HD brain, the progressive dysfunction of the corticostriatal pathway is likely to result in chronic and sustained excitotoxicity. Given the fact that the intrastriatal injection of excitotoxins represents an acute model of excitotoxicity that artificially mimicks an over-stimulation of the corticostriatal glutamatergic pathway, one should be careful when drawing conclusions regarding the role of excitotoxicity in HD.

Chapter 3

Impaired Dopaminergic Neurotransmission in R6/1 Transgenic Huntington's Disease Mice

Chapter based on the following manuscript:

Gil J, Haraldsson B, Araújo IM, Lagerkvist S, Petersén Å, and Brundin P (2006): *"Impaired Dopaminergic Neurotransmission in Transgenic Huntington's Disease Mice of the R6/1 Line"*. (Manuscript in preparation).

3.1. Summary

Previous studies have implicated a dysfunction of the nigrostriatal dopaminergic system in the neuropathology of HD. In the present study we further characterized the deficits in the regulation of this pathway in R6/1 transgenic HD mice using *in vivo* microdialysis. A set of R6/1 mice of 18 to 19 weeks of age was examined regarding the maximum capacity of the nigrostriatal neurons to release DA in the striatum upon KCl-induced plasma membrane depolarization and amphetamine-mediated DA release through DAT. High performance liquid chromatography (HPLC) was used to measure the levels of DA and its metabolites, DOPAC and homovanillic acid (HVA). In addition to DA release, we also determined the total tissue DA levels. We found that intrastriatal infusion of both KCl and amphetamine rapidly increased the local dialysate DA levels in both R6/1 and wild-type mice. However, the absolute increase was attenuated in R6/1 mice as compared to wild-type mice. In accordance with these data, we observed a significant decrease in postmortem striatal DA tissue levels in R6/1 mice. In addition, there was a significant decrease in the baseline levels of DOPAC and HVA in dialysate samples from R6/1 mice. These results further implicate an impairment of the dopaminergic nigrostriatal pathway in the neuropathology of the R6/1 transgenic HD mice.

3.2. Introduction

Several lines of evidence indicate that a dysfunction of the nigrostriatal dopaminergic pathway may contribute to the neuropathology of HD. Since the DA system plays an important function in the regulation of the striatum, it is plausible that some of the motor and cognitive symptoms that characterize HD may be due to DA (*section 1.4.2*).

In R6 mice, multiple abnormalities of the dopaminergic nigrostriatal system have been reported. At the post-synaptic level (i.e., in striatal neurons), a reduced expression of DA D1 and D2 receptors can be detected as early as 4 weeks in R6/2 mice (Cha *et al.*, 1998). A reduced expression of DARPP-32 (a phosphoprotein that mediates DA signaling transduction pathways in striatal neurons) occurs at the same time point (Bibb *et al.*, 2000; Luthi-Carter *et al.*, 2000; van Dellen *et al.*, 2000b). Moreover, R6/2 mice exhibit defects in DA-regulated ion channels (Bibb *et al.*, 2000). Basal immediate early gene (IEG) expression, which is commonly used as an index of dopaminergic signal transduction, is also reduced in the R6/2 striatum at 12 weeks (Spektor *et al.*, 2002). Interestingly, DA D2 receptor antagonist-induced IEG mRNA levels were reduced in the R6/2 striatum; whereas, DA D1 receptor agonist-induced IEG mRNA levels were surprisingly increased. This increased IEG response after D1 receptor agonist stimulation may be due to D1 receptor supersensitization, which in turn is caused by a diminished dopaminergic input (Spektor *et al.*, 2002).

Furthermore, at the presynaptic level, the nigrostriatal terminals of 16-week-old R6/1 mice were found to release reduced amounts of DA, both at baseline and after malonate stimulation, as measured by *in vivo* microdialysis (Petersén *et al.*, 2002b). This may account for the reported D1 receptor supersensitization. Moreover, 9-week-old R6/2 mice also display attenuated motor activation in response to cocaine (a DAT inhibitor that potentiates the action of physiologically released DA) (Hickey *et al.*, 2002), further supporting the notion of an impaired capacity to release DA.

In order to further characterize the dysfunction of the dopaminergic nigrostriatal pathway at the presynaptic level (i.e., at the level of DA synthesis and release), we performed *in vivo* microdialysis in 18- to 19-week-old R6/1 mice. We infused KCl (which depolarizes plasma membranes inducing the release of DA from the vesicular pool), and amphetamine (which leads to a DAT-mediated efflux of DA) through the dialysis probe. This technique allowed us to evaluate the contribution of the 2 major DA releasing routes for the reduced release of DA that was previously reported (Petersén *et al.*, 2002b).

3.3. Materials and Methods

3.3.1. Transgenic Animals

The heterozygous male R6/1 mice were purchased from Jackson Laboratories (Bar Harbor, ME, USA) and bred with wild-type females (F1 of CBA x C57BL/6J). DNA samples, derived from the tails of the offspring, were genotyped using a polymerase chain reaction (PCR) assay (Mangiarini *et al.*, 1996). The mice were housed under a 12-hour light-dark cycle with food and water *ad libitum*. All experimental procedures were conducted according to regulations set by the Ethical Committee for the use of laboratory animals at Lund University, Sweden.

3.3.2. In vivo Microdialysis

R6/1 ($n = 7$) and wild-type littermates ($n = 8$) of 18 to 19 weeks of age were anesthetized with a mixture of 1% halothane and O₂/N₂O. The anesthesia was maintained during microdialysis by free-breathing into a mask fitted over the nose of the mouse. Body temperature was maintained at 37°C using a temperature-regulating heating pad throughout the entire surgical procedure. A microdialysis probe of concentric design (CMA/11, Carnegie Medicin AB, Stockholm, Sweden; length = 2 mm; outer diameter = 0.24 mm) was inserted into the right striatum through a hole drilled in the skull, at the following stereotactic coordinates: 0.8 mm rostral to bregma; 2.2 mm lateral to the midline; 2.8 mm ventral from the dural surface; with the tooth-bar set at zero. The probes were perfused at a rate of 2 µl/minutes with sterile Ringer solution (145 mM NaCl, 3 mM KCl, 1.3 mM CaCl₂, 1 mM MgCl₂, pH 6.0; Apoteksbolaget, Täby, Sweden) through the dialysis session. Perfusate samples were collected every 20 minutes, starting 60 minutes after probe implantation (i.e., the first 120 µl were discarded). Subsequently, three stable basal values (60 minutes, with intervals of 20 minutes) were obtained, after which the perfusion was switched to KCl (60 mM), for 20 minutes. The perfusion medium was then switched back to normal Ringer solution and an additional three 20 minute-dialysate samples were collected. Amphetamine (10 µM) was then perfused through the microdialysis probe for 20 minutes, after which three more 20 minute-samples were collected in Ringer solution, yielding a total of 11 samples collected per mouse. Each 40 µl sample was divided into 2 aliquots of 20 µl each, immediately frozen in liquid nitrogen and stored at -80°C until processed.

3.3.3. Determination of the Dialysate DA, DOPAC & HVA Levels

The quantification of the levels of the monoamine neurotransmitter DA and its acidic metabolites (DOPAC and HVA) in the dialysate samples was performed by HPLC separation and electrochemical detection, according to a method developed by Lagerkvist *et al.* (unpublished protocol; Carlsson Research AB, Göteborg, Sweden). The analytical method was based on 2 chromatographic separations dedicated for amines or acids, respectively. The 2 chromatographic systems shared a common auto-injector with a 10-port valve and 2 sample loops for simultaneous injection. The acids were separated by reverse phase chromatography; whereas, the amines were separated by reverse phase ion pairing preceded by a reverse phase separation in a column switching configuration.

3.3.4. Analysis of Whole Tissue Striatal DA Levels

Immediately after microdialysis, R6/1 and wild-type mice were sacrificed by cervical dislocation and the brains were rapidly removed on ice. The 2 hemispheres were separated and the left striatum was dissected out and immediately frozen on dry ice and stored at -80°C until processing. Determination of whole tissue striatal DA levels was conducted at the Carlsson Research AB. Briefly, the striata were thawed and homogenized in 1 ml of 0.1 N perchloric acid containing 5% EDTA. After centrifugation at 14,000 *g* for 30 minutes, 200 μl of the supernatant were filtered through a 0.22 μm glass filter and 20 μl were then injected into the HPLC equipment and the DA levels were determined as above (*section 3.3.3*).

3.3.5. Evaluation of Microdialysis Probe Placement

After dissecting out the 2 brain hemispheres, the right hemisphere (i.e., the one where the microdialysis probe was inserted) was fixed for 24 hours in 4% PFA and dehydrated in 20% sucrose/0.1 M PBS. Serial coronal sections were cut on a freezing sliding microtome at 30 μm thickness and collected in PBS. Tissue from wild-type and HD mice was processed in parallel to control for staining intensity. In order to evaluate the correct placement of the microdialysis probes inside the mice striata, one series of brain sections was processed for cresyl violet (ICN Biomedicals Inc.; procedure described in *section 2.3.3*). The brain sections of each mouse were analyzed with a 10x objective fitted onto a light microscope to confirm probe tip location. All microdialysis probes had been correctly placed within the striatum.

3.3.6. Statistical Analysis

The data were analyzed with unpaired Student's *t* tests or 2-factor ANOVA with repeated measures when appropriate, using the Statview 5.4 package (Abacus Concepts). Data are presented as means \pm S.E.M. A *p* value of < 0.05 was considered statistically significant.

3.4. Results

3.4.1. Whole Tissue Striatal DA Levels in R6/1 Mice

Previous studies from our group have shown no significant differences in the whole tissue striatal levels of DA in 16-week-old R6/1 mice (Petersén *et al.*, 2002b). Interestingly, in the present study, the striatal DA tissue levels were 143 ± 11 nM for wild-type mice and 68 ± 11 nM for R6/1 mice (Student's *t* test, $p < 0.05$). Therefore, we conclude that a significant reduction in the whole tissue striatal DA levels can be detected at this age, possibly reflecting a progressive impairment of the dopaminergic nigrostriatal pathway.

3.4.2. Dialysate DA Striatal Levels in R6/1 Mice

In all samples collected during the microdialysis experiment the dialysate DA levels were consistently reduced in R6/1 as compared with wild-type mice (repeated measures 2-factor ANOVA; genotype $p < 0.001$, $F(1, 130) = 24.95$; time \times genotype $p < 0.0001$, $F(10, 130) = 20.68$) (**Figure 3.1**). Stable basal striatal dialysate DA levels were achieved 1 hour after probe implantation. Three basal fractions of 20 minutes each were collected during that period. Basal striatal dialysate DA levels were reduced by approximately 76% in R6/1 mice as compared with their wild-type littermate controls (during 20 minutes of sample collection: R6/1 = 0.610 ± 0.10 nM; wild-type = 2.49 ± 0.41 nM; Student's *t* test, $p < 0.01$), which corresponds with previous results published by our group (Petersén *et al.*, 2002b). Intrastratial KCl (60 mM) injection during 20 minutes rapidly raised the local dialysate DA levels in all mice (**Figure 3.1**). However, the release of DA induced by KCl was significantly reduced in R6/1 mice (2.90 ± 0.42 nM) compared to wild-type animals (7.87 ± 0.99 nM; Student *t* test, $p < 0.001$). After intrastratial injection of amphetamine (10 μ M), during 20 minutes, the local dialysate DA levels were 15.81 ± 1.31 nM in wild-type and 5.82 ± 0.83 nM in R6/1 mice (Student's *t* test, $p < 0.0001$) (**Figure 3.1**). These results

suggest that both routes of DA release (KCl-induced exocytosis and amphetamine-mediated DA release) are impaired in R6/1 mice.

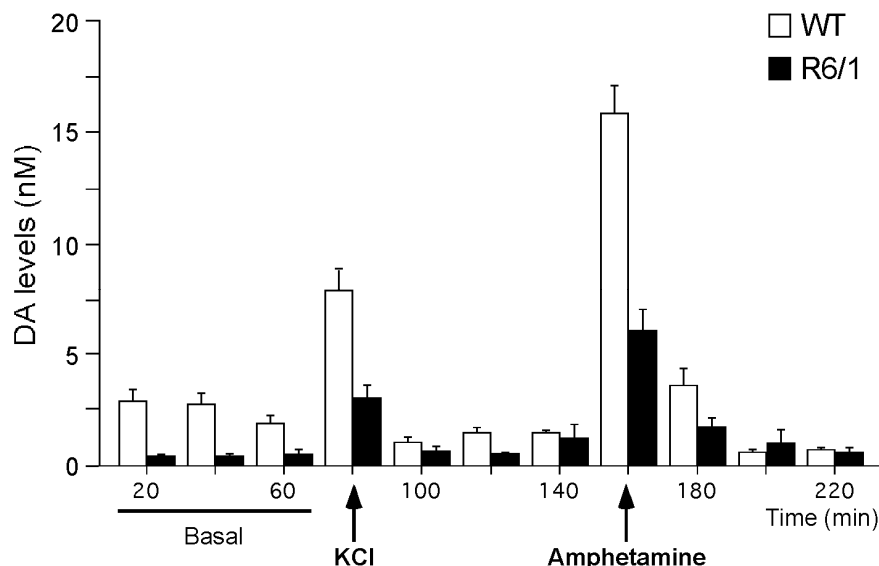


Figure 3.1 – Measurement of DA dialysate striatal levels before and after local infusion of KCl and amphetamine. Dialysate samples were collected every 20 minutes, starting 60 minutes after the implantation of the microdialysis probe. Basal levels were obtained during the first 3 samples after which KCl (60 mM) was perfused through the microdialysis probe during 20 minutes. After a recovery period of 60 minutes, amphetamine (10 μ M) was perfused for 20 minutes and 3 more subsequent 20 minute-samples were collected. There were significant reductions in DA dialysate levels at all time points in R6/1 mice as compared with their wild-type littermate controls. Data are presented as means \pm S.E.M.

3.4.3. Dialysate Basal Levels of DA Metabolites in R6/1 Mice

We also determined the basal dialysate striatal levels of the DA metabolites DOPAC and HVA (**Figure 3.2**). Interestingly, we found a 67% reduction in the basal dialysate DOPAC levels (wild-type: 162.84 ± 20.01 nM; R6/1: 53.39 ± 12.48 nM; Student's *t* test, $p < 0.001$), and a 69% decrease in the basal dialysate levels of HVA (wild-type: 179.70 ± 20.07 nM; R6/1: 56.35 ± 13.36 nM; Student's *t* test, $p < 0.001$). This significant reduction in the levels of both DA metabolites further supports the notion of an impaired dopaminergic nigrostriatal pathway in R6/1 mice.

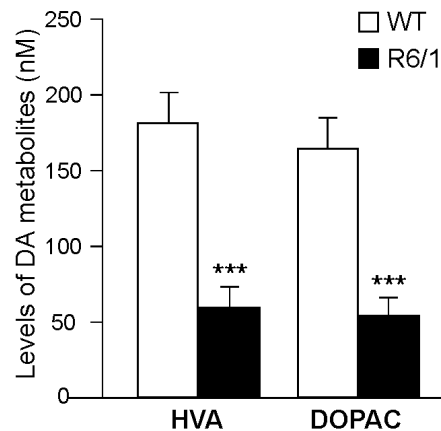


Figure 3.2 – Basal dialysate striatal levels of the DA metabolites DOPAC and HVA. Dialysate samples were collected every 20 minutes, starting 60 minutes after the implantation of the microdialysis probe. Basal levels of DOPAC and HVA were obtained during the first 3 samples and the respective averages were determined. Both DOPAC and HVA striatal basal dialysate levels were significantly reduced in R6/1 mice as compared with their wild-type littermate controls (Student's *t* test, *** $p < 0.001$). Data are presented as means \pm S.E.M.

3.5. Discussion

In this work we extended previous observations from our group (Petersén *et al.*, 2002b) and showed that both routes of DA release (membrane depolarization-induced exocytosis and DAT-mediated release) are impaired in 18- to 19-week-old R6/1 mice. Furthermore, we detected a significant decrease in whole tissue striatal DA levels, which is in accordance with studies from 9- (Hickey *et al.*, 2002) and 12-week-old (Reynolds *et al.*, 1999) R6/2 mice. Furthermore, we found a significant reduction in the basal dialysate striatal levels of both DA metabolites, DOPAC and HVA. Overall, these results further implicate a dysfunction of the nigrostriatal dopaminergic pathway in the neuropathology of R6 transgenic mice.

The cause for the impaired striatal DA release in these HD mice is not fully understood. One possibility could be the loss of dopaminergic neurons and/or a reduction in their striatal efferents. However, stereological counts revealed no differences in the total number of dopaminergic neurons in the R6/1 substantia nigra at 16 weeks of age, a time where a significant reduction in malonate-induced DA release is detected. Furthermore, when injecting a retrograde tracer

into the striatum, the number of cells back-labeled in the substantia nigra is normal in 16-week-old R6/1 mice, suggesting that their axonal striatal projections are intact (Petersén *et al.*, 2002b).

Another possible explanation for the reduced DA release could be an impairment of DA synthesis. Although no differences in the protein levels of TH (the rate-limiting enzyme in the biosynthesis of catecholamines) were initially detected in 16-week-old R6/1 mice (Petersén *et al.*, 2002b), recent evidence from our group suggest that this might not be the case (Smith *et al.*, unpublished data). Indeed, a significant reduction of about 20% in TH protein levels was observed. Furthermore, this decrease progresses over the course of the disease, reaching 70% in 40-week-old R6/1 mice (Smith *et al.*, unpublished data). Moreover, levels of TH mRNA are also decreased at both ages (Smith *et al.*, unpublished data), suggesting that the observed decrease in TH protein levels could be a direct consequence of mutant huntingtin-mediated transcriptional dysregulation (*section 1.3.3.3*). In support of this hypothesis, reduced TH protein levels have also been reported in end-stage 12-week-old R6/2 mice as assessed by fluorescence immunohistochemistry (Ariano *et al.*, 2002) and western-blotting (Yohrling *et al.*, 2003). Moreover, a similar TH decrease has been also observed in HD brains (*section 1.4.2*; Yohrling *et al.*, 2003).

Although an impairment of DA synthesis seems to be the likely cause of these pre-synaptic abnormalities, we cannot exclude the possibility that an impaired exocytotic process may also contribute to the observed reduced DA release, at least in basal conditions and after KCl-induced plasma membrane depolarization. Indeed, as discussed above (see *section 1.3.3.5*), mutant huntingtin is thought to abnormally interact with several different proteins involved in exocytosis, leading to the disruption of this process (for review see Li JY *et al.*, 2003; Smith *et al.*, 2005).

Interestingly, we found that amphetamine evoked a greater release of DA than KCl in all mice. It was recently demonstrated that amphetamine induces DA release via 2 distinct DAT-mediated mechanisms: (1) a slow process consistent with an exchange mechanism due to the reversal of the transporter; and (2) a rapid efflux through a channel-like mode of DAT that accounts for the release of a large quantity of DA molecules (Kahlig *et al.*, 2005). Therefore, it is possible that these two mechanisms can account for the massive DA release we observed upon amphetamine infusion. Nevertheless, the amphetamine-induced DAT-mediated DA release was significantly decreased in R6/1 mice as compared to wild-type controls. However, the protein levels of DAT seem to be unchanged in R6/1 mice both at 16 (Petersén *et al.*, 2002b; Smith *et al.*, unpublished data) and 40 weeks of age (Smith *et al.*, unpublished data), suggesting that a decrease in DAT is unlikely to account for our results.

Therefore, a more likely explanation for the R6/1 mice reduced response to amphetamine is an impaired DA biosynthesis.

In this study we also measured the basal dialysate striatal levels of the DA metabolites, DOPAC and HVA, and found that they too were significantly reduced in R6/1 mice. The observed decrease may reflect the reduced amount of DA that is available for catabolism in these mice. Interestingly, a reduction in whole tissue striatal DOPAC levels was also found in 9-week-old R6/2 mice (Hickey *et al.*, 2002).

It is important to point out that contradictory results showing no changes in the dopaminergic system of R6/2 mice have also been reported (Vetter *et al.*, 2003). By performing *in vitro* release experiments and *in vivo* microdialysis in freely moving 12-week-old mice, Vetter and colleagues (2003) failed to detect any significant differences at the level of electrically evoked release of [³H]DA and its modulation by DA D2 receptors, and of striatal DA levels in end-stage R6/2 mice (Vetter *et al.*, 2003). The reasons for this discrepancy are currently unknown. It may be that differences between the transgenic mouse lines (R6/1 versus R6/2), mice colonies, or *in vivo* microdialysis techniques are responsible for these discrepancies. It is interesting to point out that in our laboratory R6/2 mice failed to survive during the long periods of anesthesia that were required to perform our particular microdialysis procedure. Nevertheless, our results correspond with the recent study by Johnson and colleagues (2006) who have demonstrated a progressive and significant reduction in DA release in brain slices from R6/2 mice (Johnson *et al.*, 2006). Moreover, R6/2 mice showed an attenuated response to cocaine (Hickey *et al.*, 2002; Johnson *et al.*, 2006), and decreased activity in the open field when stimulated with a single dose of amphetamine (2.5 mg/kg) (Gil *et al.*, unpublished observations), suggesting that an impaired release of DA indeed occurs in these mice.

To conclude, we provide further evidence for an impaired release of DA and a corresponding reduction in striatal levels of this neurotransmitter and its metabolites in R6/1 mice. Since both pathways of DA release were markedly affected in R6/1 mice, we believe that this reduction is associated with a decrease in DA synthesis, which in turn is caused by a decrease in TH expression. Thus, a dysfunctional nigrostriatal pathway is likely to contribute to striatal degeneration and some of the symptoms of the disease, such as bradykinesia and rigidity, which are observed in both late-stage R6 mice and HD patients.

Chapter 4

Dysfunction of the Lateral Hypothalamus in Huntington's Disease

Chapter based on the following publication:

Petersén Å*, **Gil J***, Maat-Schieman MLC, Björkqvist M, Tanila H, Araújo IM, Smith R, Popovic N, Wierup N, Norlén P, Li JY, Roos RAC, Sundler F, Mulder H, and Brundin P (2005): "**Orexin loss in Huntington's disease**". *Hum. Mol. Genet.* **20**:744-751. * *The two authors contributed equally to this work.*
[*Commentaries by*: Khamsi R, *Nature* **432**:288 (2005); Hurtley S, *Science* **307**:483 (2005)].

4.1. Summary

Mutant huntingtin forms intracellular aggregates and is associated with neuronal death in select brain regions. Although R6/2 mice replicate many features of the disease, little neuronal death has been detected. Here we describe, for the first time, a dramatic atrophy and loss of orexin neurons in the lateral hypothalamus of R6/2 mice. Both the number of orexin neurons in the lateral hypothalamus and the CSF levels of orexin were reduced by about 72% in end-stage R6/2 mice. Correspondingly, we detected a significant atrophy and loss of orexin neurons in the lateral hypothalamus of HD patients. The lateral hypothalamus plays an important role in sleep regulation. In support, R6/2 mice develop a narcoleptic-like behavior. In addition to orexin cell loss, we also detected a significant reduction (by 38%) of melanin-concentrating hormone (MCH) neurons in end-stage R6/2 mice. MCH is an important peptide involved in the maintenance of energy homeostasis and the regulation of food intake, and the implications of this finding deserve further investigations. Our results reveal a loss of hypothalamic orexin and MCH neurons, which is a novel and potentially very important pathological feature in HD that may explain some of the symptoms of the disease, namely sleep disturbances and weight loss.

4.2. Introduction

The hypothalamus is one of the most functionally and neuroanatomically complex brain regions (**Figure 4.1**). It has long been recognized as a regulatory center that controls body homeostasis. Its functions include regulation of cardiovascular and autonomic functions, reproduction, body fluid homeostasis, energy metabolism, circadian rhythms, and the sleep-wakefulness cycle. A variety of studies suggest that multiple regions within the hypothalamus can regulate multiple physiological functions (for review see Hungs and Mignot, 2001; Taheri *et al.*, 2002). In particular, the lateral hypothalamus plays a critical role in the maintenance of wakefulness, and the regulation of the feeding behavior and energy homeostasis. Such disparate functions have been linked to distinct neuronal populations and their widespread axonal projections throughout the CNS, including the orexin (hypocretin) neurons, and the MCH-secreting neurons.

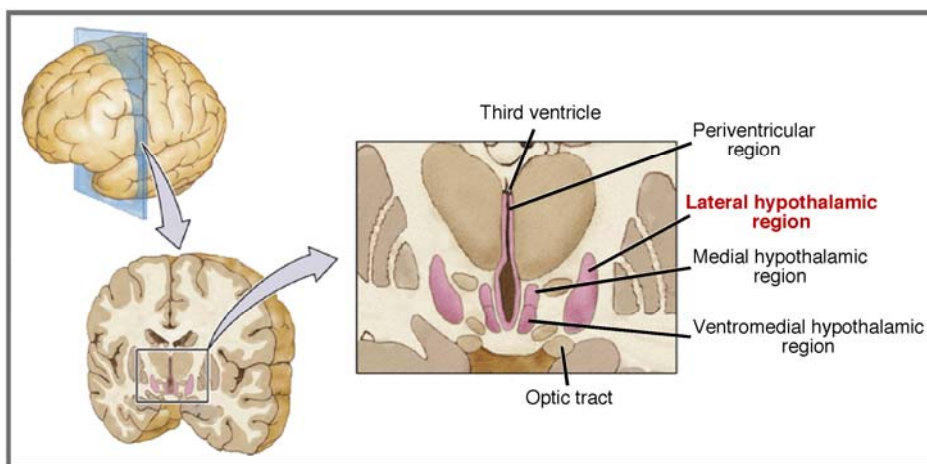


Figure 4.1. – A schematic representation of the human hypothalamus and its nuclei, viewed from a coronal perspective. The three principal regions of the hypothalamus are the periventricular, lateral, and medial regions. Adapted from Kolb and Wishaw, 2006.

Orexin neurons express the *orexin* gene, which codes for the precursor peptide prepro-orexin. Proteolytic cleavage of this precursor generates 2 orexin peptides: orexin-A (hypocretin 1; a 33 amino acid peptide) and orexin-B (hypocretin 2; a 28 amino acid peptide) (de Lecea *et al.*, 1998; Sakurai *et al.*,

1998). Orexin projections are particularly dense in monoaminergic centers and are thought to interact with the autonomic, neuroendocrine, and arousal systems (Date *et al.*, 1999). This occurs through the activation of 2 closely related GTP-binding protein (G protein)-coupled receptors, called orexin receptors 1 and 2 (OX1R and OX2R). OX1R is relatively selective for orexin-A and is coupled to the activation of the excitatory G_q subtype of G proteins. Activation of G_q proteins leads to the stimulation of phospholipase C and the influx of extracellular Ca^{2+} , which subsequently triggers the phosphatidylinositol cascade and the activation of protein kinase C. OX2R is a nonselective receptor for both orexin peptides and can be coupled either to excitatory G_q or inhibitory $G_{i/o}$ proteins, depending on the target neuron (for review see Beuckmann and Yanagisawa, 2002; Mieda and Yanagisawa, 2002).

Importantly, mice with a null mutation of either orexin (Chemelli *et al.*, 1999) or one of its receptors (Willie *et al.*, 2003), and transgenic mice with a targeted ablation of orexin neurons (Hara *et al.*, 2001) display severe disturbances in the sleep-wakefulness cycle. These sleep disturbances are similar to the symptoms observed in humans suffering from narcolepsy, a disease characterized by chronic sleepiness and a marked disorganization of the sleep/wake behaviour with abnormal manifestations of rapid eye movement (REM) sleep occurring during periods of wakefulness (for review see Siegel, 1999; Taheri *et al.*, 2002). Subsequent studies have shown that most human narcolepsy patients have reduced CSF levels of orexin (Ripley *et al.*, 2001; Dauvilliers *et al.*, 2003), and that in some cases a global loss of orexin is observed (Peyron *et al.*, 2000). Furthermore, one mutation in the *orexin* gene that impairs the peptide trafficking and processing, was found in a single case of early onset narcolepsy (Peyron *et al.*, 2000). Under normal conditions, orexins are thought to play a crucial role in sleep regulation by driving the cholinergic and monoaminergic tone throughout the sleep-wakefulness cycle. Furthermore, the suprachiasmatic nucleus (which contains neurons with a genetically identified biological clock that oscillates on a 24 hour cycle), projects to the orexin population in the lateral hypothalamus, explaining the occurrence of clock-dependent alertness (for review see Hungs and Mignot, 2001; Mignot *et al.*, 2002; Taheri *et al.*, 2002).

Another important neuronal population within the lateral hypothalamus is formed by MCH-containing neurons. MCH is a cyclic peptide formed by 19 amino acids that is generated via a proteolytic cleavage of its prepro-hormone, a process that also generates two additional peptides: neuropeptide E-I and neuropeptide G-E. Its biological functions are mediated through the activation of two G protein-coupled receptors: MCH-receptor 1 (MCHR1), which can be coupled to inhibitory G_i and excitatory G_q proteins and is expressed all over the

brain; and MCH-receptor 2 (MCHR2), which is exclusively coupled to excitatory G_q proteins and is only expressed in carnivores and primates. Although originally named due to its involvement in the regulation of skin color in fish, subsequent research showed that MCH plays a greater role in regulating various physiological functions. Indeed, MCH is believed to maintain energy homeostasis by regulating satiety, insulin and glucocorticoids levels, energy expenditure, and thermogenesis (for review see Jobst *et al.*, 2004; Shi, 2004). MCH and MCHR1 expression is up-regulated by genetic obesity and food deprivation. Intracerebroventricular injection or chronic infusion of MCH stimulates food intake and body weight gain; whereas, continuous treatment of mice with a MCHR1 antagonist suppresses appetite and decreases adiposity (for review see Shi, 2004).

Although the lateral hypothalamus has not been considered a major site for neurodegeneration in the human HD brain, several neuropathological studies of end-stage HD patients have demonstrated up to a 90% cell loss in the lateral tuberal nucleus of the hypothalamus (section 1.2.2; Kremer *et al.*, 1990, 1991). Interestingly, in humans this region is particularly enriched with NMDA receptors (Kremer *et al.*, 1993). Moreover, a recent study showed that in rat organotypic slice cultures of the lateral hypothalamus, orexin neurons are particularly susceptible to excitotoxic damage (Katsuri and Akaike, 2004). These observations suggest that excitotoxic cell death, which has been repeatedly suggested to play a role in the cell death observed in other brain regions (section 1.4.1; for review see Beal, 2000; Petersén and Brundin, 2002), may also account for the loss of lateral hypothalamic neurons in HD patients.

In this study we explore whether cell loss occurs in the lateral hypothalamus of R6/2 mice. We focused on orexin and MCH-secreting neurons, since the loss of these populations can have symptomatic implications in HD (namely, at the level of sleep disturbances and loss of body weight). Furthermore, we explored whether orexin neurons were also lost in the lateral hypothalamus of HD patients.

4.3. Materials and Methods

4.3.1. Transgenic Animals

We used transgenic HD mice of the R6/2 line and their wild-type littermates (Jackson Laboratories) in this study. The colony was maintained by crossing transgenic males with females of their background strain (F1 of CBA x

C57BL/6J). Tails of the offspring were used to obtain DNA for determination of the genotype using a PCR assay (Mangiarini *et al.*, 1996). The mice were housed in groups with *ad libitum* access to food and water at a 12-hour light/dark cycle. The experimental procedures were approved by the Ethical Committee for the use of laboratory animals at Lund University, Sweden.

4.3.2. Human HD Brains

We evaluated formalin-fixed brains of 5 HD patients (age 69 ± 6 years) and 4 controls (age 64 ± 10 years) from the Leiden University Hospital Brain Bank, Leiden, The Netherlands (Table IV).

4.3.3. Tissue Processing and Histology

R6/2 mice and wild-type littermates at 3.5, 7.5-8, 11.5-12 and 12.5 weeks ($n = 4-9/\text{genotype/age}$) of age were deeply anesthetized with pentobarbital and transcardially perfused with saline followed by 4% PFA in 0.1 M PBS. The brains were left in the fixative overnight and then dehydrated in 20% sucrose/0.1 M PBS. Coronal sections were cut in 6 series throughout the brains on a freezing sliding microtome and collected in PBS. Tissue from wild-type/controls and R6/2/HD subjects was processed in parallel for immunohistochemistry to control for labeling intensity.

Separate series of free-floating mouse sections were processed for detection of orexin-A, MCH, NeuN, and GFAP proteins. Briefly, the sections were quenched in 3% H_2O_2 /10% methanol in 0.1 M PBS for 15 minutes, and preincubated with the proper sera. The sections were then incubated overnight at room temperature (or during 48 hours at 4°C) with a rabbit polyclonal antibody against orexin-A (diluted 1:700; Phoenix Pharmaceuticals Inc., Belmont, CA, USA), a rabbit polyclonal antibody against MCH (diluted 1:500; Phoenix Pharmaceuticals Inc.), a mouse monoclonal antibody against NeuN (diluted 1:1000, Chemicon), and a rabbit polyclonal antibody against GFAP (diluted 1:700; Dako, Glostrup, Denmark), respectively. The sections were then incubated for 2 hours with the respective secondary antibodies (biotinylated horse anti-mouse IgG, diluted 1:200, Vector Laboratories; and biotinylated swine anti-rabbit IgG, diluted 1:200, Dako), and visualized with an avidin–biotin–peroxidase complex system (Vectastain ABC Elite Kit; Vector Laboratories) using DAB as the chromogen. A separate series of mice brain sections was also processed with cresyl violet (ICN Biomedicals Inc.), as described in section 2.3.3.

To evaluate whether orexin-A-positive neurons possess NIIs of mutant

huntingtin, orexin-A/EM48 double-labeling was also performed. Briefly, after preincubation in blocking solution (in 1% bovine serum albumine, BSA/0.1 M PBS) containing NHS and normal donkey serum (NDS), the sections were incubated for 48 hours at 4°C with the mouse monoclonal anti-huntingtin antibody (EM48, diluted 1:500; Chemicon; which was shown to be specific also in mouse tissue; Yu *et al.*, 2002) and the rabbit polyclonal anti-orexin-A antibody (diluted 1:700; Phoenix Pharmaceuticals Inc.). The sections were then incubated with the secondary antibodies: Texas Red dye-conjugated donkey anti-rabbit IgG (diluted 1:200, Jackson ImmunoResearch, West Grove, PA, USA) and biotinylated horse anti-mouse IgG (diluted 1:200; Vector Laboratories) for 2 hours, followed by incubation with Fluorescein (FITC)-conjugated streptavidin (diluted 1:200, Dako) for 2 hours.

Paraffin embedded human brain sections (15 µm thickness) were processed for orexin-A immunohistochemistry. Briefly, after de-waxing in xylene and rinsing in ethanol, the endogenous peroxidases were blocked in 0.3% hydrogen peroxide/methanol for 20 minutes. The sections were then incubated overnight at room temperature with the rabbit polyclonal antibody against orexin-A (diluted 1:1500; Phoenix Pharmaceuticals Inc.), and finally with the secondary antibody biotinylated swine anti-rabbit IgG (diluted 1:600; Dako) for 1 hour. The bound antibodies were visualized as described above.

4.3.4. Stereological Techniques and Cell Quantification

All morphological analyses listed below were performed on blind-coded slides, using the stereological equipment described before (*section 2.3.4*) with a 40x objective.

Due to the low numbers of orexin neurons, we were unable to perform proper stereological quantification. Instead, the density of orexin neurons in the lateral hypothalamus of R6/2 and wild-type mice ($n = 4-9/\text{genotype/age}$) was assessed in the 3 sections with the largest number of orexin immunopositive neurons per brain (distance between the sections: 150 µm). The outer border of the lateral hypothalamus was determined by delineating the region just outside the location of the orexin-immunopositive neurons. Using a systematic random sampling technique, the number of labeled cells was assessed in 25% of the delineated area. Only profiles characterized by intense dark labeling throughout the cell body were counted. Note that significantly lighter profiles were not counted, since we were uncertain whether they represented true orexin-positive cells. Profiles were included independently of the size or shape of their soma, as some cells were atrophied (see *section 4.4.1*). The same technique was used for

all mice. The average density of orexin positive neurons in the 3 sections from each mouse was used in the statistical analysis.

Due to sufficiently large enough numbers of MCH-positive neurons in the lateral hypothalamus of 8- and 12-week-old mice, their total numbers were assessed by stereological methods (Gundersen *et al.*, 1988). For systematic sampling, the frame area (2437-2442 μm^2) and the counting interval (x and y both 100 μm) were set to allow for at least a total of 200 cells to be sampled in 4 sections of the lateral hypothalamus with the highest density of MCH-positive cells (distance between the sections: 150 μm). The outer border of the lateral hypothalamus was determined by delineating the region just outside the location of the MCH-immunopositive neurons. The optical dissector was set to sample all cells below the first 2.5 μm and above the last 2.5 μm of the top and bottom surfaces of the section. Only profiles characterized by intense dark labeling throughout the cell body were counted. Significantly lighter profiles were not counted, since we were uncertain whether they represented true MCH-positive cells. Profiles were included independently of the size or shape of their soma, as some cells were atrophied (see *section 4.4.4*).

The cross-sectional soma area from 30 randomly selected orexin- or MCH-immunopositive neurons was determined in 3 to 4 sections from 4 to 7 mice per genotype and age, by delineation of their soma circumference. Neurons were selected based on the intensity of their labeling throughout the cell body and regardless of their size and shape of their soma, as some cells were atrophied (see *sections 4.4.1* and *4.4.4*). Significantly lighter profiles were not counted, since we were uncertain whether they represented true orexin- or MCH-positive cells.

In adjacent sections of the lateral hypothalamus, the density of cresyl violet stained cells, neurons (NeuN-labeled), and neurons containing NIIs (EM48-positive) were assessed in 12.5-week-old mice. The procedure was identical to the one previously established to assess the number of orexin-positive neurons. Cell counts were performed in 3 sections per brain (distance between the sections: 150 μm).

The presence of EM48-immunopositive NIIs in orexin-A-labeled neurons was analyzed in 100 randomly selected orexin-A-positive neurons in the 3 mentioned sections from 4 mice per genotype at the ages of 3.5, 7.5 and 12.5 weeks.

In the human brains, we compared sections containing orexin-A-positive cells from each individual and selected the section that appeared to have the highest density of orexin-A-positive cells. In this section, orexin-A-positive neurons were counted in 4 different fields delineated by a 1 mm^2 ocular grid.

The cross sectional soma area of 20 randomly selected orexin-A positive cell bodies/individual was also determined.

4.3.5. Radioimmunoassay

Hypothalami dissected from 12.5-week-old mice ($n = 7$ / genotype) or CSF withdrawn from the cisterna magna of 12-week-old mice ($n = 4$ / genotype) were used for peptide extraction. Using commercially available ^{125}I radioimmunoassay (RIA) kits (Phoenix Pharmaceuticals), orexin-A (CSF and brain tissue) and orexin-B (brain tissue) were measured. Duplicate samples were assayed and levels were determined against a known standard.

4.3.6. Electron Microscopy

Mice of 12 weeks of age ($n = 2$ / genotype) were perfused with 0.075 M Sørensen buffer containing 3% paraformaldehyde and 1% glutaraldehyde. Hypothalami were dissected and fixed overnight in the same fixative, rinsed in Sørensen buffer, post-fixed for 1 hour with 1% OsO_4 in the same buffer, dehydrated in acetone and embedded in Polybed 812. Ultra thin sections were cut and placed on copper grids before contrasted with 0.5% lead citrate and 4% uranyl acetate. Specimens were examined in a Philips CM10 transmission electron microscope.

4.3.7. Scoring of Narcoleptic-Like Episodes

We videorecorded and scored narcoleptic-like episodes in R6/2 and wild-type mice at the following ages: 3.5 ($n = 5$), 7.5 ($n = 5$), 11.5 ($n = 3$), and 12.5 ($n = 3$) weeks, according to the procedure described by Chemelli and colleagues (Chemelli *et al.*, 1999). Different mice were used for each age. Briefly, the mice were habituated for 3 hours in individual glass cylinders covered with bedding material before they were recorded during the first 4 hours of the dark cycle with a Sony CCD infrared videocamera. For each behavioral experiment, 1 R6/2 and 1 wild-type mouse were videorecorded simultaneously. The scoring of the episodes was carried out by 2 investigators blinded to the mouse genotype. The episodes of behavioral arrest were classified into 3 different categories according to their severity: **(1)** periods of no movement; **(2)** periods of no movement with an abrupt and/or sudden change of posture in the beginning of the episode; and **(3)** episodes involving loss of muscular tone, and/or a sudden collapse of the head and neck, occasionally causing the mouse to fall completely onto its side. The same protocol was used to evaluate the behavior of 12-week-old R6/2 mice ($n = 4$) during the light-phase of the diurnal cycle.

4.3.8. EEG and EMG Recordings

At 10 weeks of age, mice ($n = 4$ for R6/2; $n = 2$ for wild-type) were implanted with recording electrodes. One cortical screw electrode was attached to the right parietal bone to record the electroencephalogram (EEG) and a wire electrode (insulated copper, 250 μm in diameter, tip exposed to 1.5 mm, Belden, St. Louis, MI, USA) was attached between the occipital bone and the neck muscles to record the electromyography (EMG). Both electrodes were referenced to a frontal screw electrode. Two additional anchor screws were attached onto the left parietal and frontal bone, and a 3-way connector (Plastic One, Roanoke, VA, USA) fixed above the screws with dental acrylic cement. Twelve to 15 days following electrode implantation, pairs of mice (wild-type and R6/2) were videotaped and had the EEG and EMG recorded continuously (Chart 3.6.3, PowerLab/MacLab ADInstruments, Aarhus, Denmark) during the first 4 hours of their dark cycle. Videotapes were scored for narcoleptic-like episodes (section 4.3.7) and EEG parameters were analyzed with Chart 3.6.3 software.

4.3.9. Statistical Analysis

The data were analyzed with a 1- or 2-factor ANOVA when appropriate, or unpaired Student's t tests, using the Statview 5.4 package (Abacus Concepts). Data were presented as mean or median \pm S.E.M. A p value of < 0.05 was considered statistically significant.

4.4. Results

4.4.1. Orexin Loss in R6/2 Mice

We observed a progressive reduction with age in the number of orexin neurons in the R6/2 lateral hypothalamus compared to wild-type mice (2-factor ANOVA; genotype $p < 0.0001$, $F(1, 44) = 94.68$; age $p < 0.0001$, $F(3, 44) = 40.10$; age \times genotype $p < 0.0001$; $F(3, 44) = 28.12$) (**Figure 4.2**). This reduction was not apparent at 3.5 weeks of age, but after 7.5 weeks orexin cell loss was clear (**Figure 4.2.E**).

The surviving orexin neurons were significantly atrophied in R6/2 mice compared to wild-type, as assessed by measuring the cross sectional surface area of the cell bodies (2-factor ANOVA; genotype $p < 0.0001$, $F(1, 24) = 23.50$; age

$p < 0.0001$, $F(3, 24) = 13.91$; age \times genotype $p = 0.01$; $F(3, 24) = 4.49$) (**Figure 4.2.F**).

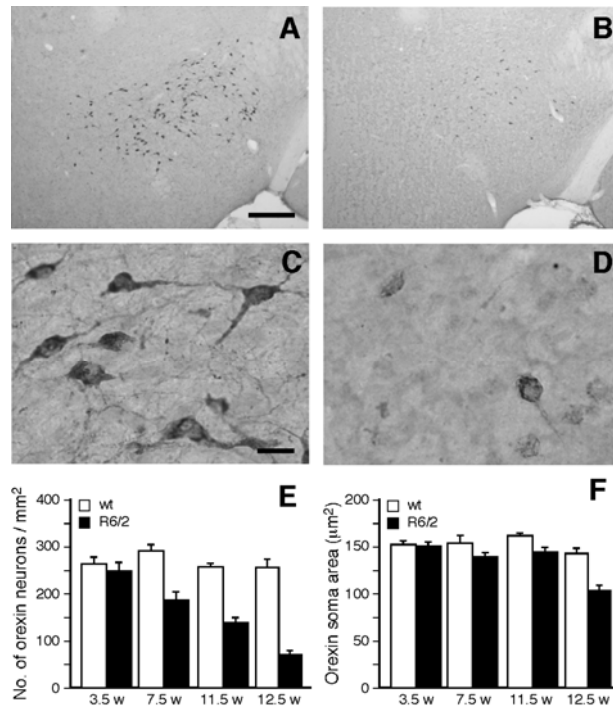


Figure 4.2. - Progressive loss and atrophy of orexin neurons in R6/2 mice. Sections of lateral hypothalamus processed for orexin-A immunohistochemistry in wild-type (**A**, **C**) and R6/2 (**B**, **D**) mice at 12.5 weeks of age. Scale bar = 200 μm (**A**) and 20 μm (**C**). (**E**) Progressive reduction in the density of orexin-immunopositive neurons ($n = 4$ to 9 / genotype/age). (**F**) Progressive decrease of the cross-sectional surface area of the somata of the orexin-positive neurons ($n = 4$ / genotype) in R6/2 mice compared to wild-type littermates. Values represent means \pm S.E.M.

To further investigate whether reduction in orexin cells counts was due to actual cell loss rather than reduced orexin protein expression in surviving cells, adjacent sections were processed for cresyl violet and NeuN immunohistochemistry. At 12.5 weeks of age, we found a significant reduction of the number of cresyl violet stained cells (wild-type: $5363 \pm 193 / \text{mm}^2$; R6/2: $4381 \pm 345 / \text{mm}^2$, Student's t test, $p < 0.05$) and cells immunopositive for the neuron-specific marker NeuN (wild-type: $3704 \pm 143 / \text{mm}^2$; R6/2: $3138 \pm 167 / \text{mm}^2$, Student's t test, $p < 0.05$) in R6/2 mice.

Although we did not use proper stereological methods to determine the total cell numbers in the lateral hypothalamus (*section 4.3.4*), we estimate that the percentage of orexin neurons (i.e., number of orexin-positive cells compared to the number of NeuN-positive neurons) in the lateral hypothalamus was around 7% in wild-type mice and 2% in R6/2 mice of 12.5 weeks of age. Moreover, according to our estimations, end-stage R6/2 mice lost around 15% of neurons in the lateral hypothalamus, among which 72% were orexin-positive. However, we cannot completely exclude the possibility that this percentage may be overestimated since we excluded lightly labeled profiles (*section 4.3.4*), which may represent a down-regulation of orexin expression, from our quantification criteria.

Using transmission electron microscopy, we observed frequent ultrastructural signs of neurodegeneration in the lateral hypothalamus of R6/2 mice, with some neurons displaying “dark degeneration” (**Figure 4.3**) as previously described in other brain regions of R6/2 mice (*section 1.6.1.2*; Iannicola *et al.*, 2000; Turmaine *et al.*, 2000; Yu *et al.*, 2003; Stack *et al.*, 2005). No gliosis was apparent in 12.5-week-old R6/2 brains as assessed in hypothalamic sections processed for GFAP immunohistochemistry (data not shown).

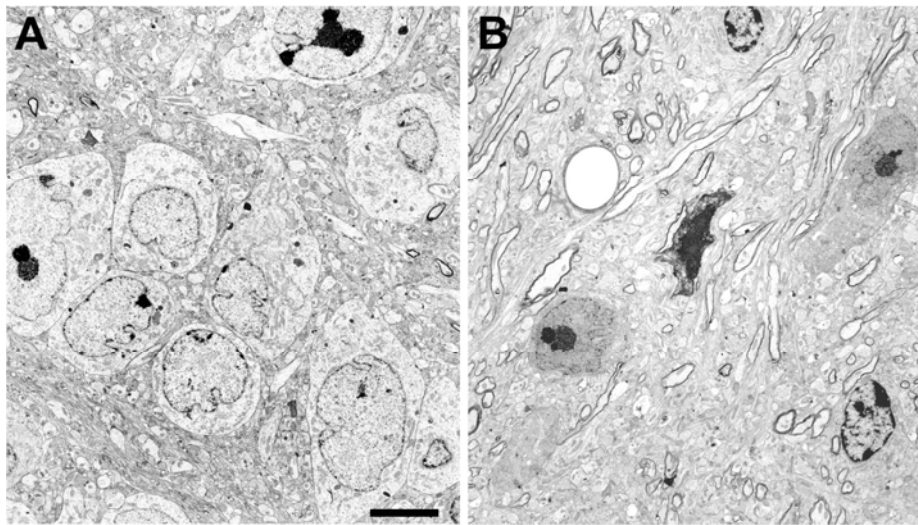


Figure 4.3. - *Dark neuron degeneration in the R6/2 lateral hypothalamus.* Transmission electron micrographs of lateral hypothalamus from a 12-week-old wild-type (A) and R6/2 mouse (B) showing examples of dark degenerating nerve cell bodies in the R6/2 mouse. Scale bar = 5 μ m.

We also studied the frequency of huntingtin inclusions in orexin immunopositive neurons in R6/2 mice. In 3.5-week-old R6/2 mice, none of the orexin neurons in the lateral hypothalamus contained EM48-immunopositive inclusions, while at 7.5 weeks $50 \pm 6\%$ of the orexin-positive neurons were EM48-positive. On average, $77.5 \pm 5\%$ of the NeuN-immunopositive neurons in the 12.5-week-old R6/2 lateral hypothalamus displayed EM48 immunoreactive inclusions, but only $57 \pm 5\%$ of the remaining orexin-positive neurons contained inclusions (Student's *t* test, $p < 0.05$).

Using RIA, we found a significant reduction of both orexin-A and orexin-B levels in R6/2 compared to wild-type mice at 12.5 weeks of age, both in the hypothalamus and in the remaining brain tissue (**Table III**).

Table III - Orexin levels in R6/2 mice.

	Hypothalamus		Brain (excluding the hypothalamus)	
	Wild-type	R6/2	Wild-type	R6/2
Orexin-A (ng/g tissue)	28.0 ± 1.5	$6.6 \pm 1.3^{***}$	17.9 ± 4.7	$2.2 \pm 1.5^*$
Orexin-B (ng/g tissue)	26.6 ± 1.3	$2.8 \pm 0.2^{***}$	15.2 ± 1.3	$2.8 \pm 0.4^{***}$

RIA measurements in 12.5-week-old mice ($n = 7$). Student's *t* test, $^{***} p < 0.0001$, $^* p < 0.05$ as compared to wild-type. Values are presented as means \pm S.E.M.

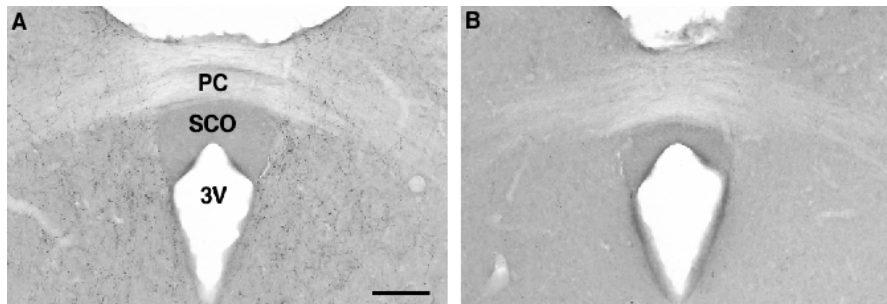


Figure 4.4. - Photomicrographs of the pineal region around the third ventricle in a 12-week-old wild-type (**A**) and R6/2 (**B**) mouse showing loss of orexin fibers in the R6/2 mouse. Scale bar = 100 μ m. *PC* (posterior commissure), *SCO* (subcommissural organ), *3V* (third ventricle).

The later result indicates that the projections of orexin neurons throughout the CNS are affected. Importantly, we found severe loss of orexin-immunoreactive fibers around the third ventricle and the subcommissural organ, a region representative of the pineal gland (Mikkelsen *et al.*, 2001), in 12.5-week-old R6/2 mice (**Figure 4.4**).

Using RIA, we also determined the levels of orexin in the CSF of 12-week-old R6/2 mice and wild-type littermate controls. Compared to the wild-type orexin CSF levels (2070 ± 130 pg/ml), end-stage R6/2 mice showed a 72% reduction in the CSF levels of this peptide (590 ± 170 pg/ml, Student's *t* test, $p < 0.001$).

4.4.2. Narcoleptic-Like Episodes in R6/2 Mice

We performed infrared video recordings of mice at different ages during the first 4 hours of their dark cycle to analyze whether the orexin loss in R6/2 mice would result in the appearance of narcoleptic-like episodes (Chemelli *et al.*, 1999). At 3.5 weeks of age, R6/2 mice were indistinguishable from wild-type controls, with periods of hyperactivity and intense exploratory behavior intercalated by prolonged periods of rest and normal sleeping (**Figure 4.5.A**). However, at 7.5 weeks of age we observed several periods of brief behavioral arrest in R6/2 mice ($n = 5$; 1 to 8 episodes/mouse; median = 6) (**Figure 4.5.A**). These episodes were characterized by a sudden interruption of purposeful motor activity associated with a change of posture that was maintained throughout the episode. This resembles the narcoleptic episodes that have been described in *orexin* knockout mice (Chemelli *et al.*, 1999). At 11.5 and 12.5 weeks, these episodes become even more frequent, and over 4 hours we observed 11 to 14 ($n = 3$; median = 11), and 10 to 14 episodes of behavioral arrest per mouse ($n = 3$; median = 13), respectively (**Figure 4.5.A**). At 12.5 weeks of age, most of the episodes occurred during the first and the third hours of the dark phase, and their duration varied between 3 and 214 seconds ($n = 3$; mean = 62 seconds). An example of the episode distribution for one R6/2 mouse is illustrated in **Figure 4.5.B**.

To further characterize this behavior in end stage mice, we divided the episodes of behavioral arrest into 3 different categories according to their severity (*section 4.3.7*). All R6/2 mice examined ($n = 3$) showed episodes of no movement (5 to 9 episodes per mouse; median = 7). Two of the mice also exhibited abrupt and sudden changes of posture; and interestingly, all 3 mice displayed narcoleptic-like episodes with complete falls onto the side (4 to 5 falls per mouse; median = 4) (**Figure 4.5.C**). These episodes were followed by sudden bouts of locomotion with hyperactivity.

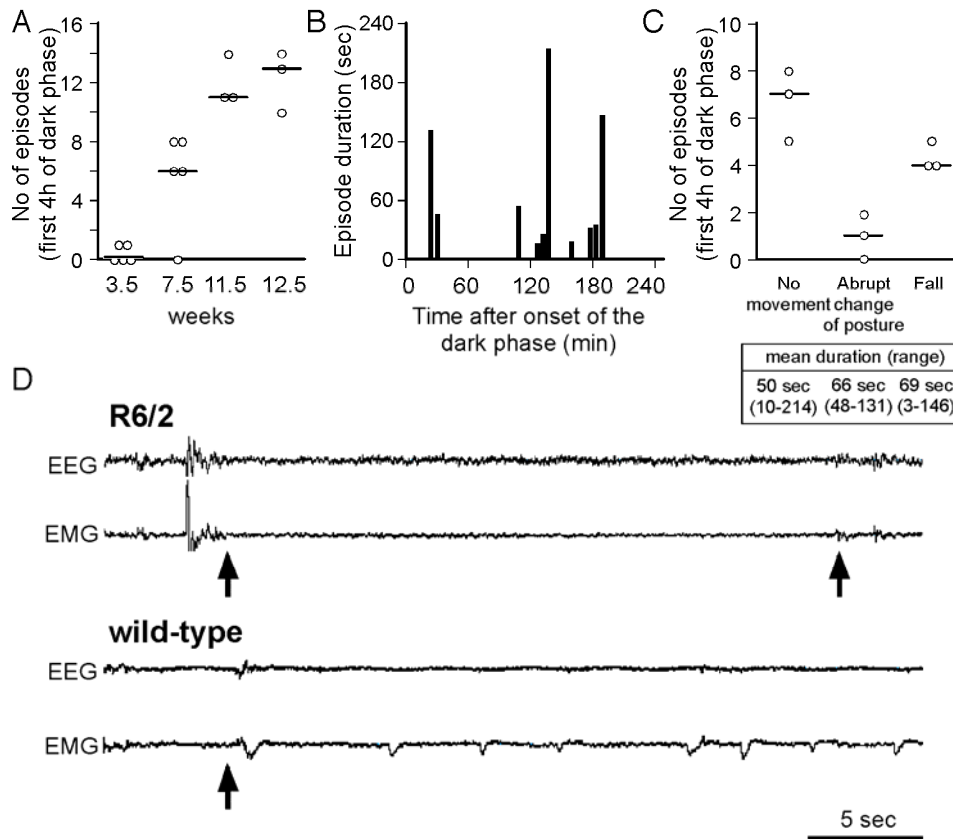


Figure 4.5.- Characterization of narcoleptic-like episodes in R6/2 mice. All analysis of narcoleptic-like episodes was performed during the first 4 hours of the dark phase, which is the active period for mice. **(A)** The total number of narcoleptic-like episodes increases with age in R6/2 mice. Different mice were used for each time-point. **(B)** The duration of the narcoleptic-like episodes for a 12.5-week-old R6/2 mouse and the period in which they occurred are illustrated by the vertical lines. **(C)** The total number of narcoleptic-like episodes per mouse divided into 3 different categories in 12.5-week-old R6/2 mice ($n = 3$). Inserted table shows the mean duration of each of the different categories of narcoleptic-like episodes. **(D)** Typical EEG / EMG recording before and during a narcoleptic-like episode in a 12.5-week-old R6/2 mouse, showing reduced EMG activity and no epileptic activity in the EEG. Arrows indicate the beginning and the end of the narcoleptic-like episode. In contrast, the EEG / EMG recording of a resting wild-type mice display continued low level EMG activity also when the mouse is not ambulatory. Arrow indicates the beginning of the period.

Using the same criteria as above, we also evaluated the behavior of 12-week-old R6/2 mice during the day, when mice are normally inactive. Interestingly, during the light-phase of their diurnal cycle, R6/2 mice generally spent less time sleeping than wild-type mice. However, they exhibited repeated, sudden episodes of behavioral arrest often associated with an abrupt change of posture. These kinds of episodes were never observed with wild-type littermate controls (data not shown).

Since R6/2 mice are known to be convulsive-prone (Mangiarini *et al.*, 1996; Gil *et al.*, unpublished observations), we subjected a separate group of 12.5-week-old R6/2 ($n = 4$) and wild-type ($n = 2$) mice to EEG / EMG recordings to determine whether the observed episodes of behavioral arrest, interpreted as narcoleptic-like, were instead caused by seizure activity. Mice were video recorded while the EEG / EMG activities were assessed, and the episodes of behavioral arrest were scored. Our video-EEG recordings revealed no epileptiform electrographic activity during episodes of motor arrest. Rather, the EEG was characterized by small amplitude theta activity and reduced EMG signal of the neck muscles (**Figure 4.5.D**). In contrast, when wild-type mice occasionally paused in their movements, EMG activity was not decreased (**Figure 4.5.D**).

4.4.3. Orexin Cell Loss in HD Brains

To ensure that loss of orexin containing neurons was also relevant to the human condition, we examined the lateral hypothalamus from HD patients.

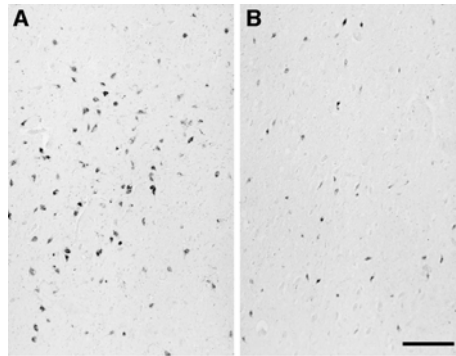


Figure 4.6. - Reduction in orexin neurons in HD patients. Representative microphotographs of orexin-A immunopositive neurons in the lateral hypothalamus of a control individual (A) and an HD patient (B). The illustration shows both atrophy of the individual neurons and a reduction in orexin immunopositive neurons in the HD patient brain compared to the control brain. Scale bar = 500 μm .

The mean number of orexin-positive neurons / mm² in the section showing the highest density of orexin-positive neurons for each subject is given in **Table IV**. In control brains from healthy individuals, the mean number of orexin-positive neurons / mm² was estimated to be 62 ± 4 neurons. In corresponding areas in brains from HD affected individuals (grade II-IV) the mean number of orexin-positive neurons was 45 ± 1 / mm² (Student's *t* test, *p* < 0.005; **Figure 4.6.A-B**, and **Table IV**). There seems to be no obvious relationship between the Vonsattel grade and the loss of orexin neurons (**Table IV**).

Table IV - Data on HD patients and controls.

	Brain Weight (g) & Fixation Time (months)	Postmortem Interval (hours)	Vonsattel Grade	CAG Repeats	No. Orexin Neurons/mm²
HD					
1	1200 g / 2 months	unknown	III	20/43	45
2	- / 5 months	< 24 hours	III	-	40
3	- / 9 months	15 hours	II	-	47
4	1175 g / 15 months	< 24 hours	III	17/46	46
5	- / 2.5 months	4 hours	IV	16/39	49
Controls					
1	1200 g / 5 months	15 hours	-	-	54
2	1510 g / unknown	13 hours	-	-	70
3	- / unknown	unknown	-	-	66
4	1300 g / unknown	6 hours	-	-	58

There was also a significant neuronal atrophy in orexin cells of HD patients, detected as a reduction in the mean cross-sectional surface area of the orexin cell bodies in HD patients (230 ± 33 μm²) compared to controls (363 ± 8 μm²) (Student's *t* test, *p* < 0.05).

4.4.4. Loss of MCH-Containing Neurons in R6/2 Mice

As stated above, we estimate that end-stage R6/2 mice lost around 15% of neurons in the lateral hypothalamus, among which 72% were orexin-positive (*section 4.4.1*). Therefore, the loss of orexin-containing neurons *per se* cannot

account for the total decrease in the estimated number of hypothalamic neurons. Thus, we sought to investigate MCH-secreting neurons, which constitute a separate neuronal population within the lateral hypothalamic region (*section 4.2*; Steininger *et al.*, 2004).

By performing MCH immunohistochemistry in brain sections from 8- and 12-week-old mice, we observed a progressive reduction with age in the number of MCH-containing neurons in the lateral hypothalamus of R6/2 mice, as compared to their wild-type littermate controls (2-factor ANOVA; genotype $p < 0.01$, $F(1, 17) = 8.55$; age $p < 0.05$, $F(1, 17) = 8.01$; age x genotype $p = 0.12$, $F(1, 17) = 2.72$) (**Figure 4.7.A**). We detected a 38% reduction in the number of MCH-positive neurons in 12-week-old R6/2 mice. The remaining neurons in end-stage R6/2 mice were significantly atrophied (2-factor ANOVA; genotype $p < 0.0001$, $F(1, 17) = 65.58$; age $p < 0.001$, $F(1, 17) = 17.98$; age x genotype $p = 0.21$; $F(1, 17) = 1.73$) (**Figure 4.7.B**). Note that the decrease in MCH neurons was not as dramatic as for orexin-positive neurons.

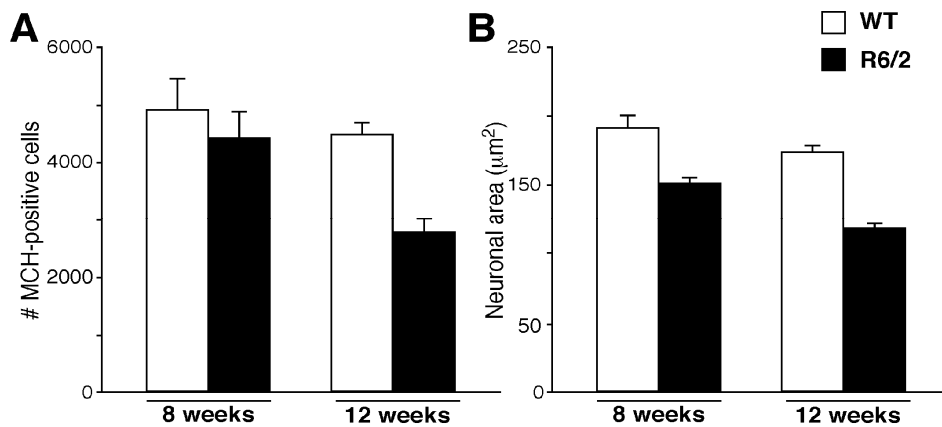


Figure 4.7. - Progressive loss and atrophy of MCH-containing neurons in R6/2 mice. **(A)** Progressive reduction in the density of MCH-immunopositive neurons in R6/2 mice compared to wild-type littermates ($n = 4$ to 7 / genotype/age). **(B)** Progressive decrease of the cross-sectional surface area of the somata of MCH-positive neurons in R6/2 mice compared to their wild-type littermates ($n = 4$ to 7 / genotype). Values represent means \pm S.E.M. (Gil and Petersén *et al.*, unpublished observations).

4.5. Discussion

In HD there is pronounced neuronal death in select brain regions. Although transgenic HD mouse models have provided valuable insight into disease mechanisms, they have not reproduced the extent and specific patterns of cell death that occur in HD patients. This is true for the R6/2 mouse, which exhibits reduced cell loss in the striatum and the cerebral cortex (*section 1.6.1.2*; Iannicola *et al.*, 2000; Turmaine *et al.*, 2000; Yu *et al.*, 2003; Stack *et al.*, 2005).

Now, for the first time, this study demonstrates progressive neuronal loss in the lateral hypothalamus of R6/2 mice. We have identified at least 2 neuronal populations that are lost in these mice: orexin and MCH-containing neurons. There was also a significant depletion of orexin in samples from hypothalamic tissue (that contain the cell bodies of the orexin neurons) and from the remaining regions of the brain (that receive orexin-projections).

Moreover, we found that HD patients display loss and atrophy of orexin-immunolabeled neurons in the lateral hypothalamus. There appears to be no obvious relationship between the Vonsattel grade and the loss of orexin neurons. This is most likely due to the fact that the Vonsattel scale is based on assessing striatal degeneration (*section 1.2.2*; Vonsattel *et al.*, 1985; for review see Vonsattel and DiFiglia, 1998). Degeneration in the hypothalamus might not follow the same time course as in the striatum.

Deficits in orexin neurotransmission result in narcoleptic-like behavior in mice (*section 4.2*; Chemelli *et al.*, 1999; Hara *et al.*, 2001; Willie *et al.*, 2003), as well as dogs (Lin *et al.*, 1999). In our study, the frequency, duration, and general appearance of the narcoleptic-like episodes in R6/2 mice are very similar to those observed both in *orexin* knock-out mice and mice with mutant orexin receptors (Chemelli *et al.*, 1999; Hara *et al.*, 2001; Willie *et al.*, 2003). Furthermore, it appears to be a relationship between the loss of orexin neurons and the gradual onset of the narcoleptic-like phenotype in R6/2 mice. Interestingly, R6/2 mice exhibit a progressive disruption of the circadian rhythm caused by dysregulation of circadian rhythm genes in the suprachiasmatic nucleus of the hypothalamus (Morton *et al.*, 2005). We have found that orexin fibers are lost in the R6/2 pineal region (**Figure 4.4**), which is involved in regulating the circadian rhythm via connections with the suprachiasmatic nucleus. Although no reports exist of HD patients actually suffering from narcolepsy, there is evidence that sleep patterns are disturbed (Petit *et al.*, 2004). A thorough evaluation of their sleep/wakefulness cycle is therefore warranted.

There is other evidence suggesting that orexin-containing neurons are sensitive to the expression of proteins with an expanded polyglutamine tail. Genetically engineered rodent models that express an ataxin-3 construct with a

large number of CAG repeats (i.e., the gene responsible for the development of the polyglutamine disorder SCA3; *section 1.1*) in orexin neurons show hypothalamic degeneration (Hara *et al.*, 2001; Beuckmann *et al.*, 2004). Other studies demonstrate that null mutant mice for HAP1 exhibit hypothalamic degeneration and die early due to impaired feeding. As well, N171-82Q HD mice show a depletion of HAP1 and hypothalamic neuronal degeneration (Li SH *et al.*, 2003). These results suggest that a disturbance in the function of critical huntingtin-interacting proteins (e.g., HAP1) may lead to neurodegeneration in the hypothalamus.

Another explanation for the vulnerability of hypothalamic orexin-containing neurons may be related to the expression of NMDA receptors. Recently, it was shown that exposing rat hypothalamic organotypic slice cultures to an excitotoxic insult results in a specific loss of orexin neurons (Katsuki and Akaike, 2004). As previously discussed, excitotoxicity is a likely contributor to cell death in HD (*section 1.4.1*; for review see Beal, 2002; Petersén and Brundin, 2002).

Despite the loss of orexin neurons in the lateral hypothalamus, the NeuN cell counts suggest that more than just orexin cells are lost on R6/2 mice. Indeed, we also found a decrease in the number of MCH-containing neurons in this brain region (**Figure 4.7**; Gil and Petersén *et al.*, unpublished observations). However, unlike the orexin neurons, this decrease appears later in the progression of the disease and the observed loss is not as severe. The later onset of the loss of MCH neurons may be partially due to the fact that MCH-containing neurons are more resistant to NMDA-induced excitotoxicity than orexin neurons. Indeed, it has been shown in rat organotypic hypothalamic slice cultures that MCH-containing neurons have a greater hyperpolarized resting membrane potential than orexin neurons. Therefore, when exposed to the same excitotoxic stimulus, the NMDA receptors present in orexin neurons may be more readily activated than those in MCH neurons (Katsuki and Akaike, 2004).

Nevertheless, the loss of MCH-containing neurons is likely to have implications for the symptoms and the progression of HD. As mentioned above, MCH is a neuromodulator involved in the regulation of energy homeostasis and food intake. Indeed, recent studies in rodents have shown that central administration of MCH promotes feeding; whereas, fasting induces an increase in the expression of this peptide (*section 4.2*; for review see Shi, 2004). Furthermore, *MCH* knock-out mice are lean as a result of hypophagia and a slightly elevated metabolic rate (Shimada *et al.*, 1998). Mice with a target deletion of the *MCHR1* gene are resistant to obesity and show increased energy expenditure (Chen *et al.*, 2002; Marsh *et al.*, 2002). Moreover, a severe loss of body weight is observed both in end-stage R6/2 mice (*section 1.6.1.4*;

Mangiarini *et al.*, 1996) and late stage HD patients (*section 1.2.1*). Whether there is a relationship between the loss of MCH-containing neurons in the lateral hypothalamus and the loss of body weight in R6/2 mice and HD patients is an exciting hypothesis that deserves further investigation. In this respect, it will be important to know if the loss of MCH-containing neurons is replicated in the human condition.

Currently, there are no biomarkers available to evaluate the progression of HD and effectiveness of therapeutic interventions. Using plasma or CSF measurements of substances secreted from brain sites, such as the hypothalamus, offer a relatively rapid and cost effective strategy to identify neurodegeneration. In end-stage R6/2 mice, both the number of orexin neurons in the lateral hypothalamus and the levels of orexin in the CSF were reduced by 72%, suggesting that orexin could be used as a biomarker to detect for hypothalamic neurodegeneration in HD. Considering the corresponding loss and atrophy of orexin neurons in the human condition, it was reasonable to speculate that orexin CSF levels may be reduced in HD patients as well. Since the publication of our initial work, two small studies have extended our results and tested this hypothesis (Gaus *et al.*, 2005; Meier *et al.*, 2005). Each study compared the orexin CSF levels from about 10 patients with genetically validated HD. However, contrary to our expectations, no changes in CSF orexin levels were detected in these HD patients (Gaus *et al.*, 2005; Meier *et al.*, 2005). A recent collaboration involving our group and three other research centers also revealed no significant changes in orexin CSF levels in a larger sample of 37 HD patients (Björkqvist *et al.*, 2006b). Moreover, in this study orexin CSF levels of 12 month-old YAC128 mice were also determined and, despite a 10% reduction in orexin neurons in the lateral hypothalamus of these mice, no decrease in the CSF levels of this peptide was detected (Björkqvist *et al.*, 2006b). Therefore, the moderate reduction in the number of orexin-positive neurons in the lateral hypothalamus of both HD patients (*section 4.4.3*) and YAC128 mice (Björkqvist *et al.*, 2006b) is insufficient to cause significant changes in the CSF levels of this peptide. It can therefore be concluded that orexin CSF levels are not a useful clinical biomarker to monitor the progression of HD.

Nevertheless, understanding the mechanisms underlying the loss of orexin and MCH neurons may shed light on the cellular events leading to neuronal death in HD. Moreover, the hypothalamic neurodegeneration may help to explain some of the non-motor symptomology of HD, such as sleep disturbances and weight loss. Finally, monitoring the loss of orexin neurons in the lateral hypothalamus may be useful for evaluating the therapeutic efficacy of novel drugs in R6/2 mice.

Chapter 5

Asialoerythropoetin is Not Effective in the R6/2 Line of Huntington's Disease Mice

Chapter based on the following publication:

Gil J, Leist M, Popovic N, Brundin P, and Petersén Å (2004):
“Asialoerythropoetin is not effective in the R6/2 line of Huntington's disease mice”. BMC Neurosci. 5:17-27.

5.1. Summary

No effective therapy is presently available for the treatment of HD. We designed this study to explore the therapeutic potential of erythropoietin (EPO), a cytokine that has been found to prevent excitotoxicity and to promote the generation of new neurons (neurogenesis). To avoid the side effects of a raised hematocrit, we used a variant of EPO, asialoEPO. R6/2 HD mice were treated with this cytokine from 5 to 12 weeks of age. We found for the first time that cell proliferation in the DG of the hippocampus was reduced by 70% in R6/2 mice. Unfortunately, asialoEPO treatment did not influence the progression of motor symptoms, weight loss, and the neuropathology in R6/2 mice. Furthermore, the reduction in hippocampal cell proliferation was not reversed by this treatment. We conclude that the chosen protocol of asialoEPO treatment is ineffective in the R6/2 model of HD. We suggest that reduced hippocampal cell proliferation is a novel neuropathological feature in R6/2 mice that warrants further examination (see *Chapter 6*).

5.2. Introduction

There is still no cure or satisfactory treatment for HD. Moreover, it is particularly challenging to perform therapeutic trials in HD patients for several reasons. First, the low prevalence of this disease in the general population often makes it difficult to recruit a sufficient number of patients for clinical trials. Second, due to the slow progression of the disease over a period of many years, treatments may require very long follow up periods. Third, there is substantial variability in the rate of progression, even in patients with similar numbers of CAG repeats. Fourth, there are no well-established objective surrogate biomarkers for HD (*section 4.5*), which means that clinical trials have to rely on cumbersome and subjective clinical rating scales as outcome parameters. The R6 mouse have served as a useful tool to evaluate new therapeutic strategies and is probably the most studied transgenic HD model in this respect (*section 1.6.3*; for review see Beal and Ferrante, 2004; Hersch and Ferrante, 2004; Li JY *et al.*, 2005). In particular, the R6/2 line has an early onset of symptoms and a fast progression of the disease, which allows for a more rapid evaluation of novel compounds.

EPO was originally discovered as a kidney-produced cytokine that regulates haematopoiesis. It was then found to protect neurons from death in a variety of conditions. One of the advantages of this compound is that it can enter the brain with peripheral administration. Receptors for EPO have been identified in the brain (Digicaylioglu *et al.*, 1995; Masuda *et al.*, 1993). EPO has been shown to be neuroprotective in animal models of focal ischemia, spinal cord injury, retinal injury, brain trauma and subarachnoid hemorrhage (Brines *et al.*, 2000; Siren *et al.*, 2001; Celik *et al.*, 2002; Gorio *et al.*, 2002; Grasso *et al.*, 2002; Junk *et al.*, 2002; Springborg *et al.*, 2003). Promising results have also been demonstrated in a phase II clinical trial for stroke (Ehrenreich *et al.*, 2002). One of the drawbacks of chronically administered EPO is an increase in the number of red-blood cells (hematocrit). However, these side-effects can be overcome by using the natural EPO metabolite asialoEPO, a molecule that appears to have a neuroprotective potency similar to EPO (Erbayraktar *et al.*, 2003; Wang *et al.*, 2004) and also has the capacity to cross the blood brain barrier (Erbayraktar *et al.*, 2003).

In addition to its neuroprotective properties, EPO seems to be essential for early embryonic neuronal development (Yu *et al.*, 2002; Tsai *et al.*, 2006) and to play an important role during adult neurogenesis (Shingo *et al.*, 2001; Tsai *et al.*, 2006). Moreover, EPO has been shown to promote the regeneration and migration of neurons in several models of acute brain injury (Wang *et al.*, 2004; Lu *et al.*, 2005; Tsai *et al.*, 2006).

One of the central dogmas of neuroscience has been the belief that neurogenesis only occurs during embryonic development. However, mounting evidence over the past 40 years has challenged that notion (for review see Gross, 2000; Temple, 2001; Kempermann, 2002). In fact, proliferation and differentiation of new neurons are now known to occur in selective regions of the adult mammalian brain, primarily the subventricular zone (SVZ) of the lateral ventricles and the subgranular zone (SGZ) of the DG of the hippocampus.

In the SVZ, neural stem cells give rise to committed progenitor cells that migrate through the rostral migratory stream (RMS) into the olfactory bulb (OB) where they differentiate into local interneurons (for review see Lie *et al.*, 2004).

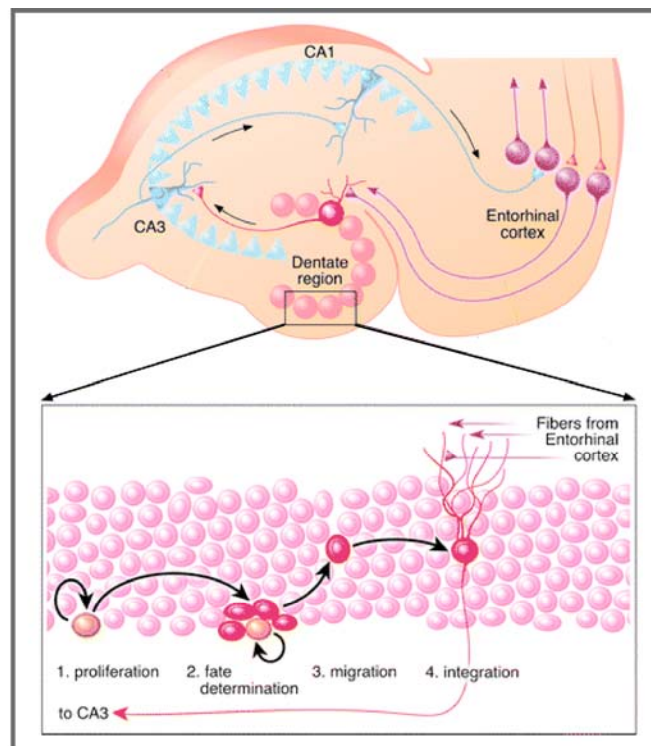


Figure 5.1. – *Hippocampal neurogenesis.* The DG of the hippocampus is one of the two neurogenic regions in the adult mammalian brain. Hippocampal neurogenesis comprises at least four distinct stages: (1) proliferation, where stem cells in the SGZ give rise to transit proliferating cells; (2) fate determination, where proliferating cells differentiate into immature neurons; (3) migration, where immature neurons migrate into the granule cell layer of the DG; and (4) integration, where immature neurons mature into new granule neurons. *Adapted from Lie et al.*, 2004.

In the SGZ of the DG, neuronal stem cells proliferate and differentiate into immature neurons. These migrate into the granule cell layer where they mature into new granule neurons, receiving inputs from the entorhinal cortex, and extending projections into the CA3 region of the hippocampus (**Figure 5.1**; for review see Lie *et al.*, 2004).

Although the functional impact of adult hippocampal neurogenesis is not yet known (for review see Kempermann *et al.*, 2004), it has been suggested to be involved in learning and memory, thus contributing to cognitive functioning (for review see van Praag *et al.*, 2002). It is a highly dynamic process that can be up-regulated by environmental enrichment, exercise, learning, estrogen, antidepressant drugs, electroconvulsive therapy, and delivery of growth factors such as BDNF and insulin growth factor 1 (IGF1). It can also be down-regulated by stress, glucocorticoids, inflammation, excitotoxicity, opiate intake, and aging (for review see Duman *et al.*, 2001a, 2001b; Kuhn *et al.*, 2001; Kempermann, 2002). The occurrence of neurogenesis in the adult brain provides a thrilling possibility to manipulate the endogenous restorative capacity in neurodegenerative disorders. Also, it is not fully explored what role neurogenesis may have in neurodegenerative diseases such as HD (for review see Armstrong and Barker, 2001).

We studied the involvement of the hippocampus in the pathology of R6/2 mice by evaluating hippocampal cell proliferation. We also tested whether stimulation of EPO-related signaling pathways would have beneficial effects in R6/2 HD mice. We used asialoEPO to selectively trigger the brain EPO receptors over a period of 7 weeks in R6/2 mice. We examined its effects on the development of motor symptoms, weight loss, striatal neuropathology and hippocampal cell proliferation.

5.3. Materials and Methods

5.3.1. Transgenic Animals

Transgenic HD mice of the R6/2 line were originally purchased from Jackson Laboratories and the colony was maintained by breeding heterozygous R6/2 males with females from their background strain (F1 of CBA x C57BL/6J). Tails of the offspring were used to obtain DNA for determination of the genotype using a PCR assay (Mangiarini *et al.*, 1996). The length of the CAG repeat in our R6/2 colony was analyzed, and was found to be stable at 142 ± 0.7 CAG repeats ($n = 18$, from 2 different generations). The mice were housed in

groups with *ad libitum* access to food and water at a 12 hours light/dark cycle. The experimental procedures followed the guidelines set by the Ethical Committee for the use of laboratory animals at Lund University, Sweden.

5.3.2. Administration of AsialoEPO and Body Weight Measurements

Mice from the same litters were divided into 3 groups ($n = 6$ to 7 mice per group). AsialoEPO was synthesized from EPO as described elsewhere (Erbayraktar *et al.*, 2003). One group of R6/2 mice was injected with asialoEPO (2.6 nmol/kg = 80 μ g/kg; in PBS) intraperitoneally (i.p.) 3 times per week, starting from age 5 weeks (when the first motor symptoms appear) until age 12 weeks. Another group of R6/2 mice and their wild-type littermates were injected (i.p.) with just the vehicle (PBS) following the same schedule. Mice were weighed once a week throughout the duration of the experiment.

5.3.3. Behavioral Testing

5.3.3.1. Rotarod

Mice were pretrained on the rotarod for 2 days before the treatment began at 5 weeks of age. On the first training day each mouse was placed on the rotarod for 120 seconds at a speed of 5 rpm. On the second day, mice were given 2 separate 120 seconds sessions at 10 rpm followed by 1 at 15 rpm. The mice were tested on the following day with 3 trials of 180 seconds at 15 rpm. The mean value of the latency to fall for these 3 trials was compared between the mice. Mice were tested once a week using a similar block of 2 trials at the ages of 5, 6, 7, 8, 10, 11 and 12 weeks.

5.3.3.2. Paw Clasping

One of the first symptoms displayed by R6/2 mice is limb dyskinesia when suspended by the tail. This symptom worsens over time until the mice clasp their paws together upon being picked up, and are unable to release this posture (section 1.6.1.3; **Figure 1.6**; Mangiarini *et al.*, 1996). Paw clasping was evaluated prior to each rotarod session. Mice were suspended by the tail 10 cm above the cage for 20 seconds. The paw clasping was scored on a scale from 0 to 2 points, where: absence of paw clasping or only the front paws pressed together yielded zero points; front paws pressed to the stomach yielded 1 point; and if front paws touched hind limbs, or both front and hind limbs were pressed

against the stomach, 2 points were noted. An individual blind to the genotype of the mice performed the assessment of paw clasping.

5.3.3.3. Motor Activity in an Open Field

The general motor activity of the mice was assessed in an open field. The open field apparatus was divided into 25 squares (5 x 5 cm each). The mice were analyzed at 10 and 12 weeks of age. They were allowed to habituate for 10 minutes and afterwards their activity was recorded for the next 10 minutes. The number of squares entered during the last 2 minutes of the recording session was evaluated. This procedure was chosen in order to increase the habituation period, during which the activity of normal mice is increased due to their exploratory behavior. Previous studies have shown that this increase in activity is the greatest during the first 20 minutes in a new environment (Zhuang *et al.*, 2001).

5.3.4. Administration of BrdU and Tissue Processing

In order to assess the genesis of new cells in the brains of 12-week-old mice, we administered the thymidine analogue bromodeoxyuridine (BrdU), which incorporates into cells undergoing DNA synthesis, and therefore has been widely used as a proliferating marker (Cooper-Kuhn and Kuhn, 2001). All mice received i.p. injections of BrdU (50 mg/kg; in PBS, pH 7.2; Sigma), every 12 hours for their last 6 days of survival. The mice were sacrificed 18 hours after the last BrdU injection. Mice were deeply anesthetized with pentobarbital and transcardially perfused with saline followed by 4% PFA in 0.1 M PBS. The brains were left in the fixative overnight and then dehydrated in 20% sucrose/0.1 M PBS. Coronal sections were cut at 4 series throughout the brain on a freezing sliding microtome at a thickness of 40 μ m and collected in PBS.

5.3.5. Immunohistochemistry

Tissue from wild-type and R6/2 mice was processed in parallel for immunohistochemistry in order to control for labeling intensity. One complete series of free-floating sections was processed for BrdU immunohistochemistry. Briefly, the sections were incubated in 1 M HCl at 65°C for 30 minutes in order to denature the DNA and allow the antibody to access the incorporated BrdU. The sections were then preincubated for 1 hour in 5% NHS and 0.25% Triton X-100 in PBS. They then were incubated for 48 hours at 4°C with a mouse monoclonal antibody against BrdU (diluted 1:50; Dako) in PBS containing 2%

NHS. After incubation with the secondary antibody biotinylated horse anti-mouse IgG (diluted 1:200; Dakopatts) for 2 hours, the bound antibodies were visualized with an avidin-biotin-peroxidase complex system (Vectastain ABC Elite Kit; Vector Laboratories) using DAB as the chromogen.

Separate series of sections were also processed for the neuronal marker NeuN, the striatal marker DARPP-32, and EM48 (for detection of NIIs). Briefly, the sections were quenched in 3% H₂O₂/10% methanol in 0.1 M PBS for 15 minutes, and preincubated with the proper sera (in the case of EM48 immunohistochemistry, the blocking solution was prepared in 1% BSA/0.1 M PBS). The sections were then incubated overnight at room temperature (or during 48 hours at 4°C) with a mouse monoclonal antibody against NeuN (diluted 1:1000; Chemicon), a rabbit polyclonal anti-DARPP-32 antibody (diluted 1:1000; Chemicon), or the mouse monoclonal anti-huntingtin antibody (EM48, diluted 1:500; Chemicon). The sections were then incubated for 2 hours with the respective secondary antibodies (biotinylated horse anti-mouse IgG, diluted 1:200, Dakopatts; and biotinylated swine anti-rabbit IgG, diluted 1:200, Dako), and visualized as described above.

BrdU/NeuN double labeling was also performed. Briefly, after DNA denaturation and preincubation in the proper sera, the sections were incubated for 48 hours at 4°C with monoclonal rat anti-BrdU (diluted 1:100, ImmunologicalsDirect, Oxfordshire, UK) and mouse anti-NeuN (diluted 1:100, Chemicon) antibodies. The sections were then incubated with the secondary antibodies Cy3-conjugated donkey anti-rat IgG (diluted 1:200, Jackson ImmunoResearch) and biotinylated horse anti-mouse IgG (Vector Laboratories) for 2 hours, followed by incubation with Alexa-488-conjugated streptavidin (diluted 1:200, Molecular Probes, Leiden, The Netherlands) for 2 hours.

5.3.6. Stereological Techniques and Cell Quantification

All morphological analyses were performed on blind-coded slides. The number of BrdU-immunopositive cells in the SGZ of the DG of the dorsal hippocampus was assessed by counting all positive cells in 7 to 9 sections per mouse (from -1.34 mm to -2.80 mm from bregma) using conventional light microscopy with a 40x objective. The distance between the sections was about 120 µm. The total number of cells assessed in 7 to 9 adjacent sections per mouse was expressed as the average number of cells per section.

Due to the large number of BrdU-immunopositive cells in the SVZ (located adjacent to the ventricle in the striatum), the total number of labeled cells in this region was assessed with stereological techniques (Gundersen *et al.*, 1988). We used the stereological equipment described before (*section 2.3.4*) with a 100x

objective. For systematic sampling, the frame area (808 - 843 μm^2) and the counting interval (x and y both 75 μm) were set to allow for at least a total of 200 cells to be sampled in 5 adjacent sections (distance between the sections: 120 μm) with the SVZ (five sections anterior to the appearance of the anterior commissure at +0.14 mm from bregma) and the optical dissector was set to sample all cells below the first 2.5 μm and above the last 2.5 μm of both surfaces of the section.

For neuronal quantification in the DG, 4 mice from each group were randomly selected and the number of NeuN-positive neurons in the DG was determined. Since the DG is densely populated with neurons, we were able to use stereological techniques (100x objective; frame area: 187 - 249 μm^2 ; counting interval: x and y both 150 μm). The number of neurons was determined in 7 adjacent sections (120 μm apart; from -1.34 mm to -2.80 mm from bregma).

The number of EM48-immunopositive neurons in the striatum was assessed using the stereological equipment (with a 40x objective) and applying the same stereological principles (frame area: 2452 - 2498 μm^2 ; counting interval: x and y both 500 μm). The number of EM48-positive neurons was determined in 5 adjacent sections (120 μm apart) of the striatum beginning at the 2 sections anterior to the first appearance of the anterior commissure.

The striatal volume was calculated in 4 randomly selected mice per group using the stereological equipment (with a 10x objective). The striatum was delineated in 5 adjacent sections (120 μm apart) processed for DARPP-32 immunohistochemistry. The quantification began at 2 sections anterior to the appearance of the anterior commissure. Volume was calculated by taking into account the frequency of sections (1:4) and their thickness (40 μm), according to the Cavalieri principle (Gundersen *et al.*, 1988). Using the stereological equipment (with a 40x objective), 45 randomly selected DARPP-32-positive cell bodies per striatum were delineated to assess their cross-sectional area (15 neurons per section in 3 sections per mouse).

5.3.7. Statistical Analysis

The data were analyzed using the Statview 5.4 package (Abacus Concepts). Unpaired Student's *t*, 1-factor ANOVA followed by the Bonferroni-Dunn post-hoc test, and 2-factor ANOVA with repeated measures when appropriate were applied. Data are presented as means \pm S.E.M. A *p* value of < 0.05 was considered statistically significant.

5.4. Results

5.4.1. AsialoEPO Does Not Reverse Motor Impairments in R6/2 Mice

Mice were assessed weekly over 7 weeks on the rotarod task (2-factor repeated measures ANOVA; significant difference between the 3 groups: $p = 0.0001$, $F(2, 96) = 16.61$; significant effect of time: $p = 0.0009$, $F(6, 96) = 4.16$). There was no effect of asialoEPO on the development of motor deficits in the R6/2 mice as assessed by the time spent on the rotarod (**Figure 5.2.A**).

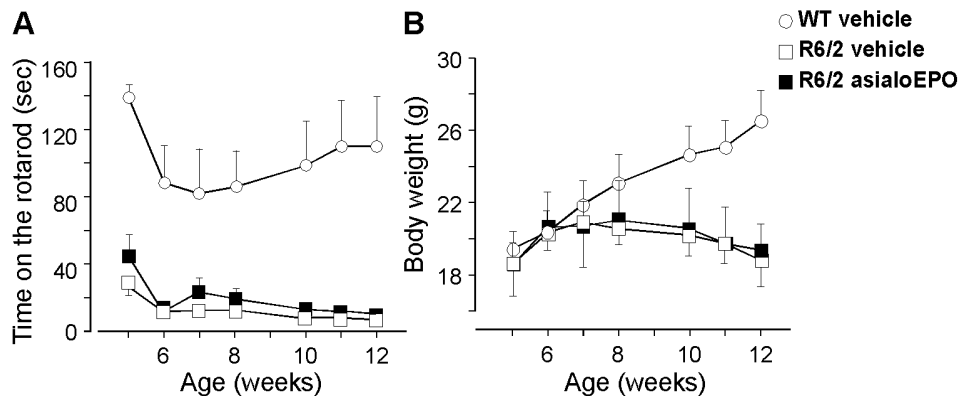


Figure 5.2. - No effect of asialoEPO on the decline in rotarod performance or body weight in R6/2 mice. **(A)** Mice were tested weekly on the rotarod for 3 trials of 180 seconds each, at the speed of 15 rpm. The mean latency to fall for the 3 trials was compared between mice. The testing began at 5 weeks and continued until 12 weeks of age. Administration of asialoEPO three times weekly from 5 to 12 weeks of age did not significantly affect the decline in rotarod performance in R6/2 mice. **(B)** Mice were weighed weekly during the treatment period. There was no effect of asialoEPO on the progressive reduction in body weight in R6/2 mice. Values are represented as means \pm S.E.M.

Open field was used to assess motor activity in mice at 10 and 12 weeks of age (**Table V**). The data were analyzed using 2-factor repeated measures ANOVA. There was a significant difference between the 3 groups ($p = 0.0004$, $F(2, 15) = 13.7$) and a significant time \times group interaction ($p < 0.05$, $F(2, 15) = 4.30$). AsialoEPO did not influence the decreased activity displayed by R6/2 mice.

Table V - No effect of asialoEPO on open field activity in R6/2 mice.

Age (weeks)	wild-type (n = 7)	R6/2 vehicle (n = 5)	R6/2 asialoEPO (n = 6)
10 weeks	66 ± 12	44 ± 14	20 ± 10
12 weeks	75 ± 7	11 ± 5	12 ± 7

The activity of the mice was assessed at 10 and 12 weeks of age in an open field. The open field was divided into 25 equal squares of 5 x 5 cm each. After 18 minutes of habituation to the new environment, the number of squares entered by the mice during 2 minutes was determined as a measure of general activity. Data are presented as means ± S.E.M.

In addition, all mice were assessed weekly with regard to their development of paw clasping. No wild-type mice ever showed clasping behaviour. Regardless of the treatment, around 80% of the R6/2 mice scored 1 point in the clasping scale at week 7. At week 10, all R6/2 mice scored 2 points.

5.4.2. No Effect of AsialoEPO on Body Weight

As mentioned above, an important symptom in R6/2 mice is progressive loss body weight (*section 1.6.1.4*; Mangiarini *et al.*, 1996). The body weight was assessed weekly from 5 to 12 weeks of age (**Figure 5.2.B**). The data were analyzed using 2-factor repeated measures ANOVA. There was a significant effect of time ($p < 0.0001$, $F(6, 96) = 1.55$) and significant time x group interaction ($p < 0.0001$, $F(12, 96) = 1.32$). However, asialoEPO treatment did not affect the loss of body weight observed in R6/2 mice ($p = 0.26$, $F(2, 96) = 1.47$).

5.4.3. AsialoEPO Treatment Does Not Reverse Striatal Neuropathology in R6/2 Mice

At 12 weeks of age, 5 striatal sections per mouse were assessed for NIIs. We detected 426000 ± 31000 NIIs in the vehicle-treated R6/2 mice and 407000 ± 45000 NIIs in the asialoEPO-treated mice (Student's *t* test, $p = 0.73$).

To assess for atrophy we measured the striatal volume in striatal sections processed for DARPP-32. The striatal volume measured 8.23 ± 0.53 mm³ in wild-type mice, 5.14 ± 0.21 mm³ in vehicle-treated R6/2 mice, and 5.26 ± 0.07 mm³ in asialoEPO-treated R6/2 mice (1-factor ANOVA; significant difference between the 3 groups: $p = 0.0008$, $F(2, 6) = 29.01$). As expected, there was a significant difference between both R6/2 groups as compared with the wild-type controls (Bonferroni-Dunn post-hoc test; wild-type versus vehicle-treated R6/2

mice: $p = 0.0005$; wild-type versus asialoEPO-treated R6/2 mice: $p = 0.0006$), and no difference between vehicle- and asialoEPO-treated R6/2 mice (Bonferroni-Dunn post-hoc test, $p = 0.813$).

Moreover, the cross sectional analysis of striatal DARPP-32-immunopositive neuronal area also demonstrated no changes in atrophy with asialoEPO treatment. Soma area was $78 \pm 6 \mu\text{m}^2$ for wild-type mice, $55 \pm 3 \mu\text{m}^2$ for vehicle-treated R6/2 mice, and $59 \pm 1 \mu\text{m}^2$ for asialoEPO-treated R6/2 mice (1-factor ANOVA; significant difference between the 3 groups: $p = 0.013$, $F(2, 6) = 9.64$). Again, there was a significant difference between both R6/2 groups and the wild-type group (Bonferroni-Dunn post hoc test; wild-type versus vehicle-treated R6/2 mice: $p = 0.006$; wild-type versus asialoEPO-treated R6/2 mice: $p = 0.014$) but not between asialoEPO- and vehicle-treated R6/2 mice (Bonferroni-Dunn post-hoc test, $p = 0.504$).

5.4.4. AsialoEPO Administration Had No Effect on the Reduced BrdU Labeling in the R6/2 Mouse Dentate Gyrus

EPO was shown to possess neurogenic properties (Shingo *et al.*, 2001).

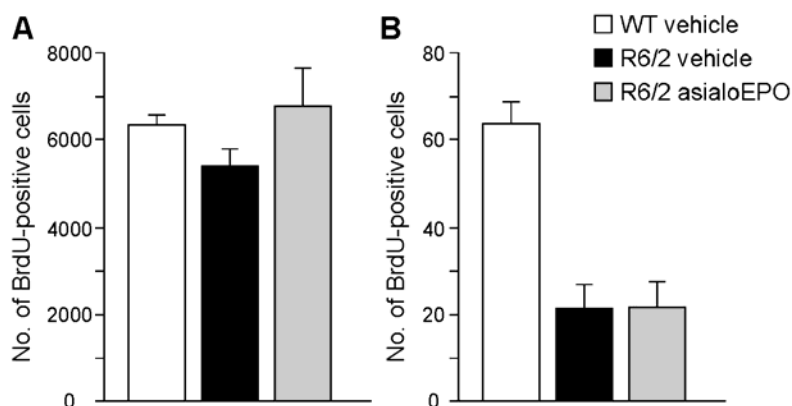


Figure 5.3. - Reduced BrdU-labeling in the R6/2 DG with no influence by asialoEPO treatment. All mice were i.p. injected with 50 mg/kg of BrdU every 12 hours for their last 6 days of survival to assess cell proliferation at 12 weeks of age. **(A)** The number of BrdU-labeled cells was assessed by stereological techniques in the SVZ in 5 striatal sections per mouse. In this region there was no significant reduction in the number of BrdU-labeled cells between the groups. **(B)** In the DG, BrdU-labeled cells were assessed in 7 to 9 sections per mouse as the mean number per section. There was a reduction in the number of BrdU-labeled cells in R6/2 mice compared to wild-type mice. The administration of asialoEPO was not able to reverse this reduced cell proliferation. Data are presented as means \pm S.E.M.

Therefore, we sought to investigate whether cell proliferation in the 2 neurogenic brain regions (subependymal layer of the SVZ and SGZ of the DG) was altered in R6/2 mice and whether asialoEPO treatment would impact this cell proliferation. We injected all mice with BrdU (50 mg/kg) during the last 6 days before they were sacrificed. In the subependymal layer of the SVZ there was a slight trend towards a reduction in the number of BrdU labeled cells in R6/2 mice compared to their wild-type littermates at the age of 12 weeks (1-factor ANOVA; $p = 0.23$, $F(2, 16) = 1.63$) (**Figure 5.3.A**). However, in the DG there was a significant difference between the groups (1-factor ANOVA; $p < 0.0001$, $F(2, 16) = 23.50$). We found a profound reduction in the number of BrdU labeled cells in R6/2 compared to the wild-type mice (Bonferroni-Dunn post-hoc test, $p < 0.0001$) (**Figures 5.3.B** and **5.4**). However, the administration of asialoEPO was not able to reverse this decreased hippocampal cell proliferation (Bonferroni-Dunn post-hoc test, $p = 0.98$).

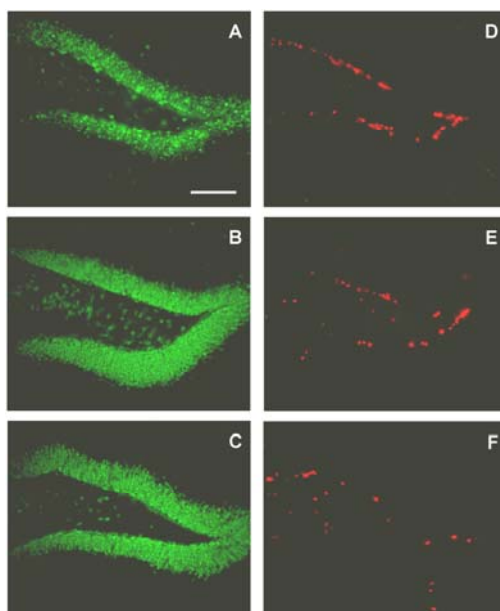


Figure 5.4. – *BrdU-labeled cells in the DG of the hippocampus of wild-type and R6/2 mice.* Hippocampal sections from 12-week-old R6/2 and wild-type mice were processed for BrdU/NeuN double-labeling. Photomicrographs showing representative NeuN labeling of the DG in a wild-type (**A**), a vehicle-treated R6/2 (**B**) and an asialoEPO-treated R6/2 (**C**) mouse. Photomicrographs showing representative BrdU-labeling in the same sections of the DG in a wild-type (**D**), a vehicle-treated R6/2 (**E**) and an asialoEPO-treated R6/2 (**F**) mouse. Scale bar = 100 μm .

Finally, using stereological techniques, we calculated the total number of mature neurons (NeuN-positive) in the DG of 12-week-old mice. We found 116967 ± 15056 neurons in wild-type mice, 141694 ± 4679 neurons in vehicle-treated R6/2 mice, and 157301 ± 20065 neurons in asialoEPO-treated R6/2 mice (1-factor ANOVA; $p = 0.20$, $F(2, 9) = 1.91$). These results suggest that the reduction in cell proliferation observed in R6/2 mice was not likely due to loss of neurons.

5.5. Discussion

The underlying mechanisms responsible for HD are still not fully understood, although excitotoxicity (*section 1.4.1*) and oxidative stress (*section 1.4.3*) have been suggested to be involved in the pathogenesis of the disease (for review see DiFiglia, 1990; Davies and Ramsden, 2001; Petersén and Brundin, 2002). Since administration of EPO has been shown to be protective against such insults (Siren *et al.*, 2001; Celik *et al.*, 2002; Ehrenreich *et al.*, 2002; Junk *et al.*, 2002; Erbayraktar *et al.*, 2003), we tested whether asialoEPO, an EPO analogue, exerts beneficial effects in R6/2 HD mice. We injected R6/2 mice 3 times weekly with asialoEPO, starting at five weeks of age (when symptoms begin to manifest) and ending at 12 weeks of age. We attempt to assess for the potential beneficial effects of this compound by measuring rotarod performance, paw claspings, open field activity, body weight changes, striatal huntingtin inclusions, striatal and neuronal atrophy, and cell proliferation. Despite all of these assessments, we were unable to find any beneficial effects of asialoEPO.

There may be several reasons why asialoEPO did not reverse the HD pathology and symptoms in R6/2 mice. It has been previously shown that EPO has neuroprotective effects in acute neurodegenerative paradigms characterized by extensive cell death, such as hypoxia and ischemia (Brines *et al.*, 2000; Siren *et al.*, 2001; for review see Cerami *et al.*, 2002). The same is true for asialoEPO (Erbayraktar *et al.*, 2003; Wang *et al.*, 2004). However, the R6/2 HD mouse model is a chronic neuropathological model with reduced cell death (*section 1.6.1.2*; Iannicola *et al.*, 2000; Turmaine *et al.*, 2000; Yu *et al.*, 2003; Stack *et al.*, 2005; *Chapter 4*).

Moreover, one of the proposed neuroprotective mechanisms for EPO relies upon functional transcriptional machinery. EPO is thought to activate EPO receptors that are linked to the Janus kinase 2 (Jak2) pathway, where activation of this pathway promotes the nuclear translocation of nuclear factor- κ B (NF κ B). Once in the nucleus, NF κ B up-regulates neuroprotective genes, such as the

caspase inhibitors X-linked inhibitor of apoptosis proteins (XIAP) and cellular inhibitor of apoptosis proteins-2 (c-IAP2) (Digicaylioglu and Lipton, 2001). Given that R6/2 mice display transcriptional abnormalities (*section 1.6.2.1*; Luthi-Carter *et al.*, 2000, 2002, 2003; Zucher *et al.*, 2005), it is possible that the EPO-mediated up-regulation of neuroprotective genes is compromised in these mice. Furthermore, since most of these genes have anti-apoptotic functions, their effects are likely to be minimal in the R6/2 brain, where little apoptosis has been documented (*section 1.6.1.2*; Iannicola *et al.*, 2000; Turmaine *et al.*, 2000; Yu *et al.*, 2003; *Chapter 4*).

This study is the first to demonstrate an impairment of cell proliferation in the hippocampus of R6/2 mice. In this region, the majority (approximately 80%) of the surviving BrdU-labeled cells are known to mature into neurons (for review see Duman *et al.*, 2001a, 2001b; *section 6.4.2*). Interestingly, during the process of submitting this work for publication, another study was published showing reduced cell proliferation in the DG of R6/1 mice (Lazic *et al.*, 2004), indicating that compromised DG cell proliferation is a novel feature of the R6 lines.

The underlying mechanism for the reduced cell proliferation in the R6/2 mice is not yet determined. Various factors may be responsible, including stress, increased levels of glucocorticoids, or an accelerated aging process. A more detailed discussion of these mechanisms can be found in the next chapter (*section 6.5*). Suffice to say, the mice in the present study were subjected to much handling stress with the weekly injections and behavioral testing and stress can have a negative impact on cell proliferation (for review see Duman *et al.*, 2001a). Therefore, in this study it would have been appropriate to have a non-handled control group to assess for the influence of stress. Furthermore, future studies need to determine whether the decrease number of hippocampal proliferating cells in R6/2 is due to increased death of the proliferating cells or to impaired cell proliferation. Our results suggest the latter since we did not find a loss in the total number of neurons (NeuN-positive cells) in the DG of R6/2 mice.

Neurogenesis has been suggested to play an important role in hippocampal function, which could explain some of the cognitive deficits characteristic of HD. Therefore, treatments aimed at restoring hippocampal neurogenesis are likely to have beneficial effects. In support of this hypothesis, a recent study has shown that fluoxetine (a serotonin-reuptake inhibitor commonly used for the treatment of depression) administration to R6/1 mice reversed the neurogenesis deficits in the DG and improved hippocampal-dependent cognitive impairments (Grote *et al.*, 2005). Moreover, environmental enrichment, which can slow the disease progression both in R6/2 (Hockly *et al.*, 2002) and R6/1 (van Dellen *et*

al., 2000a) mice, was recently shown to partially restore the deficit in DG cell proliferation in R6/1 mice (Lazic *et al.*, 2006). These results demonstrate that a restoration of hippocampal neurogenesis may ameliorate some of the symptoms of R6 mice.

Unfortunately, in this study we were unable to restore hippocampal cell proliferation with asialoEPO administration in the R6/2 mice. Interestingly, all studies reporting the neurogenic properties of EPO were performed in acute animal models of neurodegeneration, such as stroke (Wang *et al.*, 2004; Tsai *et al.*, 2006) and traumatic brain injury (Lu *et al.*, 2005). Again, it might be the case that EPO (and its derivative asialoEPO) are not so effective in promoting neurogenesis in chronic degeneration models. Furthermore, in this study asialoEPO treatment was initiated when the mice were 5-week-old, which might be too late in the disease process to obtain an effect at the level of DG cell proliferation. The evaluation of DG cell proliferation and neurogenesis throughout the lifespan of R6/2 mice will be the focus of *Chapter 6*.

Chapter 6

Reduced Hippocampal Neurogenesis in R6/2 Transgenic Huntington's Disease Mice

Chapter based on the following publication:

Gil J, Mohapel P, Araújo IM, Popovic N, Li JY, Brundin P, and Petersén Å (2005): "*Reduced hippocampal neurogenesis in R6/2 transgenic Huntington's disease mice*". *Neurobiol. Dis.* **20**:744-751.

6.1. Summary

In this study we extended our previous findings (*Chapter 5*; Gil *et al.*, 2004) and investigated to what extent cell proliferation and neurogenesis are altered in R6/2 transgenic HD mice. Using the thymidine analogue BrdU, we found a decrease in the number of proliferating cells in the DG of R6/2 mice over the course of the disease progression. This reduction was first detected in pre-symptomatic mice, and by 11.5 weeks R6/2 mice had 66% fewer newly born cells in the hippocampus. These results were confirmed by immunohistochemistry for the cell cycle markers Ki-67 (11.5 weeks: 72% reduction), proliferating cell nuclear antigen (PCNA; 11.5 weeks: 36% reduction), and for the transcription factor NeuroD (11.5 weeks: 79.5% reduction). We did not observe changes in cell proliferation in the R6/2 SVZ, indicating that the decrease in cell proliferation is specific for the hippocampus. This decrease corresponded to a reduction in neuronal production, as assessed by double immunolabeling for BrdU and the neuronal marker NeuN and by immunohistochemistry for the neuroblast marker doublecortin. We conclude that diminished hippocampal neurogenesis is a novel neuropathological feature in R6/2 mice that occurs early in the disease process, and therefore could be assessed when evaluating potential therapies.

6.2. Introduction

Given the capacity of the adult brain to generate new neurons, adult neuronal stem cells have been proposed as an endogenous cellular source for the treatment of various neurodegenerative diseases (for review see Lie *et al.*, 2004; Mohapel and Brundin, 2004). However, there is still controversy whether neurogenesis is compromised with neurodegenerative conditions, with different groups reporting contradictory results in animal models and patients of Alzheimer's disease (AD) (Haughey *et al.*, 2002a, 2002b; Jin *et al.*, 2004a, 2004b) and Parkinson's disease (PD) (Fallon *et al.*, 2000; Hoglinger *et al.*, 2004; Zhao *et al.*, 2003; Frielingsdorf *et al.*, 2004).

It is possible that altered neurogenesis is an important pathological hallmark in HD. It was recently reported that there is an increased number of proliferating cells in the subependymal layer of the SVZ adjacent to the striatum of human HD brains (Curtis *et al.*, 2003, 2005a, 2005b, 2006). These newborn cells were identified with the cell cycle marker PCNA and half were found to coexpress the glial marker GFAP while only 5% expressed the neuronal marker β III-tubulin (Curtis *et al.*, 2003). However, in this study hippocampal neurogenesis was never examined. We have shown that cell proliferation is reduced in the DG of end-stage R6/2 mice (Gil *et al.*, 2004; Chapter 5), a study that is in agreement with the work of Lazic and colleagues (2004, 2006) that demonstrated a reduction in hippocampal cell proliferation in R6/1 transgenic HD mice (Lazic *et al.*, 2004, 2006).

In order to further characterize the involvement of hippocampal neuropathology in R6/2 mice, in this study we extend our previous observations and used several markers to evaluate cell proliferation and neurogenesis throughout the lifespan of R6/2 mice.

6.3. Materials and Methods

6.3.1. Transgenic Animals

Transgenic HD mice of the R6/2 line were originally purchased from Jackson Laboratories and the colony was maintained by breeding heterozygous R6/2 males with females from their background strain (F1 of CBA x C57BL/6J). Tails of the offspring were used to obtain DNA for determination of the genotype using a PCR assay (Mangiarini *et al.*, 1997). The mice were housed in groups with *ad libitum* access to food and water at a 12 hours light/dark cycle.

The experimental procedures followed the guidelines set by the Ethical Committee for the use of laboratory animals at Lund University, Sweden.

6.3.2. Administration of BrdU and Tissue Processing

Generation of newborn cells was assessed by injecting 50 mg/kg of the thymidine analogue BrdU (in PBS, pH 7.2; Sigma) i.p. every 12 hours for 3 consecutive days. Note that administration of BrdU over a period of 6 days (*section 5.3.4*) was more than sufficient to detect proliferating cells. Therefore, in order to minimize the handling of mice, we were able to reduce the number of BrdU injections and still detect changes in cell proliferation. At the age of 3.5, 7.5 and 11.5 weeks of age, mice were sacrificed 18 hours after the last BrdU injection. To analyze the neuronal differentiation of the newborn cells that incorporated BrdU, a separate set of mice at the age of 5.5 and 10 weeks were sacrificed 2 weeks after the last BrdU injection, which was administered at 3.5 and 8 weeks of age, respectively. Mice at 2 weeks of age were sacrificed without prior BrdU injection due to their young age. Mice were deeply anesthetized with pentobarbital and transcardially perfused with saline followed by 4% PFA in 0.1 M PBS. The brains were left in fixative overnight and then dehydrated in 20% sucrose / 0.1 M PBS. Six series of coronal sections were cut throughout the brain on a sliding freezing microtome at a thickness of 30 μ m and collected in PBS.

6.3.3. Immunohistochemistry

Tissue from wild-type and R6/2 mice was processed in parallel for immunohistochemistry to control for labeling intensity. One series of free-floating sections was processed for BrdU immunohistochemistry exactly as described in *section 5.3.5*.

Separate series of sections were also processed for the proliferative marker Ki-67, the neural-specific intermediate filament nestin, the transcription factor NeuroD, and doublecortin, a marker for newly differentiated and migrating neuroblasts. Briefly, after quenching in 3% H₂O₂/10% methanol in 0.1 M PBS for 15 minutes, and preincubation with the proper sera, the sections were incubated for 48 hours at 4°C with a mouse monoclonal antibody against Ki-67 (diluted 1:120, Novocastra, Newcastle, UK), a monoclonal mouse anti-rat nestin antibody (diluted 1:200, BD Biosciences Pharmingen, Heidelberg, Germany), a polyclonal goat antibody against NeuroD (diluted 1:200, Santa Cruz Biotechnology, Santa Cruz, CA, USA), or a polyclonal goat anti-doublecortin antibody (diluted 1:400, Santa Cruz Biotechnology), respectively. The sections were then incubated for 2 hours with the respective secondary antibodies

(biotinylated horse anti-mouse IgG, diluted 1:200; Dakopatts, and biotinylated horse anti-goat IgG, diluted 1:200; Vector Laboratories), and visualized with an avidin-biotin-peroxidase complex system using DAB as the chromogen (Vectastain ABC Elite Kit, Vector Laboratories).

Immunohistochemistry for the cell cycle marker PCNA was also performed. A separate series of brain sections were first incubated in 10 mM sodium citrate buffer (in PBS, pH 6.0) at 95°C for 5 minutes. This step was repeated twice in order to unmask the antigens. After quenching and preincubation with 5% normal swine serum (NSS) for 1 hour, the sections were incubated with a rabbit polyclonal antibody against PCNA (diluted 1:200, Santa Cruz Biotechnology) for 48 hours at 4°C. The sections were then incubated with the secondary antibody biotinylated swine anti-rabbit IgG (Dako), and visualized as described above.

Neuronal differentiation was also assessed by BrdU/NeuN double labeling, exactly as described in *section 5.3.5*.

6.3.4. Stereological Techniques and Cell Quantification

All morphological analyses were performed on blind-coded slides. The number of BrdU-immunopositive cells in the SGZ of the DG of the dorsal hippocampus was assessed as described on *section 5.3.6* (the distance between the sections was 150 μm). The same procedure was also used to determine the numbers of Ki-67-, PCNA-, nestin-, NeuroD-, and doublecortin-labeled cells within this region.

The total number of BrdU-labeled cells in the SVZ was estimated by stereological techniques (frame area: 163 μm^2 ; counting interval: x and y both 75 μm), as described on *section 5.3.6* (the distance between the sections was 150 μm). The total number of PCNA-positive cells in this region was also determined by stereological techniques, using the same method. The total volume of the SVZ was calculated taking into account the frequency of sections (1:6) and their thickness (30 μm), according to the Cavalieri principle (Gundersen *et al.*, 1988).

For the sections that were processed for BrdU/NeuN immunohistochemistry, 50 BrdU-labeled cells per mouse were analyzed for co-labeling with NeuN, using a confocal laser-scanning microscope (Leica DM IRE3 microscope, Leica Confocal Software Version 2.77, Wetzlar, Germany) at 1 μm optical thickness. BrdU and NeuN were considered to be co-localized if nuclear co-localization was observed over the extent of the nucleus in consecutive 1 μm z-stacks, profiles of green and red fluorescence coincided, and when co-localization was

confirmed in x - y , x - z , and y - z cross-sections produced by orthogonal reconstructions from z -series.

6.3.5. Statistical Analysis

The data were analyzed with a 2-factor ANOVA or unpaired Student's t tests, when appropriate, using the Statview 5.4 package (Abacus Concepts). Data are presented as means \pm S.E.M. A p value of < 0.05 was considered statistically significant.

6.4. Results

6.4.1. R6/2 Mice Exhibit Decreased Hippocampal Cell Proliferation With the Progression of the Disease

Using BrdU to label dividing cells we observed an age-related decline in the number of proliferating cells in mice of both genotypes (2-factor ANOVA; genotype $p < 0.0001$, $F(1, 38) = 46.97$; age $p < 0.0001$, $F(2, 38) = 80.93$; age \times genotype $p = 0.50$, $F(2, 38) = 0.71$) (**Figure 6.1**).

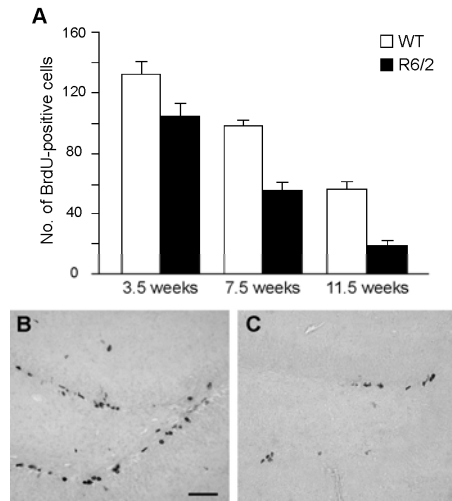


Figure 6.1. - Progressive reduction in the number of proliferating BrdU-labeled cells in the DG of R6/2 and wild-type mice. There was an age related decline in the number of BrdU-labeled cells in the DG of all mice (A). Compared to wild-type littermates, R6/2 mice displayed significantly less BrdU-labeled cells at all ages examined. Values represent means \pm S.E.M. Representative sections of the DG processed for BrdU immunohistochemistry in wild-type (B) and R6/2 mice (C) at 11.5 weeks of age. Scale bar = 50 μ m.

However, compared to wild-type littermates, R6/2 mice exhibited significantly fewer BrdU-labeled cells. Already by 3.5 weeks, R6/2 mice displayed a significant 21% reduction in the number of BrdU-positive cells compared to their wild-type littermate controls. Nestin is an intermediate filament protein that is expressed in neural progenitor/stem cells in the CNS, thus being widely used as a marker for cell proliferation (for review see Wiese *et al.*, 2004). When examining for nestin labeling we were able to confirm the results obtained with BrdU. We found a trend for a similar degree of reduction (19%) in the number of nestin-positive cells in 3.5-week-old R6/2 mice (wild-type: 377 ± 25 cells/section; R6/2: 304 ± 24 cells/section, Student's *t* test $p = 0.057$). At 7.5 weeks, an age at which motor symptoms are present, BrdU cell numbers further declined to 43% compared to wild-type mice. At 11.5 weeks, at a more advanced stage of motor deterioration, R6/2 mice showed a reduction of 66% in BrdU-labeled cells compared to wild-type mice (**Figure 6.1**).

Ki-67 is a nuclear protein that is expressed in all phases of the cell cycle except during the resting phase, and thus can be used as a marker for cell proliferation during the initial phase of adult neurogenesis (Kee *et al.*, 2002).

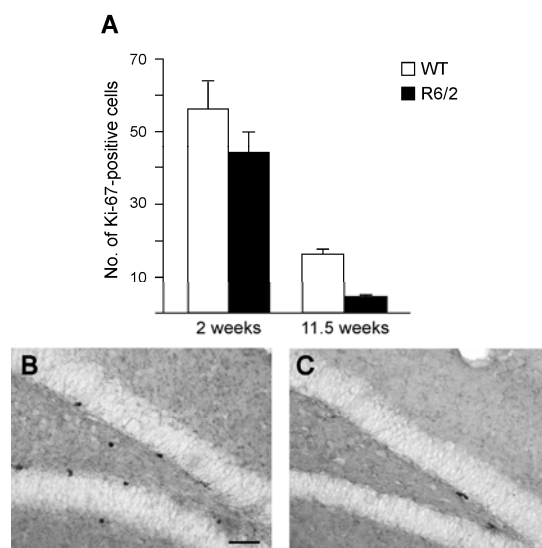


Figure 6.2. - Reduced cell proliferation in the R6/2 DG as assessed with the endogenous cell proliferation marker Ki-67. There was a progressive reduction in Ki-67 positive cells in the DG of both R6/2 and wild-type mice (**A**). The R6/2 mice displayed significantly fewer Ki-67-positive cells. Values represent means \pm S.E.M. Representative photomicrographs of the DG processed for Ki-67 immunohistochemistry in wild-type (**B**) and R6/2 mice (**C**) at 11.5 weeks of age. Scale bar = 50 μ m.

Ki-67 was used to assess cell proliferation in 2- and 11.5-week-old mice (two-factor ANOVA; genotype $p < 0.05$, $F(1, 22) = 6.83$; age $p < 0.0001$, $F(1, 22) = 198.97$; age x genotype $p = 0.44$, $F(1, 22) = 0.61$) (**Figure 6.2.A**). We found a non-significant trend towards a decrease in the number of Ki-67-positive cells (20% reduction) in 2-week-old R6/2 mice. Assessment of Ki-67-positive cells at 11.5 weeks of age confirmed the BrdU analysis, with 72% fewer Ki-67-labeled cells in R6/2 mice compared to wild-type littermates (**Figure 6.2**).

Since the cell cycle marker PCNA has been used in previous studies assessing cell proliferation in human HD tissue (Curtis *et al.*, 2003, 2005a, 2005b, 2006), we also used this marker to evaluate cell proliferation in 2- and 11.5-week-old R6/2 mice (2-factor ANOVA; genotype $p < 0.005$, $F(1, 22) = 11.04$; age $p < 0.0001$, $F(1, 22) = 84.09$; age x genotype $p = 0.65$, $F(1, 22) = 0.21$).

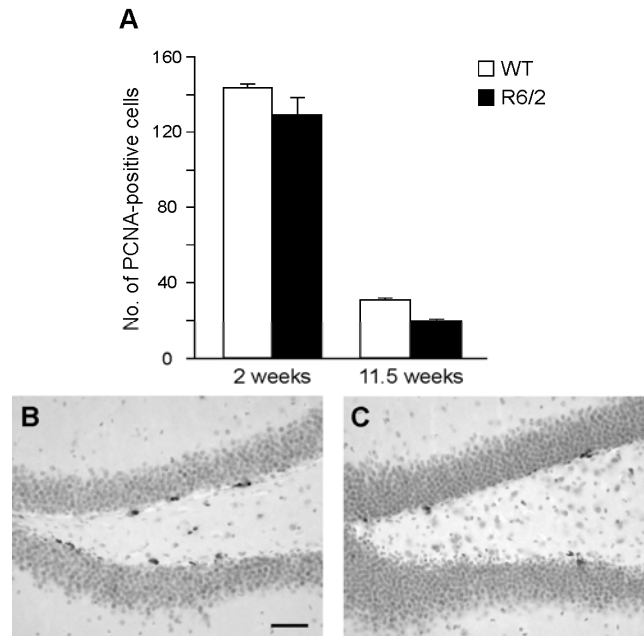


Figure 6.3. - Reduced cell proliferation in the R6/2 DG as assessed with the cell cycle marker PCNA. There was a progressive decrease in the number of PCNA-immunopositive cells with increasing age in the DG of both R6/2 and wild-type mice (**A**). Significantly fewer PCNA-positive cells were found in R6/2 mice. Values represent means \pm S.E.M. Representative sections of the DG processed for PCNA immunohistochemistry in wild-type (**B**) and R6/2 mice (**C**) at 11.5 weeks of age. Scale bar = 50 μ m.

Again, we observed a non-significant trend towards a decrease in the number of PCNA-labeled cells at the early age of 2 weeks in R6/2 mice (10% reduction) (**Figure 6.3.A**). However, this marker was less sensitive at detecting decreases in cell proliferation at 11.5 weeks of age, since we only observed about a 36% decrease in the number of PCNA-labeled cells (**Figure 6.3**), compared to 66% and 72% with BrdU and Ki-67, respectively.

Neuro D is a helix-loop-helix transcription factor that is expressed during development in the mammalian brain. Mutant mice homozygous for a deletion at the *NeuroD* locus fail to develop a granule cell layer within the DG, which is due to a severe defect in the proliferation of hippocampal precursor cells and to a delayed differentiation of these precursor cells into granule cells (Liu *et al.*, 2000). Interestingly, a recent study has also shown that NeuroD interacts with both normal and mutant huntingtin (*section 1.3.1*; Marcora *et al.*, 2003). When we labeled for NeuroD, we observed a significant 79.5% reduction in the number of NeuroD-positive cells in the DG of 11.5-week-old R6/2 mice (Student's *t* test, $p < 0.01$) (**Figure 6.4**).

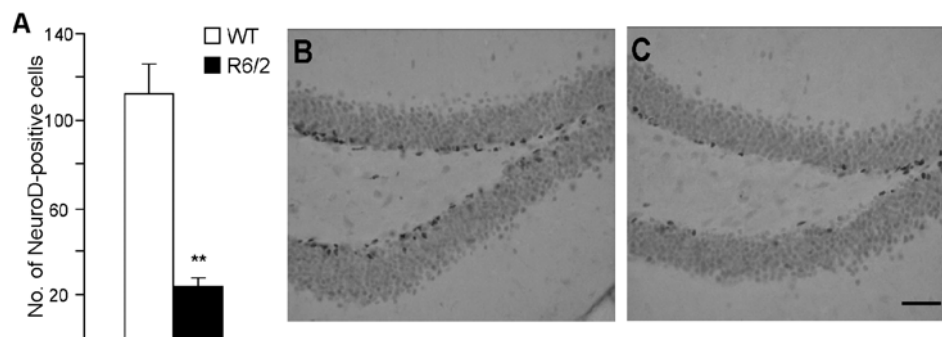


Figure 6.4. - Reduced cell proliferation in the DG of R6/2 mice as assessed with the transcription factor *NeuroD*. (A) There was a significant decrease in the number of NeuroD-immunopositive cells in the DG of 11.5-week-old R6/2 mice as compared with wild-type mice (Student's *t* test, ** $p < 0.01$). Values represent means \pm S.E.M. Representative photomicrographs of the DG processed for NeuroD immunohistochemistry in wild-type (B) and R6/2 mice (C) at 11.5 weeks of age. Scale bar = 50 μ m. (Gil and van der Burg *et al.*, unpublished observations).

6.4.2. Decreased Hippocampal Neurogenesis at Both Early and at End Stage of Disease in R6/2 Mice

Three and a half and 8-week-old mice were injected with BrdU (every 12 h, during 3 days) and allowed to survive for an additional 2 weeks before being

sacrificed. The total number of BrdU-labeled cells 2 weeks after the last BrdU injection was significantly lower in R6/2 as compared to wild-type mice at both ages (2-factor ANOVA; genotype $p < 0.0001$, $F(1, 17) = 52.75$; age $p < 0.0001$, $F(1, 17) = 72.46$; genotype x age $p < 0.005$, $F(1, 17) = 12.99$) (**Figure 6.5.A**).

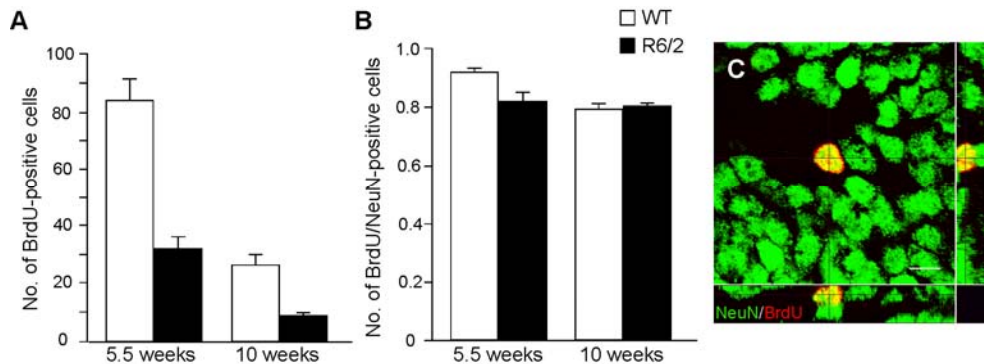


Figure 6.5. - Decreased hippocampal neurogenesis in R6/2 mice. To study whether the reduced cell proliferation reflected a decrease in neurogenesis, 5.5- and 10-week-old mice were sacrificed 2 weeks after the last BrdU injection to allow for differentiation of the proliferating cells that incorporated BrdU. **(A)** A significant reduction in BrdU-labeled cells was found in the DG of R6/2 mice at both ages compared to wild-type mice. **(B)** In the DG of both 5.5- and 10-week-old wild-type and R6/2 mice, around 80-90% of the BrdU-labeled cells were NeuN-positive. Values represent means \pm S.E.M. **(C)** A representative confocal image of a cell immunopositive for both BrdU (red) and NeuN (green) in the DG of a 10-week-old R6/2 mouse. Scale bar = 8 μ m.

Interestingly, if the average number of BrdU-labelled cells at 5.5 weeks (2 weeks post-injection; **Figure 6.5**) was compared with the cell proliferation numbers at 3.5 weeks (18 h post-injection; **Figure 6.1**), there were 35% less BrdU-positive cells in wild-type and 69% less BrdU-positive cells in R6/2 mice at 5.5 weeks of age. Similarly, if one compares the BrdU numbers at 10 weeks (2 weeks post-injection; **Figure 6.5**) with the cell proliferation numbers at 7.5 weeks (18h post-injection; **Figure 6.1**), one finds 73% less BrdU-positive cells in wild-type and 84% less BrdU-positive cells in R6/2 mice at 10 weeks of age. Therefore, waiting 2 weeks after the last BrdU injection allowed us to determine the survival rate of newly born precursor cells.

We also evaluated the proportion of precursor cells that become neurons by confocal analysis. We estimated that about 80-90% of the BrdU-labeled cells co-expressed the specific neuronal marker NeuN at both 5.5 and 10 weeks of age (2-factor ANOVA; genotype $p = 0.08$, $F(1, 17) = 3.50$; age $p < 0.01$, $F(1, 17) =$

9.85; age x genotype $p < 0.05$, $F(1, 17) = 6.87$) (Figures 6.5.B and C). In order to determine the nature of the remaining BrdU-positive cells, we performed a double-labeling for BrdU and the glial marker GFAP (data not shown). However, due to the fact that the DG is a very dense and compact cell layer and BrdU is localized in the nucleus whereas GFAP is present in the cytoplasm, it was virtually impossible to conduct a proper double-labeling determination with the confocal microscope.

Doublecortin is a microtubule binding protein that is expressed in newly differentiated and migrating neuroblasts (Brown *et al.*, 2003). In 10-week-old R6/2 mice, we also observed a significant 65% reduction in the number of doublecortin-labeled cells (Student's t test, $p < 0.01$), further indicating a reduction in hippocampal neurogenesis (Figure 6.6).

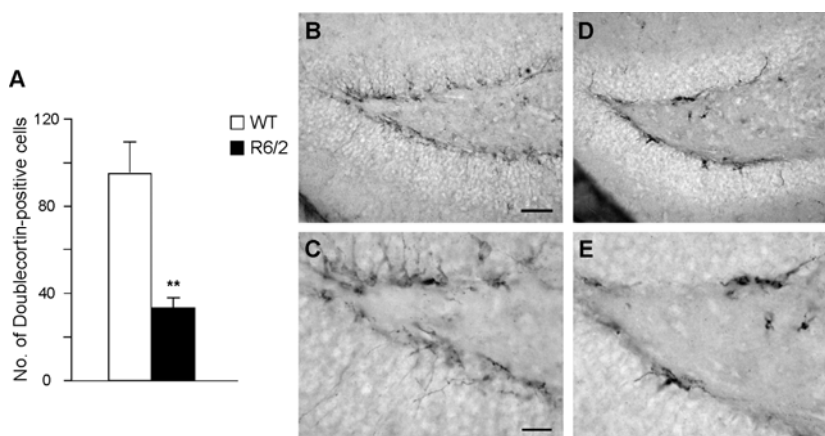


Figure 6.6. - Decreased number of neuroblasts in the DG of R6/2 mice. (A) The reduced hippocampal neurogenesis in R6/2 mice was confirmed by a significant decrease in the number of doublecortin-immunopositive neuroblasts in the DG of 10-week-old R6/2 mice as compared to wild-type controls (Student's t test, $** p < 0.01$). Values represent means \pm S.E.M. Representative photomicrographs of the DG processed for doublecortin immunohistochemistry in wild-type (B, C) and R6/2 mice (D, E) at 10 weeks of age. Scale bar = 50 μm (B, D) and = 20 μm (C, E).

6.4.3. R6/2 Mice Exhibit Normal Proliferation in the SVZ

We evaluated the volume of the SVZ, the other neurogenic zone in the adult brain, in young and old R6/2 and wild-type mice. The total volume of the SVZ was $0.072 \pm 0.004 \text{ mm}^3$ in wild-type and $0.072 \pm 0.003 \text{ mm}^3$ in R6/2 mice at 3.5 weeks, and $0.071 \pm 0.003 \text{ mm}^3$ in wild-type and $0.057 \pm 0.003 \text{ mm}^3$ in R6/2 mice at 11.5 weeks of age. Two-factor ANOVA revealed a significant difference

between the age groups ($p < 0.05$, $F(1, 26) = 5.28$). However, no difference between the genotypes ($p = 0.051$, $F(1, 26) = 4.17$), or any interaction between age and genotype ($p = 0.054$, $F(1, 26) = 4.08$) were detected.

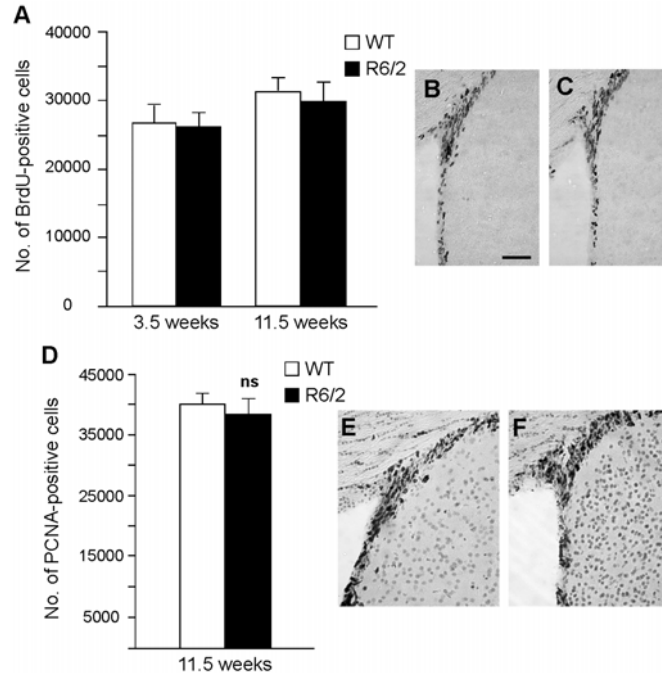


Figure 6.7. - No difference in cell proliferation in the SVZ of R6/2 mice. Cell proliferation in the SVZ of 3.5- and 11.5-week-old R6/2 mice and wild-type littermates was examined using stereological assessment of BrdU-labeled cells (**A**). Representative sections of the SVZ processed for BrdU immunohistochemistry in wild-type (**B**) and R6/2 mice (**C**) at 11.5 weeks of age. The cell cycle marker PCNA was also used to assess cell proliferation in the SVZ of 11.5-week-old R6/2 mice (**D**). Again, no significant difference in the number of PCNA-positive cells was detected between the two genotypes (Student's *t* test, n.s., non-significant). Representative photomicrographs of the SVZ processed for PCNA immunohistochemistry in wild-type (**E**) and R6/2 mice (**F**) at 11.5 weeks of age. Scale bar = 100 μ m. Values represent means \pm S.E.M.

We then examined the total number of BrdU-labeled cells in this region and found no significant differences between R6/2 and wild-type mice at both ages (2-factor ANOVA; significant effect of age: $p < 0.04$, $F(1, 26) = 4.98$; no significant effect of genotype: $p = 0.43$, $F(1, 26) = 0.64$; no significant interaction age x genotype: $p = 0.84$, $F(1, 26) = 0.04$). (**Figures 6.7.A-C**).

Furthermore, the total number of PCNA-labeled cells in the SVZ did not differ between 11.5-week-old R6/2 and wild-type mice (Student's *t* test, $p = 0.56$) (Figures 6.7.D-F).

These results further confirm our previous published observations of reduced cell proliferation that is restricted to the DG and does not affect the SVZ in 12-week-old R6/2 mice (Gil *et al.*, 2004; Chapter 5).

6.5. Discussion

In this study we report an age-related decline in hippocampal cell proliferation, both in R6/2 HD mice and in wild-type littermate controls. The reduction in hippocampal cell proliferation with aging in wild-type mice is in agreement with previous studies (Bizon and Gallagher, 2003). Nevertheless, R6/2 mice exhibited a greater reduction in the number of BrdU-positive cells than that expected with normal aging. This reduction can be detected as early as 2 weeks of age, before any behavioral or widespread neuropathological features have been reported in R6/2 mice. Therefore, reduced neurogenesis may constitute one of the initial pathological steps in the disease process.

Our study is the first to systematically investigate progressive changes in neurogenesis in a HD model. We previously showed a reduction in cell proliferation in R6/2 mice (Gil *et al.*, 2004; Chapter 5), which has been confirmed by Lazic and coworkers in R6/1 mice (Lazic *et al.*, 2004, 2006). In the present study we extended our knowledge of this deficit by showing the progressive nature of the reduced cell proliferation using a variety of different cell cycle markers; i.e. BrdU, Ki-67, and PCNA. Furthermore, we demonstrate that 80-90% of the surviving proliferating cells became neurons in both wild-type and R6/2 mice, a similar percentage to what has been reported previously (for review see Duman *et al.*, 2001a, 2001b). We also found a reduction in the survival rate of newly born precursor cells both in wild-type and R6/2 mice. In agreement, a massive reduction in the number of BrdU-labeled cells is commonly reported during the first days up to more than two weeks after the last administration of BrdU and is thought to be due to cell death (Gould *et al.*, 1999; Dayer *et al.*, 2003).

Several recently published studies have failed to replicate our findings, in that no differences in basal cell proliferation were detected in the DG of R6/1 (Grote *et al.*, 2005) or R6/2 mice (Jin *et al.*, 2005; Phillips *et al.*, 2005). The reasons for these discrepancies are currently unknown. They may be attributable to differences between different mice colonies, protocols of BrdU administration

or the methods used to quantify BrdU-labeling. It is interesting to note that in all these reports stereological counting methods were used to determine the total number of DG proliferating cells (Grote *et al.*, 2005; Jin *et al.*, 2005; Phillips *et al.*, 2005); whereby, in our hands we are unable to use this technique due to the inability to count at least 200 labeled cells, which is one of the basic tenants of stereological principles (*sections 5.3.4 and 6.3.4*; Gundersen *et al.*, 1988). These authors do not state whether or not they met this basic stereological requirement; but, if they did not, a great bias would be introduced into their counting procedure.

Nevertheless, in the study by Phillips and colleagues (2005), R6/2 mice failed to up-regulate DG neurogenesis in response to KA-induced seizures (a very robust method of inducing DG neurogenesis), confirming that indeed these mice show a compromised neurogenic process (Phillips *et al.*, 2005). These authors also speculate that the reduced cell proliferation in response to seizures is attributed to the surrounding environment in which these progenitor cells are located, rather than any intrinsic impairment of the precursor cells itself (Phillips *et al.*, 2005). However, this hypothesis was based on the fact that neurospheres derived from the SVZ of 8-week-old R6/2 and wild-type mice have the same proliferative capacity (Chu-LaGraff *et al.*, 2001; Phillips *et al.*, 2005), which is in agreement with the normal cell proliferation observed in the R6/2 SVZ. Since neurospheres derived from the adult DG are difficult to maintain in culture (Phillips *et al.*, 2005), one should be careful when speculating about the actual intrinsic proliferative capacity of the precursor cells in this neurogenic brain region.

Classically, HD is considered a neurodegenerative disease in that dysfunction and death of neurons underlie most, if not all, of the symptoms. Although the cerebral cortex, the striatum and the hypothalamus are the major sites for neuropathology in HD (*section 1.2.2*), some studies have reported cell loss also in the hippocampus of HD patients (Rosas *et al.*, 2003; for review see Vonsattel and DiFiglia, 1998). Keeping in mind that R6/2 mice show reduced neuronal death (*section 1.6.1.2*; Iannicola *et al.*, 2000; Turmaine *et al.*, 2000; Helmlinger *et al.*, 2002; Yu *et al.*, 2003; Stack *et al.*, 2005; *Chapter 4*), we have shown no neuronal loss in the DG of the hippocampus with NeuN immunohistochemistry (Gil *et al.*, 2004; *Chapter 5*) and FJ staining (Gil *et al.*, unpublished observations). Nevertheless there is strong electrophysiological and behavioral evidence for hippocampal dysfunction (Murphy *et al.*, 2000) in these mice. It remains to be seen if the disturbed neurogenesis in R6 mice participates in hippocampal dysfunction. Nevertheless, Grote and colleagues (2006) have recently shown an improvement of the cognitive function in R6/1 mice upon

recovery of DG cell proliferation followed by fluoxetine treatment (Gore *et al.*, 2006).

Given that expanded CAG repeats in huntingtin can lead to the dysregulation of transcription, intracellular trafficking and metabolism (*section 1.3*; for review see Li and Li, 2004), it is plausible that they may also interfere with the proliferative capacity of progenitor cells. Indeed, huntingtin is known to interact with the cell cycle machinery (for review see Li and Li, 2004). Huntingtin can also become associated with the centrosome and microtubules (Gutekunst *et al.*, 1995; Hoffner *et al.*, 2002), the latter through interaction with β -tubulin (*section 1.3.1*; Hoffner *et al.*, 2002). Interestingly, the HEAT repeat motifs present in the huntingtin sequence (Andrade and Bork, 1995) are also found in a number of proteins that are involved in mitotic progression, chromosomal dynamics and segregation (*section 1.3.1*; Neuwald *et al.*, 2000) and several of these proteins exert their functions via microtubules. Dysfunctional microtubule dynamics caused by mutant huntingtin may be a more broad phenomenon in HD, since a reduced proliferative capacity is not only found in the brain but also in the pancreas of end-stage R6/2 mice (Björkqvist *et al.*, 2005).

As stated above (*section 1.3.1*), normal huntingtin and the huntingtin-associated proteins HAP1 and MLK2 modulate and stimulate the activity of NeuroD (Marcora *et al.*, 2003), a transcription factor that is crucial for the development of a functional DG (Liu *et al.*, 2000). NeuroD is also expressed in the pancreas, where it plays an important role in the morphogenesis of normal islets (Huang *et al.*, 2002). The relationship between normal huntingtin, NeuroD and genesis of new cells (both in the DG and in the pancreas) raises the exciting possibility that an abnormal interaction between mutant huntingtin and NeuroD could contribute, at least in part, for the compromised generation of new cells observed both in the DG and in the pancreas of R6/2 HD mice. Arguing against this hypothesis, the study of Marcora and co-workers (2003) showed that NeuroD activity could also be stimulated by mutant huntingtin *in vitro* (Marcora *et al.*, 2003). However, as the authors suggested, the aggregates of mutant huntingtin that are formed *in vivo* may interfere with NeuroD activation. Interestingly, we found a drastic decrease in the number of NeuroD-positive cells in the DG of R6/2 mice (**Figure 6.4**; Gil and van der Burg *et al.*, unpublished observations). Whether this decrease is a cause or a consequence of the observed reduced cell proliferation remains to be elucidated. Further experiments are needed in order to conclude if a compromised NeuroD pathway (due, for instance, to its sequestration into NIIs of mutant huntingtin) is contributing to a reduction in the generation of new cells (neurons and pancreatic cells), or if this decrease in the number of NeuroD-positive cells simply reflects the down-regulation of another cell proliferation marker.

Interestingly, a disturbed NeuroD function would also explain the down-regulation of certain genes that are regulated by this transcription factor. One example is the neurotrophin BDNF, whose expression is regulated by huntingtin and NeuroD, and that has been shown to be down-regulated in HD (*sections 1.3.1 and 1.3.3.3*; Zuccato *et al.*, 2001; Luthi-Carter *et al.*, 2002; Canals *et al.*, 2004; Spires *et al.*, 2004). BDNF has also been shown to stimulate cell proliferation in the neurogenic zones and to promote migration of progenitor cells from the SVZ to non-neurogenic regions like the striatum and septum, the thalamus and the hypothalamus (Benraiss *et al.*, 2001; Pencea *et al.*, 2001; Mohapel *et al.*, 2005). Therefore, one can speculate that the down-regulation of BDNF observed in HD (Zuccato *et al.*, 2001; Luthi-Carter *et al.*, 2002; Canals *et al.*, 2004; Spires *et al.*, 2004) can also contribute to the decrease in cell proliferation.

A recent study showing a reduction in cell proliferation, both in the DG and the SVZ, in PD brains has also implicated the dopaminergic system in the regulation of neurogenesis (Hoglinger *et al.*, 2004). In this paper the authors also show that experimental depletion of DA in rodents decreases precursor cell proliferation in both the DG and the SVZ. Moreover, a selective agonist of D2-like receptors is enough to completely restore proliferation, further supporting the idea that DA can promote cell proliferation (Hoglinger *et al.*, 2004). As stated above, several studies have shown that a dopaminergic dysfunction may also be implicated in HD (*section 1.4.2*). In fact, R6 mice display a deficient dopaminergic neurotransmission (Bibb *et al.*, 2000; Petersén *et al.*, 2002b; *Chapter 3*). Whether this dysfunction in the dopaminergic neurotransmission is contributing to the observed compromised neurogenesis in R6/2 mice, is a hypothesis that needs to be further evaluated.

Still another factor that can account for these results is an increase in the levels of glucocorticoids, which are known to down-regulate neurogenesis (*section 5.2*; Cameron and McKay, 1999). Importantly, we have recently shown a progressive increase in the serum and urine levels of corticosterone in R6/2 mice (*section 1.6.1.4*; Björkqvist *et al.*, 2006a). Therefore, it is possible that the alterations in the hypothalamic-pituitary-adrenal axis (Björkqvist *et al.*, 2006a) may contribute to the progressive decrease in cell proliferation and neurogenesis in R6/2 mice.

In contrast with the decrease observed in the DG, in the SVZ we found no difference between R6/2 and wild-type mice in the number of proliferating cells. This is in agreement with our previous examination of BrdU-labeled cells in the SVZ in 12-week-old R6/2 mice (Gil *et al.*, 2004; *Chapter 5*). We also assessed the total number of PCNA-positive cells in the SVZ of 11.5-week-old mice and found again no differences. Phillips and colleagues (2005) have recently

extended these results and demonstrated that the number and migration of neuroblasts generated in the SVZ is not altered in R6/2 mice (Phillips *et al.*, 2005). Similar findings in the R6/1 model were also recently published (Lazic *et al.*, 2006). However, contradictory results were reported in HD human tissue, where an increased cell proliferation in the SVZ (estimated by assessing the number of PCNA-positive cells) was described (Curtis *et al.*, 2003, 2005a, 2005b, 2006).

The discrepancy between the results in R6 mice and HD patients could be due to several factors. For instance, the R6 mice express a higher number of CAG repeats and display a greater frequency of inclusions than HD patients. Alternatively, as suggested by Phillips and co-workers (2005), it may be the case that R6 mice simply do not live long enough for that phenomenon to be detected (Phillips *et al.*, 2005).

On the other hand, it has been suggested that PCNA can also be expressed in cells undergoing DNA repair (Tomasevic *et al.*, 1998), and therefore caution should be taken when evaluating cell proliferation results that are exclusively based on PCNA immunohistochemistry. Although in theory BrdU could also label cells undergoing apoptosis and DNA repair, this is unlikely to be the case with the low BrdU concentration used in our study. Indeed, several experimental data have shown that BrdU-positive cells mature into neurons in the rodent DG, that irradiation reduces the amount of BrdU labeling while increasing DNA repair and apoptosis, and no BrdU labeling has been detected in cells undergoing apoptosis (Cooper-Kuhn and Kuhn, 2002). Nevertheless, the validation of the results obtained with BrdU labeling with immunohistochemistry for endogenous cell cycle markers like Ki-67 and PCNA is the best option in order to draw definite conclusions regarding changes in cell proliferation.

Finally, one can speculate that cell loss in the caudate nucleus of HD patients is the actual trigger for the increased SVZ cell proliferation reported by Curtis and colleagues (Curtis *et al.*, 2003, 2005a, 2005b, 2006). In agreement with this scenario, an increased neurogenesis was also observed in the striatum of the QA-lesion rat model of HD (Tattersfield *et al.*, 2004), where an excitotoxicity-induced striatal lesion was enough to promote SVZ neurogenesis. Similar results were also obtained with other lesion paradigms, such as rat models of stroke (Arvidsson *et al.*, 2002; Parent *et al.*, 2002) and PD (Fallon *et al.*, 2000). On the other hand, the cell death occurring in the striatum of R6/2 mice (*section 1.6.1.2*; Iannicola *et al.*, 2000; Turmaine *et al.*, 2000; Yu *et al.*, 2003; Stack *et al.*, 2005) may not be enough to stimulate cell proliferation in the adjacent SVZ. Interestingly, R6/2 mice failed to up-regulate cell proliferation in the SVZ in response to QA-induced excitotoxic striatal lesions (Phillips *et al.*, 2005), in

agreement with the well documented striatal resistance to excitotoxic insults (Hansson *et al.*, 1999, 2001b), and further supporting the hypothesis of an overt striatal cell death as being the actual trigger for SVZ proliferation in HD patients. Nevertheless, treatment of R6/2 mice with fibroblast growth factor 2 (FGF2) stimulated SVZ cell proliferation (by 150%), as well as the migration of new neurons from this region into the cerebral cortex and striatum (where they differentiate into DARPP-32-expressing medium spiny neurons) (Jin *et al.*, 2005). Furthermore, FGF2 treatment reduced the number of NIIs, improved motor function, and increased the life span of these animals by 20%, suggesting that potentiation of SVZ neurogenesis may be used for the treatment of HD (Jin *et al.*, 2005).

We conclude that the progressive decline in hippocampal cell proliferation observed in R6/2 HD mice is a novel neuropathological feature that occurs early in the progression of the disease, before the appearance of any other HD symptoms. Therefore, cell proliferation might be assessed when evaluating the efficacy of potential therapies in this HD mouse model. Nevertheless, future studies are still needed in order to evaluate hippocampal neurogenesis in the human HD brain.

Chapter 7

**Final Conclusions
&
Future Directions**

7.1. Final Conclusions

The work presented in this thesis has broadened our understanding of the varied neuropathology associated with HD. We attempted to evaluate the impact of nonstriatal brain regions on striatal degeneration. We also looked to other brain structures to understand how they could contribute to a wide array of HD symptoms. We utilized several different rodent models of HD to address these questions. Due to the diverse nature of the final conclusions of the studies included in this thesis, each are summarized under a separate and specific aim (*section 1.7*):

1) To evaluate the striatal response to an excitotoxic insult that mimicks an excessive activation of the glutamatergic corticostriatal pathway in the newly generated rat model (Chapter 2).

We conclude that the newly generated transgenic HD rat model, which expresses a huntingtin fragment of intermediate size bearing 51 CAG repeats under the control of the rat *Hdh* promoter (von Hörsten *et al.*, 2003), was not resistant to QA-induced excitotoxic striatal lesions. By comparing our results with those obtained with different HD transgenic mouse models, we hypothesize that sensitivity/resistance to striatal excitotoxic insults is a function of the length of the expressed mutated huntingtin gene. Moreover, since the intrastriatal injection of excitotoxins represents an acute insult, they may not model well the more chronic dysfunction of the corticostriatal pathway associated with sustained excitotoxicity that occurs in the human HD brain.

2) To further characterize the impairment of the dopaminergic nigrostriatal pathway in the R6/1 mouse, by using in vivo microdialysis (Chapter 3).

We present further evidence implicating a dysfunction of the dopaminergic nigrostriatal pathway in the neuropathology of R6 mice. By performing *in vivo* microdialysis in R6/1 mice, we were able to detect several disturbances of this pathway at the presynaptic level, namely a reduction of striatal DA release (both by exocytosis and through an efflux via the DAT). This decrease was accompanied by a reduction in the striatal levels of this neurotransmitter and its metabolites (DOPAC and HVA). A disturbance in the synthesis of DA (due to a reduction of TH expression) (Ariano *et al.*, 2002; Yohrling *et al.*, 2003; Smith *et al.*, unpublished data) is likely to be the underlying cause of the impairment of both DA release routes. We speculate that the dysfunction of the dopaminergic nigrostriatal pathway may in fact contribute to the neurodegeneration of striatal neurons. Moreover, the deficient dopaminergic neurotransmission is likely to be

responsible for some of the motor symptoms of the disease (e.g., bradikinesia and rigidity), especially in late-stage HD patients and transgenic HD mice.

3) To determine whether the lateral hypothalamus, a structure involved in the regulation of several peripheral and endocrine functions, is affected by HD pathology in both R6/2 mice and human HD brains (Chapter 4).

We report, for the first time, loss of specific neuronal populations in the lateral hypothalamus of R6/2 mice. These populations express either orexin (involved in the regulation of the sleep/wakefulness cycle), or MCH (which controls energy homeostasis and food intake). Importantly, reduction in the number of orexin neurons was also observed in human HD brains, extending initial studies that indicated loss of somatostatin-positive neurons in another region of the hypothalamus, the lateral tuberal nucleus (Kremer *et al.*, 1990, 1991). Moreover, loss of orexin in the R6/2 mice is accompanied by the development of a narcoleptic-like phenotype resembling *orexin* knockout mice (Chemelli *et al.*, 1999). Evaluating the implications of loss of MCH neurons is beyond the scope of this thesis. However, it is likely that loss of these neurons do contribute, at least in part, to the reduced body weight observed in both human HD patients and R6/2 mice.

4) To study the contribution of the DG of the hippocampus, a structure important for cognitive functioning, on new neuron production and in HD pathology in R6/2 mice (Chapters 5 and 6).

We discovered a progressive and specific impairment of neurogenesis in the DG of the hippocampus in R6/2 mice. The decrease in cell proliferation was first observed at a time when no widespread neuropathological, motor, or cognitive symptoms are known to occur. As the HD mice age and the disease symptoms and pathology increasingly manifest, there is an even further decline in DG neurogenesis. Interestingly, the decrease in neurogenesis appears to be restricted to the hippocampus, since we observed no evidence of reduced cell proliferation in the SVZ of R6/2 mice. Importantly, one of the mechanisms that can account, at least in part, for these observations is a reduction in dopaminergic neurotransmission, in accordance with the results presented on *Chapter 3*. Since a similar reduction in cell proliferation was reported to occur in the DG of R6/1 mice (Lazic *et al.*, 2004, 2006), we conclude that a reduced neurogenesis is a common feature of the R6 lines, constituting a novel neuropathological feature of these transgenic models. A reduced neurogenesis may have functional implications in HD, for instance at the cognitive level.

5) *To assess the effects of a novel neuroprotective compound (asialoEPO) on motor function, striatal neuropathology and hippocampal cell proliferation in R6/2 mice (Chapter 5).*

Evaluation of hippocampal cell proliferation in R6 mice is a potential method for determining the efficacy of new therapeutic strategies. Therefore, we evaluated whether asialoEPO, an EPO analogue, has any beneficial effects on motor symptoms, neuropathology, or cell proliferation in R6/2 mice. In our hands this compound had no benefits on any of the outcome variables, including hippocampal cell proliferation. We conclude that this compound is not an effective candidate for the treatment of HD-related symptomology.

To conclude, we provide further evidence implicating the involvement of brain regions that directly interact with the striatum (i.e., the substantia nigra) in striatal degeneration, which may impact the development of motor symptoms in HD. Moreover, we also demonstrate that other nonstriatal brain regions, specifically the lateral hypothalamus and the DG of the hippocampus, are also afflicted in R6/2 HD mice and, in the case of the lateral hypothalamus, in HD human brains. The observed alterations (loss of orexin- and MCH-containing neurons in the lateral hypothalamus and decreased neurogenesis in the DG) are likely to have significant functional implications. These may include disturbances of the sleep/wakefulness cycle and development of a narcoleptic-like behaviour, loss of body weight, and cognitive impairment.

7.2. Future Directions

The field of HD has been the focus of intensive research during the past decade, especially after the identification of the gene and the mutation responsible for the disease (The Huntington's Disease Collaborative Research Group, 1993). This discovery led to the generation of the R6 lines, the first HD transgenic mouse models (Mangiarini *et al.*, 1996). Despite the efforts of a multidisciplinary approach from a broad array of researchers, a cure for this devastating neurodegenerative disorder still eludes us. A cure for HD will depend on our ability to understand the mechanisms underlying the neurodegeneration caused by the expression of mutant huntingtin.

The research presented in this thesis, as is often the case in science, leaves many more questions unanswered and deserving further investigation. More specifically, it will be important to further characterize the sleep disturbances in HD patients. Furthermore, the impact of loss of MCH-containing neurons in the lateral hypothalamus of R6/2 mice deserves further attention, and a relationship

between loss of MCH and the decreased body weight observed in R6/2 mice is currently under investigation. Moreover, a validation of these results in human HD samples is of primary importance. Finally, assessing hippocampal neurogenesis in HD human brains will be important. Determining the exact mechanisms responsible for the reduced neurogenesis may shed some more light on the pathogenesis of HD. Ultimately, the answer to these questions will clearly define the importance of these nonstriatal brain regions for the pathology of HD. The development of new therapies specifically designed to ameliorate the nonstriatal symptoms is likely to improve the quality of life as well as increase life expectancy of patients afflicted with this devastating disorder.

References

- Alam ZI, Halliwell B, and Jenner P (2000): "No evidence for increased oxidative damage to lipids, proteins, or DNA in Huntington's disease". *J Neurochem* **75**:840-846.
- Andrade MA, and Bork P (1995): "HEAT repeats in the Huntington's disease protein". *Nat Genet* **11**:115-116.
- Andreassen OA, Dedeoglu A, Stanojevic V, Hughes DB, Browne SE, Leech CA, Ferrante RJ, Habener JF, Beal MF, and Thomas MK (2002): "Huntington's disease of the endocrine pancreas: insulin deficiency and diabetes mellitus due to impaired insulin gene expression". *Neurobiol Dis* **11**:410-424.
- Arenas J, Campos Y, Ribacoba R, Martin MA, Rubio JC, Ablanedo P, and Cabello A (1998): "Complex I defect in muscle from patients with Huntington's disease". *Ann Neurol* **43**:397-400.
- Ariano MA, Aronin N, DiFiglia M, Tagle DA, Sibley DR, Leavitt BR, Hayden MR, and Levine MS (2002): "Striatal neurochemical changes in transgenic models of Huntington's disease". *J Neurosci Res* **68**:716-729.
- Armstrong RJ, and Barker RA (2001): "Neurodegeneration: a failure of neuroregeneration?" *Lancet* **358**:1174-1176.
- Arvidsson A, Collin T, Kirik D, Kokaia Z, and Lindvall O (2002): "Neuronal replacement from endogenous precursors in the adult brain after stroke". *Nat Med* **8**:963-970.
- Augood SJ, Faull RL, and Emson PC (1997): "Dopamine D1 and D2 receptor gene expression in the striatum in Huntington's disease". *Ann Neurol* **42**:215-221.
- Bäckman L, and Farde L (2001): "Dopamine and cognitive functioning: brain imaging findings in Huntington's disease and normal aging". *Scand J Psychol* **42**:287-296.
- Bauer A, Zilles K, Matusch A, Holzmann C, Riess O, and von Hörsten S (2005): "Regional and subtype selective changes of neurotransmitter receptor density in a rat transgenic for the Huntington's disease mutation". *J Neurochem* **94**:639-650.
- Beal MF (2000): "Energetics in the pathogenesis of neurodegenerative diseases". *Trends Neurosci* **23**:298-304.
- Beal MF, and Ferrante RJ (2004): "Experimental therapeutics in transgenic mouse models of Huntington's disease". *Nat Rev Neurosci* **5**:373-384.
- Beal MF, Ferrante RJ, Swartz KJ, and Kowall NW (1991): "Chronic quinolinic acid lesions in rats closely resemble Huntington's disease". *J Neurosci*

- 11:1649-1659.
- Beal MF, Kowall NW, Ellison DW, Mazurek MF, Swartz KJ, and Martin JB (1986): "Replication of the neurochemical characteristics of Huntington's disease by quinolinic acid". *Nature* **321**:168-171.
- Becher MW, Kotzuc JA, Sharp AH, Davies SW, Bates GP, Price DL, and Ross CA (1998): "Intranuclear neuronal inclusions in Huntington's disease and dentatorubral and pallidolusian atrophy: correlation between the density of inclusions and IT15 CAG triplet repeat length". *Neurobiol Dis* **4**:387-397.
- Behrens PF, Franz P, Woodman B, Lindenberg KS, and Landwehrmeyer GB (2002): "Impaired glutamate transport and glutamate-glutamine cycling: downstream effects of the Huntington mutation". *Brain* **125**:1908-1922.
- Benraiss A, Chmielnicki E, Lerner K, Roh D, and Goldman SA (2001): "Adenoviral brain-derived neurotrophic factor induces both neostriatal and olfactory neuronal recruitment from endogenous progenitor cells in the adult forebrain". *J Neurosci* **21**:6718-6731.
- Berke SJ, and Paulson HL (2003): "Protein aggregation and the ubiquitin proteasome pathway: gaining the UPPer hand on neurodegeneration". *Curr Opin Genet Dev* **13**:253-261.
- Beuckmann CT, Sinton CM, Williams SC, Richardson JA, Hammer RE, Sakurai T, and Yanagisawa M (2004): "Expression of a poly-glutamine-ataxin-3 transgene in orexin neurons induces narcolepsy-cataplexy in the rat". *J Neurosci* **24**:4469-4477.
- Beuckmann CT, and Yanagisawa M (2002): "Orexins: from neuropeptides to energy homeostasis and sleep/wake regulation". *J Mol Med* **80**:329-342.
- Bibb JA, Yan Z, Svenningsson P, Snyder GL, Pieribone VA, Horiuchi A, Nairn AC, Messer A, and Greengard P (2000): "Severe deficiencies in dopamine signaling in presymptomatic Huntington's disease mice". *Proc Natl Acad Sci USA* **97**:6809-6814.
- Bizon JL, and Gallagher M (2003): "Production of new cells in the rat dentate gyrus over the lifespan: relation to cognitive decline". *Eur J Neurosci* **18**:215-219.
- Björkqvist M, Fex M, Wierup N, Petersén Å, Gil J, Bacos K, Popovic N, Li JY, Sundler F, Brundin P, and Mulder H (2005): "The R6/2 transgenic mouse model of Huntington's disease develops diabetes due to deficient β -cell mass". *Hum Mol Genet* **14**:565-574.
- Björkqvist M, Petersén Å, Bacos K, Isaacs J, Norlén P, Gil J, Popovic N, Sundler F, Bates GP, Tabrizi SJ, Brundin P, and Mulder H (2006a): "Progressive alterations in the hypothalamic-pituitary-adrenal axis in the R6/2 transgenic mouse model of Huntington's disease". *Hum Mol Genet* **15**:1713-1721.

- Björkqvist M, Petersén Å, Nielsen J, Ecker D, Mulder H, Hayden M, Landwehrmeyer B, Brundin P, and Leavitt B (2006b): "Cerebrospinal fluid levels of orexin-A are not a clinically useful biomarker for Huntington disease." *Clin Genet* **70**:78-79.
- Bogdanov MB, Andreassen OA, Dedeoglu A, Ferrante RJ, and Beal MF (2001): "Increased oxidative damage to DNA in a transgenic mouse model of Huntington's disease". *J Neurochem* **79**:1246-1249.
- Bohnen NI, Koeppe RA, Meyer P, Ficaró E, Wernette K, Kilbourn MR, Kuhl DE, Frey KA, and Albin RL (2000): "Decreased striatal monoaminergic terminals in Huntington disease". *Neurology* **54**:1753-1759.
- Bolivar VJ, Manley K, and Messer A (2003): "Exploratory activity and fear conditioning abnormalities develop early in R6/2 Huntington's disease transgenic mice". *Behav Neurosci* **117**:1233-1242.
- Bolivar VJ, Manley K, and Messer A (2004): "Early exploratory behavior abnormalities in R6/1 Huntington's disease transgenic mice". *Brain Res* **1005**:29-35.
- Brouillet E, Conde F, Beal MF, and Hantraye P (1999): "Replicating Huntington's disease phenotype in experimental animals". *Prog Neurobiol* **59**:427-468.
- Brown JP, Couillard-Despres S, Cooper-Kuhn CM, Winkler J, Aigner L, and Kuhn HG (2003): "Transient expression of doublecortin during adult neurogenesis". *J Comp Neurol* **467**:1-10.
- Browne SE, Bowling AC, MacGarvey U, Baik MJ, Berger SC, Muqit MM, Bird ED, and Beal MF (1997): "Oxidative damage and metabolic dysfunction in Huntington's disease: selective vulnerability of the basal ganglia". *Ann Neurol* **41**:646-653.
- Butterworth NJ, Williams L, Bullock JY, Love DR, Faull RL, and Dragunow M (1998): "Trinucleotide (CAG) repeat length is positively correlated with the degree of DNA fragmentation in Huntington's disease striatum". *Neuroscience* **87**:49-53.
- Cameron HA, and McKay RD (1999): "Restoring production of hippocampal neurons in old age". *Nat Neurosci* **2**:894-897.
- Canals JM, Pineda JR, Torres-Peraza JF, Bosch M, Martin-Ibanez R, Munoz MT, Mengod G, Ernfors P, and Alberch J (2004): "Brain-derived neurotrophic factor regulates the onset and severity of motor dysfunction associated with enkephalinergic neuronal degeneration in Huntington's disease". *J Neurosci* **24**:7727-7739.
- Cao C, Temel Y, Blokland A, Ozen H, Steinbusch HW, Vlamings R, Nguyen HP, von Horsten S, Schmitz C, and Visser-Vandewalle V (2006): "Progressive deterioration of reaction time performance and choreiform

- symptoms in a new Huntington's disease transgenic rat model*". Behav Brain Res **170**:257-261.
- Carter RJ, Lione LA, Humby T, Mangiarini L, Mahal A, Bates GP, Dunnett SB, and Morton AJ (1999): "*Characterization of progressive motor deficits in mice transgenic for the human Huntington's disease mutation*". Neurosci **19**:3248-3257.
- Celik M, Gokmen N, Erbayraktar S, Akhisaroglu M, Konakc S, Ulukus C, Genc S, Genc K, Sagiroglu E, Cerami A, and Brines M (2002): "*Erythropoietin prevents motor neuron apoptosis and neurologic disability in experimental spinal cord ischemic injury*". Proc Natl Acad Sci USA **99**:2258-2263.
- Cepeda C, Ariano MA, Calvert CR, Flores-Hernandez J, Chandler SH, Leavitt BR, Hayden MR, and Levine MS (2001): "*NMDA receptor function in mouse models of Huntington disease*". J Neurosci Res **66**:525-539.
- Cepeda C, Hurst RS, Calvert CR, Hernandez-Echeagaray E, Nguyen OK, Jocoy E, Christian LJ, Ariano MA, and Levine MS (2003): "*Transient and progressive electrophysiological alterations in the corticostriatal pathway in a mouse model of Huntington's disease*". J Neurosci **23**:961-969.
- Cerami A, Brines M, Ghezzi P, Cerami C, and Itri LM (2002): "*Neuroprotective properties of epoetin alfa*". Nephrol Dial Transplant **17**:8-12.
- Cha JH, Kosinski CM, Kerner JA, Alsdorf SA, Mangiarini L, Davies SW, Penney JB, Bates GP, and Young AB (1998): "*Altered brain neurotransmitter receptors in transgenic mice expressing a portion of an abnormal human huntington disease gene*". Proc Natl Acad Sci USA **95**:6480-6485.
- Chan EY, Luthi-Carter R, Strand A, Solano SM, Hanson SA, DeJohn MM, Kooperberg C, Chase KO, DiFiglia M, Young AB, Leavitt BR, Cha JH, Aronin N, Hayden MR, and Olson JM (2002): "*Increased huntingtin protein length reduces the number of polyglutamine-induced gene expression changes in mouse models of Huntington's disease*". Hum Mol Genet **11**:1939-1951.
- Chemelli RM, Willie JT, Sinton CM, Elmquist JK, Scammell T, Lee C, Richardson JA, Williams SC, Xiong Y, Kisanuki Y, Fitch TE, Nakazato M, Hammer RE, Saper CB, and Yanagisawa M. (1999): "*Narcolepsy in orexin knockout mice: molecular genetics of sleep regulation*". Cell **98**:437-451.
- Chen M, Ona VO, Li M, Ferrante RJ, Fink KB, Zhu S, Bian J, Guo L, Farrell LA, Hersch SM, Hobbs W, Vonsattel JP, Cha JH, and Friedlander RM (2000): "*Minocycline inhibits caspase-1 and caspase-3 expression and delays mortality in a transgenic mouse model of Huntington disease*". Nat Med **6**:797-801.
- Chen Y, Hu C, Hsu CK, Zhang Q, Bi C, Asnicar M, Hsiung HM, Fox N, Sliker

-
- LJ, Yang DD, Heiman ML, and Shi Y (2002): "Targeted disruption of the melanin-concentrating hormone receptor-1 results in hyperphagia and resistance to diet-induced obesity". *Endocrinology* **143**:2469-2477.
- Chu-LaGraff Q, Kang X, and Messer A (2001): "Expression of the Huntington's disease transgene in neural stem cell cultures from R6/2 transgenic mice". *Brain Res Bull* **56**:307-312.
- Ciechanover A, and Brundin P (2003): "The ubiquitin proteasome system in neurodegenerative diseases: sometimes the chicken, sometimes the egg". *Neuron* **40**:427-446.
- Cooper-Kuhn CM, and Kuhn HG (2002): "Is it all DNA repair? Methodological considerations for detecting neurogenesis in the adult brain". *Brain Res Dev Brain Res* **134**:13-21.
- Curtis MA, Faull RL, and Glass M (2006): "A novel population of progenitor cells expressing cannabinoid receptors in the subependymal layer of the adult normal and Huntington's disease human brain." *J Chem Neuroanat* **31**:210-215.
- Curtis MA, Penney EB, Pearson AG, van Roon-Mom WM, Butterworth NJ, Dragunow M, Connor B, and Faull RL (2003): "Increased cell proliferation and neurogenesis in the adult human Huntington's disease brain". *Proc Natl Acad Sci USA* **100**:9023-9027.
- Curtis MA, Penney EB, Pearson J, Dragunow M, Connor B, and Faull RL (2005a): "The distribution of progenitor cells in the subependymal layer of the lateral ventricle in the normal and Huntington's disease human brain." *Neuroscience* **132**:777-788.
- Curtis MA, Waldvogel HJ, Synek B, and Faull RL (2005b): "A histochemical and immunohistochemical analysis of the subependymal layer in the normal and Huntington's disease brain". *J Chem Neuroanat* **30**:55-66.
- Date Y, Ueta Y, Yamashita H, Yamaguchi H, Matsukura S, Kangawa K, Sakurai T, Yanagisawa M, and Nakazato M (1999): "Orexins, orexigenic hypothalamic peptides, interact with autonomic, neuroendocrine and neuroregulatory systems". *Proc Natl Acad Sci USA* **96**:748-753.
- Dauvilliers Y, Baumann CR, Carlander B, Bischof M, Blatter T, Lecendreux M, Maly F, Besset A, Touchon J, Billiard M, Tafti M, and Bassetti CL (2003): "CSF hypocretin-1 levels in narcolepsy, Kleine-Levin syndrome, and other hypersomnias and neurological conditions". *J Neurol Neurosurg Psychiatry* **74**:1667-1673.
- Davies S, and Ramsden DB (2001): "Huntington's disease". *J Clin Pathol: Mol Pathol* **54**:409-413.
- Davies SW, Turmaine M, Cozens BA, DiFiglia M, Sharp AH, Ross CA, Scherzinger E, Wanker EE, Mangiarini L, and Bates GP (1997): "Formation

- of neuronal intranuclear inclusions underlies the neurological dysfunction in mice transgenic for the HD mutation*". Cell **90**:537-548.
- Dayer AG, Ford AA, Cleaver KM, Yassaee M, and Cameron HA (2003): "Short-term and long-term survival of new neurons in the rat dentate gyrus". J Comp Neurol **460**:563-572.
- Deckel AW, Elder R, and Fuhrer G (2002a): "Biphasic developmental changes in Ca²⁺/calmodulin-dependent proteins in R6/2 Huntington's disease mice". Neuroreport **13**:707-711.
- Deckel AW, Gordinier A, Nuttal D, Tang V, Kuwada C, Freitas R, and Gary KA (2001): "Reduced activity and protein expression of NOS in R6/2 HD transgenic mice: effects of L-NAME on symptom progression". Brain Res **919**:70-81.
- Deckel AW, Tang V, Nuttal D, Gary K, and Elder R (2002b): "Altered neuronal nitric oxide synthase expression contributes to disease progression in Huntington's disease transgenic mice". Brain Res **939**:76-86.
- de Lecea L, Kilduff TS, Peyron C, Gao X, Foye PE, Danielson PE, Fukuhara C, Battenberg EL, Gautvik VT, Bartlett FS 2nd, Frankel WN, van den Pol AN, Bloom FE, Gautvik KM, and Sutcliffe JG (1998): "The hypocretins: hypothalamus-specific peptides with neuroexcitatory activity". Proc Natl Acad Sci USA **95**:322-327.
- DiFiglia M (1990): "Excitotoxic injury of the neostriatum: a model for Huntington's disease". Trends Neurosci **13**:286-289.
- DiFiglia M, Sapp E, Chase KO, Davies SW, Bates GP, Vonsattel JP, and Aronin N (1997a): "Aggregation of huntingtin in neuronal intranuclear inclusions and dystrophic neurites in brain". Science **277**:1990-1993.
- DiFiglia M, Sapp E, Chase KO, Davies SW, Bates GP, Vonsattel JP, and Aronin N (1997b): "Huntingtin localization in brains of normal and Huntington's disease patients". Ann Neurol **42**:604-12.
- Digicaylioglu M, Bichet S, Marti HH, Wenger RH, Rivas LA, Bauer C, and Gassmann M (1995): "Localization of specific erythropoietin binding sites in defined areas of the mouse brain". Proc Natl Acad Sci USA **92**:3717-3720.
- Digicaylioglu M, and Lipton SA (2001): "Erythropoietin-mediated neuroprotection involves cross-talk between Jak2 and NF-kappaB signalling cascades". Nature **412**:641-647.
- Djousse L, Knowlton B, Cupples LA, Marder K, Shoulson I, and Myers RH. (2002): "Weight loss in early stage of Huntington's disease". Neurology **59**:1325-1330.
- Dragatsis I, Levine MS, and Zeitlin S (2000): "Inactivation of Hdh in the brain and testis results in progressive neurodegeneration and sterility in mice". Nat Genet **26**:300-306.

- Dragunow M, Faull RL, Lawlor P, Beilharz EJ, Singleton K, Walker EB, and Mee E (1995): "In situ evidence for DNA fragmentation in Huntington's disease striatum and Alzheimer's disease temporal lobes". *Neuroreport* **6**:1053-1057.
- Duman RS, Malberg J, and Nakagawa S (2001a): "Regulation of adult neurogenesis by psychotropic drugs and stress". *J Pharmacol Exp Ther* **299**:401-407.
- Duman RS, Nakagawa S, and Malberg J (2001b): "Regulation of adult neurogenesis by antidepressant treatment". *Neuropsychopharmacology* **25**:836-844.
- Dunah AW, Jeong H, Griffin A, Kim YM, Standaert DG, Hersch SM, Mouradian MM, Young AB, Tanese N, and Krainc D (2002): "Sp1 and TAFIII30 transcriptional activity disrupted in early Huntington's disease". *Science* **296**:2238-2243.
- Duyao MP, Auerbach AB, Ryan A, Persichetti F, Barnes GT, McNeil SM, Ge P, Vonsattel JP, Gusella JF, Joyner AL, et al. (1995): "Inactivation of the mouse Huntington's disease gene homolog Hdh". *Science* **269**:407-410.
- Ehrenreich H, Hasselblatt M, Dembowski C, Cepek L, Lewczuk P, Stiefel M, Rustenbeck HH, Breiter N, Jacob S, Knerlich F, Bohn M, Poser W, Ruther E, Kochen M, Gefeller O, Gleiter C, Wessel TC, De Ryck M, Itri L, Prange H, Cerami A, Brines M, and Siren AL (2002): "Erythropoietin therapy for acute stroke is both safe and beneficial". *Mol Med* **8**:495-505.
- Erbayraktar S, Grasso G, Sfacteria A, Xie QW, Coleman T, Kreilgaard M, Torup L, Sager T, Erbayraktar Z, Gokmen N, Yilmaz O, Ghezzi P, Villa P, Fratelli M, Casagrande S, Leist M, Helboe L, Gerwein J, Christensen S, Geist MA, Pedersen LO, Cerami-Hand C, Wuerth JP, Cerami A, and Brines M (2003): "Asialoerythropoietin is a nonerythropoietic cytokine with broad neuroprotective activity in vivo". *Proc Natl Acad Sci USA* **100**: 6741-6746.
- Fain JN, Del Mar NA, Meade CA, Reiner A, and Goldowitz D (2001): "Abnormalities in the functioning of adipocytes from R6/2 mice that are transgenic for the Huntington's disease mutation". *Hum Mol Genet* **10**:145-152.
- Fallon J, Reid S, Kinyamu R, Opole I, Opole R, Baratta J, Korc M, Endo TL, Duong A, Nguyen G, Karkehabadhi M, Twardzik D, Patel S, and Loughlin S (2000): "In vivo induction of massive proliferation, directed migration, and differentiation of neural cells in the adult mammalian brain". *Proc Natl Acad Sci USA* **97**:14686-14691.
- Farrer LA (1985): "Diabetes mellitus in Huntington disease". *Clin Genet* **27**:62-67.
- Ferrante RJ, and Kowall NW (1987): "Tyrosine hydroxylase-like

- immunoreactivity is distributed in the matrix compartment of normal human and Huntington's disease striatum*". Brain Res **416**:141-146.
- Ferrante RJ, Kowall NW, Cipolloni PB, Storey E, and Beal MF (1993): "Excitotoxic lesions in primates as a model for Huntington's disease: histopathologic and neurochemical characterization". Exp Neurol **119**:46-71.
- Frielingdorf H, Schwarz K, Brundin P, and Mohapel P (2004): "No evidence for new dopaminergic neurons in the adult mammalian substantia nigra". Proc Natl Acad Sci USA **101**:10177-10182.
- Gafni J, and Ellerby LM (2002): "Calpain activation in Huntington's disease". J Neurosci **22**:4842-4849.
- Gatchel JR, and Zoghbi HY (2005): "Diseases of unstable repeat expansion: mechanisms and common principles". Nat Rev Genet **6**:743-755.
- Gaus SE, Lin L, and Mignot E (2005): "CSF hypocretin levels are normal in Huntington's disease patients." **28**:1607-1608.
- Gauthier LR, Charrin BC, Borrell-Pages M, Dompierre JP, Rangone H, Cordelieres FP, De Mey J, MacDonald ME, Lessmann V, Humbert S, and Saudou F (2004): "Huntingtin controls neurotrophic support and survival of neurons by enhancing BDNF vesicular transport along microtubules." Cell **118**:127-138.
- Gervais FG, Singaraja R, Xanthoudakis S, Gutekunst CA, Leavitt BR, Metzler M, Hackam AS, Tam J, Vaillancourt JP, Houtzager V, Rasper DM, Roy S, Hayden MR, and Nicholson DW (2002): "Recruitment and activation of caspase-8 by the Huntingtin-interacting protein Hip-1 and a novel partner Hippi". Nat Cell Biol **4**:95-105.
- Gil JM, Leist M, Popovic N, Brundin P, and Petersén Å (2004): "Asialoerythropoietin is not effective in the R6/2 line of Huntington's disease mice". BMC Neurosci **5**:17-27.
- Ginovart N, Lundin A, Farde L, Halldin C, Backman L, Swahn CG, Pauli S, and Sedvall G (1997): "PET study of the pre- and post-synaptic dopaminergic markers for the neurodegenerative process in Huntington's disease". Brain **120**:503-514.
- Goldberg YP, Nicholson DW, Rasper DM, Kalchman MA, Koide HB, Graham RK, Bromm M, Kazemi-Esfarjani P, Thornberry NA, Vaillancourt JP, and Hayden MR (1996): "Cleavage of huntingtin by apopain, a proapoptotic cysteine protease, is modulated by the polyglutamine tract". Nat Genet **13**:442-449.
- Gorio A, Gokmen N, Erbayraktar S, Yilmaz O, Madaschi L, Cichetti C, Di Giulio AM, Vardar E, Cerami A, and Brines M (2002): "Recombinant human erythropoietin counteracts secondary injury and markedly enhances

-
- neurological recovery from experimental spinal cord trauma*". Proc Natl Acad Sci USA **99**:9450-9455.
- Gould E, Beylin A, Tanapat P, Reeves A, and Shors TJ (1999): "*Learning enhances adult neurogenesis in the hippocampal formation*". Nat Neurosci **2**:260-265.
- Gourfinkel-An I, Parain K, Hartmann A, Mangiarini L, Brice A, Bates G, and Hirsch (2003): "*Changes in GAD67 mRNA expression evidenced by in situ hybridization in the brain of R6/2 transgenic mice*". J Neurochem **86**:1369-1378.
- Graham RK, Deng Y, Slow EJ, Haigh B, Bissada N, Lu G, Pearson J, Shehadeh J, Bertram L, Murphy Z, Warby SC, Doty CN, Roy S, Wellington CL, Leavitt BR, Raymond LA, Nicholson DW, and Hayden MR (2006): "*Cleavage at the caspase-6 site is required for neuronal dysfunction and degeneration due to mutant huntingtin*." Cell **125**:1179-1191.
- Graham RK, Slow EJ, Deng Y, Bissada N, Lu G, Pearson J, Shehadeh J, Leavitt BR, Raymond LA, and Hayden MR (2005): "*Levels of mutant huntingtin influence the phenotypic severity of Huntington disease in YAC128 mouse models*." Neurobiol Dis **21**:444-455.
- Grasso G, Buemi M, Alafaci C, Sfacteria A, Passalacqua M, Sturiale A, Calapai G, De Vico G, Piedimonte G, Salpietro FM, and Tomasello F (2022): "*Beneficial effects of systemic administration of recombinant human erythropoietin in rabbits subjected to subarachnoid hemorrhage*". Proc Natl Acad Sci USA **99**:5627-5631.
- Gross CG. (2000): "*Neurogenesis in the adult brain: death of a dogma*". Nat Rev Neurosci **1**:67-73.
- Grote HE, Bull ND, Howard ML, van Dellen A, Blakemore C, Bartlett PF, and Hannan A (2005): "*Cognitive disorders and neurogenesis deficits in Huntington's disease mice are rescued by fluoxetine*". Eur J Neurosci **22**:2081-2088.
- Gu M, Gash MT, Mann VM, Javoy-Agid F, Cooper JM, and Schapira AH (1996): "*Mitochondrial defect in Huntington's disease caudate nucleus*". Ann Neurol **39**:385-389.
- Gunawardena S, and Goldstein LS (2005): "*Polyglutamine diseases and transport problems: deadly traffic jams on neuronal highways*". Arch Neurol **62**:46-51.
- Gundersen HJ, Bendtsen TF, Korbo L, Marcussen N, Moller A, Nielsen K, Nyengaard JR, Pakkenberg B, Sorensen FB, Vesterby A, et al. (1988): "*Some new, simple and efficient stereological methods and their use in pathological research and diagnosis*". Apmis **96**:379-394.
- Gusella JF (2001): "*Huntington Disease*". Encyclopedia of Life Sciences,

- Nature Publishing Group (www.els.net).
- Gusella JF, and MacDonald ME (1998): "*Huntingtin: a single bait hooks many species*". *Curr Opin Neurobiol* **8**:425-430.
- Gusella JF, and MacDonald ME (2000): "*Molecular genetics: unmasking polyglutamine triggers in neurodegenerative disease*". *Nat Rev Neurosci* **1**:109-115.
- Gutkunst CA, Levey AI, Heilman CJ, Whaley WL, Yi H, Nash NR, Rees HD, Madden JJ, and Hersch SM (1995): "*Identification and localization of huntingtin in brain and human lymphoblastoid cell lines with anti-fusion protein antibodies*". *Proc Natl Acad Sci USA* **92**:8710-8714.
- Gutkunst CA, Li SH, Yi H, Mulroy JS, Kuemmerle S, Jones R, Rye D, Ferrante RJ, Hersch SM, and Li XJ (1999): "*Nuclear and neuropil aggregates in Huntington's disease: relationship to neuropathology*". *J Neurosci* **19**:2522-2534.
- Hansson O, Castilho RF, Korhonen L, Lindholm D, Bates GP, and Brundin P. (2001a): "*Partial resistance to malonate-induced striatal cell death in transgenic mouse models of Huntington's disease is dependent on age and CAG repeat length*". *J Neurochem* **78**:694-703.
- Hansson O, Guatteo E, Mercuri NB, Bernardi G, Li XJ, Castilho RF, and Brundin P (2001b): "*Resistance to NMDA toxicity correlates with appearance of nuclear inclusions, behavioural deficits and changes in calcium homeostasis in mice transgenic for exon 1 of the huntington gene*". *Eur J Neurosci* **14**:1492-1504.
- Hansson O, Petersén Å, Leist M, Nicotera P, Castilho RF, and Brundin P (1999): "*Transgenic mice expressing a Huntington's disease mutation are resistant to quinolinic acid-induced striatal excitotoxicity*". *Proc Natl Acad Sci USA* **96**:8727-8732.
- Hara J, Beuckmann CT, Nambu T, Willie JT, Chemelli RM, Sinton CM, Sugiyama F, Yagami K, Goto K, Yanagisawa M, and Sakurai T (2001): "*Genetic ablation of orexin neurons in mice results in narcolepsy, hypophagia, and obesity*". *Neuron* **30**:345-354.
- Haughey NJ, Liu D, Nath A, Borchard AC, and Mattson MP (2002a): "*Disruption of neurogenesis in the subventricular zone of adult mice, and in human cortical neuronal precursor cells in culture, by amyloid beta-peptide: implications for the pathogenesis of Alzheimer's disease*". *Neuromolecular Med* **1**:125-135.
- Haughey NJ, Nath A, Chan SL, Borchard AC, Rao MS, and Mattson MP (2002b): "*Disruption of neurogenesis by amyloid beta-peptide, and perturbed neural progenitor cell homeostasis, in models of Alzheimer's disease*". *J Neurochem* **83**:1509-1524.

- Hedreen JC, and Folstein SE (1995): "Early loss of neostriatal striosome neurons in Huntington's disease". *J Neuropathol Exp Neurol* **54**:105-120.
- Helmlinger D, Yvert G, Picaud S, Merienne K, Sahel J, Mandel JL, and Devys D (2002): "Progressive retinal degeneration and dysfunction in R6 Huntington's disease mice". *Hum Mol Genet* **11**:3351-3359.
- Hersch SM, and Ferrante RJ (2004): "Translating therapies for Huntington's disease from genetic animal models to clinical trials". *NeuroRx* **1**:298-306.
- Heuser IJ, Chase TN, and Mouradian MM (1991): "The limbic-hypothalamic-pituitary-adrenal axis in Huntington's disease". *Biol Psychiatry* **30**:943-952.
- Hickey MA, and Chesselet MF (2003a): "Apoptosis in Huntington's disease". *Prog Neuropsychopharmacol Biol Psychiatry* **27**:255-265.
- Hickey MA, and Chesselet MF (2003b): "The use of transgenic and knock-in mice to study Huntington's disease". *Cytogenet Genome Res* **100**:276-286.
- Hickey MA, and Morton AJ (2000): "Mice transgenic for the Huntington's disease mutation are resistant to chronic 3-nitropropionic acid-induced striatal toxicity". *J Neurochem* **75**:2163-2171.
- Hickey MA, Reynolds GP, and Morton AJ (2002): "The role of dopamine in motor symptoms in the R6/2 transgenic mouse model of Huntington's disease". *J Neurochem* **81**:46-59.
- Ho LW, Carmichael J, Swartz J, Wyttenbach A, Rankin J, and Rubinsztein DC (2001): "The molecular biology of Huntington's disease". *Psychol Med* **31**:3-14.
- Hockly E, Cordery PM, Woodman B, Mahal A, van Dellen A, Blakemore C, Lewis CM, Hannan AJ, and Bates GP (2002): "Environmental enrichment slows disease progression in R6/2 Huntington's disease mice". *Ann Neurol* **51**:235-242.
- Hockly E, Woodman B, Mahal A, Lewis CM, and Bates G. (2003): "Standardization and statistical approaches to therapeutic trials in the R6/2 mouse". *Brain Res Bull* **61**:469-79.
- Hodgson JG, Agopyan N, Gutekunst CA, Leavitt BR, LePiane F, Singaraja R, Smith DJ, Bissada N, McCutcheon K, Nasir J, Jamot L, Li XJ, Stevens ME, Rosemond E, Roder JC, Phillips AG, Rubin EM, Hersch SM, and Hayden MR (1999): "A YAC mouse model for Huntington's disease with full-length mutant huntingtin, cytoplasmic toxicity, and selective striatal neurodegeneration". *Neuron* **23**:181-192.
- Hoffner G, Kahlem P, and Djian P (2002): "Perinuclear localization of huntingtin as a consequence of its binding to microtubules through an interaction with beta-tubulin: relevance to Huntington's disease". *J Cell Sci* **115**:941-948.
- Hoglinger GU, Rizk P, Muriel MP, Duyckaerts C, Oertel WH, Caille I, and

- Hirsch EC (2004): “*Dopamine depletion impairs precursor cell proliferation in Parkinson disease*”. *Nat Neurosci* **7**:726-735.
- Huang HP, Chu K, Nemoz-Gaillard E, Elberg D, and Tsai MJ (2002): “*Neogenesis of beta-cells in adult BETA2/NeuroD-deficient mice*”. *Mol Endocrinol* **16**:541-551.
- Hungs M, and Mignot E (2001): “*Hypocretin/orexin, sleep and narcolepsy*”. *Bioessays* **23**:397-408.
- Hurlbert MS, Zhou W, Wasmeier C, Kaddis FG, Hutton JC, and Freed CR (1999): “*Mice transgenic for an expanded CAG repeat in the Huntington's disease gene develop diabetes*”. *Diabetes* **48**:649-651.
- Iannicola C, Moreno S, Oliverio S, Nardacci R, Ciofi-Luzzatto A, and Piacentini M (2000): “*Early alterations in gene expression and cell morphology in a mouse model of Huntington's disease*”. *J Neurochem* **75**:830-839.
- Jarabek BR, Yasuda RP, and Wolfe BB (2004): “*Regulation of proteins affecting NMDA receptor-induced excitotoxicity in a Huntington's mouse model*”. *Brain* **127**:505–516.
- Jenkins BG, Koroshetz WJ, Beal MF, and Rosen BR (1993): “*Evidence for impairment of energy metabolism in vivo in Huntington's disease using localized IH NMR spectroscopy*”. *Neurology* **43**:2689-2695.
- Jin K, Galvan V, Xie L, Mao XO, Gorostiza OF, Bredesen DE, and Greenberg DA (2004a): “*Enhanced neurogenesis in Alzheimer's disease transgenic (PDGF-APP^{Sw,Ind}) mice*”. *Proc Natl Acad Sci USA* **101**:13363-13367.
- Jin K, LaFevre-Bernt M, Sun Y, Chen S, Gafni J, Crippen D, Logvinova A, Ross CA, Greenberg DA, and Ellerby LM (2005): “*FGF-2 promotes neurogenesis and neuroprotection and prolongs survival in a transgenic mouse model of Huntington's disease*”. *Proc Natl Acad Sci USA* **102**:18189-18194.
- Jin K, Peel AL, Mao XO, Xie L, Cottrell BA, Henshall DC, and Greenberg DA (2004b): “*Increased hippocampal neurogenesis in Alzheimer's disease*”. *Proc Natl Acad Sci USA* **101**:343-347.
- Jobst EE, Enriori PJ, and Cowley MA (2004): “*The electrophysiology of feeding circuits*”. *Trends Endocrinol Metab* **15**:488-499.
- Johnson MA, Rajan V, Miller CE, and Wightman RM (2006): “*Dopamine release is severely compromised in the R6/2 mouse model of Huntington's disease*”. *J Neurochem* **97**:737-746.
- Junk AK, Mammis A, Savitz SI, Singh M, Roth S, Malhotra S, Rosenbaum PS, Cerami A, Brines M, and Rosenbaum DM (2002): “*Erythropoietin administration protects retinal neurons from acute ischemia-reperfusion injury*”. *Proc Natl Acad Sci USA* **99**:10659-10664.
- Kahlem P, Green H, and Djian P (1998): “*Transglutaminase action imitates Huntington's disease: selective polymerization of Huntingtin containing*”

- expanded polyglutamine*". Mol Cell **1**:595-601.
- Kahlig KM, Binda F, Khoshbouei H, Blakely RD, McMahon DG, Javitch JA, and Galli A (2005): "Amphetamine induces dopamine efflux through a dopamine transporter channel". Proc Natl Acad Sci USA **102**:3495-3500.
- Kantor O, Temel Y, Holzmann C, Raber K, Nguyen HP, Cao C, Turkoglu HO, Rutten BP, Visser-Vandewalle V, Steinbusch HW, Blokland A, Korr H, Riess O, von Hörsten S, and Schmitz C (2006): "Selective striatal neuron loss and alterations in behavior correlate with impaired striatal function in Huntington's disease transgenic rats". Neurobiol Dis **22**:538-547.
- Karpuj MV, Garren H, Slunt H, Price DL, Gusella J, Becher MW, and Steinman L (1999): "Transglutaminase aggregates huntingtin into nonamyloidogenic polymers, and its enzymatic activity increases in Huntington's disease brain nuclei". Proc Natl Acad Sci USA **96**:7388-7393.
- Kassubek J, Gaus W, and Landwehrmeyer GB (2004): "Evidence for more widespread cerebral pathology in early HD: an MRI-based morphometric analysis". Neurology **62**:523-524.
- Katsuki H, and Akaike A (2004): "Excitotoxic degeneration of hypothalamic orexin neurons in slice culture". Neurobiol Dis **15**:61-69.
- Kee N, Sivalingam S, Boonstra R, and Wojtowicz JM (2002): "The utility of Ki-67 and BrdU as proliferative markers of adult neurogenesis". J Neurosci Methods **115**:97-105.
- Kegel KB, Kim M, Sapp E, McIntyre C, Castano JG, Aronin N, and DiFiglia M (2000): "Huntingtin expression stimulates endosomal-lysosomal activity, endosome tubulation, and autophagy". J Neurosci **20**:7268-7278.
- Kempermann G (2002): "Why new neurons? Possible functions for adult hippocampal neurogenesis". J Neurosci **22**:635-638.
- Kempermann G, Wiskott L, and Gage FH (2004): "Functional significance of adult neurogenesis". Curr Opin Neurobiol **14**:186-191.
- Kiechle T, Dedeoglu A, Kubilus J, Kowall NW, Beal MF, Friedlander RM, Hersch SM, and Ferrante RJ (2002): "Cytochrome C and caspase-9 expression in Huntington's disease". Neuromolecular Med **1**:183-195.
- Kim YJ, Sapp E, Cuiffo BG, Sobin L, Yoder J, Kegel KB, Qin ZH, Detloff P, Aronin N, and DiFiglia M (2006): "Lysosomal proteases are involved in generation of N-terminal huntingtin fragments." Neurobiol Dis **22**:346-356.
- Kim YJ, Yi Y, Sapp E, Wang Y, Cuiffo B, Kegel KB, Qin ZH, Aronin N, and DiFiglia M (2001): "Caspase 3-cleaved N-terminal fragments of wild-type and mutant huntingtin are present in normal and Huntington's disease brains, associate with membranes, and undergo calpain-dependent proteolysis". Proc Natl Acad Sci USA **98**:12784-12789.
- Kirkwood SC, Su JL, Conneally P, and Foroud T (2001): "Progression of

- symptoms in the early and middle stages of Huntington disease*". Arch Neurol **58**:273-278.
- Klapstein GJ, Fisher RS, Zanjani H, Cepeda C, Jokel ES, Chesselet MF, and Levine MS (2001): "*Electrophysiological and morphological changes in striatal spiny neurons in R6/2 Huntington's disease transgenic mice*". J Neurophysiol **86**:2667-2677.
- Kolb B, and Whishaw IQ (2006): "*An Introduction to Brain and Behaviour*", Second Edition, New York: Worth Publishers.
- Koroshetz WJ, Jenkins BG, Rosen BR, and Beal MF (1997): "*Energy metabolism defects in Huntington's disease and effects of coenzyme Q10*". Ann Neurol **41**:160-165.
- Kosinski CM, Cha JH, Young AB, Mangiarini L, Bates G, Schiefer J, and Schwarz M (1999): "*Intranuclear inclusions in subtypes of striatal neurons in Huntington's disease transgenic mice*". Neuroreport **10**:3891-3896.
- Kremer HP, Roos RA, Dingjan GM, Bots GT, Bruyn GW, and Hofman MA (1991): "*The hypothalamic lateral tuberal nucleus and the characteristics of neuronal loss in Huntington's disease*". Neurosci Lett **132**:101-104.
- Kremer HP, Roos RA, Dingjan G, Marani E, and Bots GT (1990): "*Atrophy of the hypothalamic lateral tuberal nucleus in Huntington's disease*". J Neuropathol Exp Neurol **49**:371-382.
- Kremer B, Tallaksen-Greene SJ, and Albin RL (1993): "*AMPA and NMDA binding sites in the hypothalamic lateral tuberal nucleus: implications for Huntington's disease*". Neurology **43**:1593-1595.
- Kuemmerle S, Gutekunst CA, Klein AM, Li XJ, Li SH, Beal MF, Hersch SM, and Ferrante RJ (1999): "*Huntington aggregates may not predict neuronal death in Huntington's disease*". Ann Neurol **46**:842-849.
- Kuhn HG, Palmer TD, and Fuchs E (2001): "*Adult neurogenesis: a compensatory mechanism for neuronal damage*". Eur Arch Psychiatry Clin Neurosci **251**:152-158.
- Laforet GA, Sapp E, Chase K, McIntyre C, Boyce FM, Campbell M, Cadigan BA, Warzecki L, Tagle DA, Reddy PH, Cepeda C, Calvert CR, Jokel ES, Klapstein GJ, Ariano MA, Levine MS, DiFiglia M, and Aronin N (2001): "*Changes in cortical and striatal neurons predict behavioral and electrophysiological abnormalities in a transgenic murine model of Huntington's disease*". J Neurosci **21**:9112-9123.
- Landles C, and Bates GP (2004): "*Huntingtin and the molecular pathogenesis of Huntington's disease. Fourth in molecular medicine review series*". EMBO Rep **5**:958-963.
- La Spada AR, and Taylor JP (2003): "*Polyglutamines placed into context*". Neuron **38**:681-684.

- Lazic SE, Grote H, Armstrong RJ, Blakemore C, Hannan AJ, van Dellen A, and Barker RA (2004): "Decreased hippocampal cell proliferation in R6/1 Huntington's mice". *Neuroreport* **15**:811-813.
- Lazic SE, Grote HE, Blakemore C, Hannan AJ, van Dellen A, Phillips W, and Barker RA (2006): "Neurogenesis in the R6/1 transgenic mouse model of Huntington's disease: effects of environmental enrichment". *Eur J Neurosci* **23**:1829-1838.
- Leblhuber F, Peichl M, Neubauer C, Reisecker F, Steinparz FX, Windhager E, and Maschek W (1995): "Serum dehydroepiandrosterone and cortisol measurements in Huntington's chorea". *J Neurol Sci* **132**:76-79.
- Levine MS, Cepeda C, Hickey MA, Fleming SM, and Chesselet MF (2004): "Genetic mouse models of Huntington's and Parkinson's diseases: illuminating but imperfect". *Trends Neurosci* **27**:691-697.
- Levine MS, Klapstein GJ, Koppel A, Gruen E, Cepeda C, Vargas ME, Jokel ES, Carpenter EM, Zanjani H, Hurst RS, Efstratiadis A, Zeitlin S, and Chesselet MF (1999): "Enhanced sensitivity to N-methyl-D-aspartate receptor activation in transgenic and knockin mouse models of Huntington's disease". *J Neurosci Res* **58**:515-532.
- Li H, Li SH, Cheng AL, Mangiarini L, Bates GP, and Li XJ (1999): "Ultrastructural localization and progressive formation of neuropil aggregates in Huntington's disease transgenic mice". *Hum Mol Genet* **8**:1227-1236.
- Li H, Wyman T, Yu ZX, Li SH, and Li XJ (2003): "Abnormal association of mutant huntingtin with synaptic vesicles inhibits glutamate release". *Hum Mol Genet* **12**:2021-2030.
- Li JY, Plomann M, and Brundin P (2003): "Huntington's disease: a synaptopathy?" *Trends Mol Med* **9**:414-420.
- Li JY, Popovic N, and Brundin P (2005): "The use of the R6 transgenic mouse models of Huntington's disease in attempts to develop novel therapeutic strategies". *NeuroRx* **2**:447-464.
- Li SH, and Li XJ (2004): "Huntingtin-protein interactions and the pathogenesis of Huntington's disease". *Trends Genet* **20**:146-154.
- Li SH, Yu ZX, Li CL, Nguyen HP, Zhou YX, Deng C, and Li XJ (2003): "Lack of huntingtin-associated protein-1 causes neuronal death resembling hypothalamic degeneration in Huntington's disease". *J Neurosci* **23**:6956-6964.
- Lie DC, Song H, Colamarino SA, Ming GL, and Gage FH (2004): "Neurogenesis in the adult brain: new strategies for central nervous system diseases". *Annu Rev Pharmacol Toxicol* **44**:399-421.

- Lievens JC, Woodman B, Mahal A, Spasic-Bosovic O, Samuel D, Kerkerian-Le Goff L, and Bates GP (2001): "Impaired glutamate uptake in the R6 huntington's disease transgenic mice". *Neurobiol Dis* **8**:807-821.
- Lin L, Faraco J, Li R, Kadotani H, Rogers W, Lin X, Qiu X, de Jong PJ, Nishino S, and Mignot E (1999): "The sleep disorder canine narcolepsy is caused by a mutation in the hypocretin (orexin) receptor 2 gene". *Cell* **98**:365-376.
- Lione LA, Carter RJ, Hunt MJ, Bates GP, Morton AJ, and Dunnett SB (1999): "Selective discrimination learning impairments in mice expressing the human Huntington's disease mutation". *J Neurosci* **19**:10428-10437.
- Lodi R, Schapira AH, Manners D, Styles P, Wood NW, Taylor DJ, and Warner TT (2000): "Abnormal in vivo skeletal muscle energy metabolism in Huntington's disease and dentatorubropallidolusian atrophy". *Ann Neurol* **48**:72-76.
- Liu M, Pleasure SJ, Collins AE, Noebels JL, Naya FJ, Tsai MJ, and Lowenstein DH (2000): "Loss of BETA2/NeuroD leads to malformation of the dentate gyrus and epilepsy". *Proc Natl Acad Sci USA* **97**:865-870.
- Lu D, Mahmood A, Qu C, Goussev A, Schallert T, and Chopp M (2005): "Erythropoietin enhances neurogenesis and restores spatial memory in rats after traumatic brain injury". *J Neurotrauma* **22**:1011-1017.
- Luesse HG, Schiefer J, Spruenken A, Puls C, Block F, and Kosinski CM (2001): "Evaluation of R6/2 HD transgenic mice for therapeutic studies in Huntington's disease: behavioral testing and impact of diabetes mellitus". *Behav Brain Res* **126**:185-195.
- Luthi-Carter R, Apostol BL, Dunah AW, DeJohn MM, Farrell LA, Bates GP, Young AB, Standaert DG, Thompson LM, and Cha JH (2003): "Complex alteration of NMDA receptors in transgenic Huntington's disease mouse brain: analysis of mRNA and protein expression, plasma membrane association, interacting proteins, and phosphorylation". *Neurobiol Dis* **14**:624-636.
- Luthi-Carter R, Hanson SA, Strand AD, Bergstrom DA, Chun W, Peters NL, Woods AM, Chan EY, Kooperberg C, Krainc D, Young AB, Tapscott SJ, and Olson JM (2002): "Dysregulation of gene expression in the R6/2 model of polyglutamine disease: parallel changes in muscle and brain". *Hum Mol Genet* **11**:1911-1926.
- Luthi-Carter R, Strand A, Peters NL, Solano SM, Hollingsworth ZR, Menon AS, Frey AS, Spektor BS, Penney EB, Schilling G, Ross CA, Borchelt DR, Tapscott SJ, Young AB, Cha JH, and Olson JM (2000): "Decreased expression of striatal signaling genes in a mouse model of Huntington's disease". *Hum Mol Genet* **9**:1259-1271.
- Ma L, Morton AJ, and Nicholson LF (2003): "Microglia density decreases with

- age in a mouse model of Huntington's disease". *Glia* **43**:274-280.
- Mangiarini L, Sathasivam K, Mahal A, Mott R, Seller M, and Bates GP (1997): "Instability of highly expanded CAG repeats in mice transgenic for the Huntington's disease mutation". *Nat Genet.* **15**:197-200.
- Mangiarini L, Sathasivam K, Seller M, Cozens B, Harper A, Hetherington C, Lawton M, Trotter Y, Lehrach H, Davies SW, and Bates GP (1996): "Exon 1 of the HD gene with an expanded CAG repeat is sufficient to cause a progressive neurological phenotype in transgenic mice". *Cell* **87**:493-506.
- Marcora E, Gowan K, and Lee JE (2003): "Stimulation of NeuroD activity by huntingtin and huntingtin-associated proteins HAP1 and MLK2". *Proc Natl Acad Sci USA* **100**:9578-9583.
- Markianos M, Panas M, Kalfakis N, and Vassilopoulos D (2005): "Plasma testosterone in male patients with Huntington's disease: relations to severity of illness and dementia". *Ann Neurol* **57**:520-525.
- Marsh DJ, Weingarth DT, Novi DE, Chen HY, Trumbauer ME, Chen AS, Guan XM, Jiang MM, Feng Y, Camacho RE, Shen Z, Frazier EG, Yu H, Metzger JM, Kuca SJ, Shearman LP, Gopal-Truter S, MacNeil DJ, Strack AM, MacIntyre DE, Van der Ploeg LH, and Qian S (2002): "Melanin-concentrating hormone 1 receptor-deficient mice are lean, hyperactive, and hyperphagic and have altered metabolism". *Proc Natl Acad Sci USA* **99**:3240-3245.
- Marsh JL, Pallos J, and Thompson LM (2003): "Fly models of Huntington's disease". *Hum Mol Genet* **12**:R187-193.
- Masuda S, Nagao M, Takahata K, Konishi Y, Gallyas F Jr, Tabira T, and Sasaki R (1993): "Functional erythropoietin receptor of the cells with neural characteristics. Comparison with receptor properties of erythroid cells". *J Biol Chem* **268**:11208-11216.
- Meade CA, Deng YP, Fusco FR, Del Mar N, Hersch S, Goldowitz D, and Reiner A (2002): "Cellular localization and development of neuronal intranuclear inclusions in striatal and cortical neurons in R6/2 transgenic mice". *J Comp Neurol* **449**:241-269.
- Meier A, Mollenhauer B, Cohrs S, Rodenbeck A, Jordan W, Meller J, and Otto M (2005): "Normal hypocretin-1 (orexin-A) levels in the cerebrospinal fluid of patients with Huntington's disease". *Brain Res* **1063**:201-203.
- Menalled LB, and Chesselet MF (2002): "Mouse models of Huntington's disease". *Trends Pharmacol Sci* **23**:32-39.
- Mieda M, and Yanagisawa M (2002): "Sleep, feeding, and neuropeptides: roles of orexins and orexin receptors". *Curr Opin Neurobiol* **12**:339-345.
- Mignot E, Lammers GJ, Ripley B, Okun M, Nevsimalova S, Overeem S, Vankova J, Black J, Harsh J, Bassetti C, Schrader H, and Nishino S (2002):

- "The role of cerebrospinal fluid hypocretin measurement in the diagnosis of narcolepsy and other hypersomnias"*. Arch Neurol **59**:1553-1562.
- Mignot E, Taheri S, and Nishino S (2002): *"Sleeping with the hypothalamus: emerging therapeutic targets for sleep disorders"*. Nat Neurosci **5**:1071-1075.
- Mikkelsen JD, Hauser F, deLecea L, Sutcliffe JG, Kilduff TS, Calgari C, Pevet P, and Simonneaux V (2001): *"Hypocretin (orexin) in the rat pineal gland: a central transmitter with effects on noradrenaline-induced release of melatonin"*. Eur J Neurosci **14**:419-425.
- Modregger J, DiProspero NA, Charles V, Tagle DA, and Plomann M (2002): *"PACSIN 1 interacts with huntingtin and is absent from synaptic varicosities in presymptomatic Huntington's disease brains"*. Hum Mol Genet **11**:2547-2558.
- Mohapel P, and Brundin P (2004): *"Harnessing endogenous stem cells to treat neurodegenerative disorders of the basal ganglia"*. Parkinsonism Relat Disord **10**:259-264.
- Mohapel P, Frielingsdorf H, Haggblad J, Zachrisson O, and Brundin P (2005): *"Platelet-derived growth factor (PDGF-BB) and brain-derived neurotrophic factor (BDNF) induce striatal neurogenesis in adult rats with 6-hydroxydopamine lesions"*. Neuroscience **132**:767-776.
- Morton AJ and Edwardson JM (2001): *"Progressive depletion of complexin II in a transgenic mouse model of Huntington's disease"*. J Neurochem **76**:166-172.
- Morton AJ, Faull RL, and Edwardson JM (2001): *"Abnormalities in the synaptic vesicle fusion machinery in Huntington's disease"*. Brain Res Bull **56**:111-117.
- Morton AJ, Lagan MA, Skepper JN, and Dunnett SB (2000): *"Progressive formation of inclusions in the striatum and hippocampus of mice transgenic for the human Huntington's disease mutation"*. J Neurocytol **29**:679-702.
- Morton AJ, and Leavens W (2000): *"Mice transgenic for the human Huntington's disease mutation have reduced sensitivity to kainic acid toxicity"*. Brain Res Bull **52**:51-59.
- Morton AJ, Wood NI, Hastings MH, Hurelbrink C, Barker RA, and Maywood ES (2005): *"Disintegration of the sleep-wake cycle and circadian timing in Huntington's disease"*. J Neurosci **25**:157-63.
- Murphy KP, Carter RJ, Lione LA, Mangiarini L, Mahal A, Bates GP, Dunnett SB, and Morton AJ (2000): *"Abnormal synaptic plasticity and impaired spatial cognition in mice transgenic for exon 1 of the human Huntington's disease gene"*. J Neurosci **20**:5115-5123.
- Nagata E, Sawa A, Ross CA, and Snyder SH (2004): *"Autophagosome-like*

-
- vacuole formation in Huntington's disease lymphoblasts*". Neuroreport **15**:1325-1328.
- Nasir J, Floresco SB, O'Kusky JR, Diewert VM, Richman JM, Zeisler J, Borowski A, Marth JD, Phillips AG, and Hayden MR (1995): "*Targeted disruption of the Huntington's disease gene results in embryonic lethality and behavioral and morphological changes in heterozygotes*". Cell **81**:811-823.
- Neuwald AF, and Hirano T (2000): "*HEAT repeats associated with condensins, cohesins, and other complexes involved in chromosome-related functions*". Genome Res **10**:1445-1452.
- Nicnocaill B, Haraldsson B, Hansson O, O'Connor WT, and Brundin P (2001): "*Altered striatal amino acid neurotransmitter release monitored using microdialysis in R6/1 Huntington transgenic mice*". Eur J Neurosci **13**:206-210.
- Nguyen HP, Kobbe P, Rahne H, Worpel T, Jager B, Stephan M, Pabst R, Holzmann C, Riess O, Korr H, Kantor O, Petrasch-Parwez E, Wetzel R, Osmand A, and von Horsten S. (2006): "*Behavioral abnormalities precede neuropathological markers in rats transgenic for Huntington's Disease.*" Hum Mol Genet *in press*.
- Ona VO, Li M, Vonsattel JP, Andrews LJ, Khan SQ, Chung WM, Frey AS, Menon AS, Li XJ, Stieg PE, Yuan J, Penney JB, Young AB, Cha JH, and Friedlander RM (1999): "*Inhibition of caspase-1 slows disease progression in a mouse model of Huntington's disease*". Nature **399**:263-267.
- Oyanagi K, Takeda S, Takahashi H, Ohama E, and Ikuta F (1989): "*A quantitative investigation of the substantia nigra in Huntington's disease*". Ann Neurol **26**:13-19.
- Panov AV, Gutekunst CA, Leavitt BR, Hayden MR, Burke JR, Strittmatter WJ, and Greenamyre JT (2002): "*Early mitochondrial calcium defects in Huntington's disease are a direct effect of polyglutamines*". Nat Neurosci **5**:731-736.
- Papalexí E, Persson A, Björkqvist M, Petersén Å, Woodman B, Bates GP, Sundler F, Mulder H, Brundin P, and Popovic N (2005): "*Reduction of GnRH and infertility in the R6/2 mouse model of Huntington's disease*". Eur J Neurosci **22**:1541-1546.
- Parent JM, Vexler ZS, Gong C, Derugin N, and Ferriero DM (2002): "*Rat forebrain neurogenesis and striatal neuron replacement after focal stroke*". Ann Neurol **52**:802-813.
- Parker WD Jr, Boyson SJ, Luder AS, and Parks JK (1990): "*Evidence for a defect in NADH: ubiquinone oxidoreductase (complex I) in Huntington's disease.*" Neurology **40**:1231-1234.

- Pencea V, Bingaman KD, Wiegand SJ, and Luskin MB (2001): "Infusion of brain-derived neurotrophic factor into the lateral ventricle of the adult rat leads to new neurons in the parenchyma of the striatum, septum, thalamus, and hypothalamus". *J Neurosci* **21**:6706-6717.
- Perez-Severiano F, Escalante B, Vergara P, Rios C, and Segovia J (2002): "Age-dependent changes in nitric oxide synthase activity and protein expression in striata of mice transgenic for the Huntington's disease mutation". *Brain Res* **951**:36-42.
- Perutz MF, Johnson T, Suzuki M, and Finch JT (1994): "Glutamine repeats as polar zippers: their possible role in inherited neurodegenerative diseases". *Proc Natl Acad Sci USA* **91**:5355-5358.
- Petersén Å, and Brundin P (2002): "Huntington's disease: the mystery unfolds?" *Int Rev Neurobiol* **53**:315-339.
- Petersén Å, Chase K, Puschban Z, DiFiglia M, Brundin P, and Aronin N (2002a): "Maintenance of susceptibility to neurodegeneration following intrastriatal injections of quinolinic acid in a new transgenic mouse model of Huntington's disease". *Exp Neurol* **175**:297-300.
- Petersén Å, Gil J, Maat-Schieman MLC, Björkqvist M, Tanila H, Araújo IM, Smith R, Popovic N, Wierup N, Norlén P, Li JY, Roos RAC, Sundler F, Mulder H, and Brundin P (2005): "Orexin loss in Huntington's disease". *Hum Mol Genet* **14**:39-47.
- Petersén Å, Hansson O, Puschban Z, Sapp E, Romero N, Castilho RF, Sulzer D, Rice M, DiFiglia M, Przedborski S, and Brundin P (2001): "Mice transgenic for exon 1 of the Huntington's disease gene display reduced striatal sensitivity to neurotoxicity induced by dopamine and 6-hydroxydopamine". *Eur J Neurosci* **14**:1425-1435.
- Petersén Å, Puschban Z, Lotharius J, Nicniocaill B, Wiekop P, O'Connor WT, and Brundin P (2002b): "Evidence for dysfunction of the nigrostriatal pathway in the R6/1 line of transgenic Huntington's disease mice". *Neurobiol Dis* **11**:134-146.
- Petit D, Gagnon JF, Fantini ML, Ferini-Strambi L, and Montplaisir J (2004): "Sleep and quantitative EEG in neurodegenerative disorders". *J Psychosom Res* **56**:487-496.
- Peyron C, Faraco J, Rogers W, Ripley B, Overeem S, Charnay Y, Nevsimalova S, Aldrich M, Reynolds D, Albin R, Li R, Hungs M, Pedrazzoli M, Padigaru M, Kucherlapati M, Fan J, Maki R, Lammers GJ, Bouras C, Kucherlapati R, Nishino S, and Mignot E. (2000): "A mutation in a case of early onset narcolepsy and a generalized absence of hypocretin peptides in human narcoleptic brains". *Nat Med* **6**:991-997.

- Phillips W, Morton AJ, and Barker RA (2005): “*Abnormalities of neurogenesis in the R6/2 mouse model of Huntington's disease are attributable to the in vivo microenvironment*”. *J Neurosci* **25**:11564-11576.
- Pineda JR, Canals JM, Bosch M, Adell A, Mengod G, Artigas F, Ernfors P, and Alberch J (2005): “*Brain-derived neurotrophic factor modulates dopaminergic deficits in a transgenic mouse model of Huntington's disease*”. *J Neurochem* **93**:1057-1068.
- Portera-Cailliau C, Hedreen JC, Price DL, and Koliatsos VE (1995): “*Evidence for apoptotic cell death in Huntington disease and excitotoxic animal models*”. *J Neurosci* **15**:3775-3787.
- Qin ZH, Wang Y, Kegel KB, Kazantsev A, Apostol BL, Thompson LM, Yoder J, Aronin N, and DiFiglia M (2003): “*Autophagy regulates the processing of amino terminal huntingtin fragments*”. *Hum Mol Genet* **12**:3231-3244.
- Ravikumar B, Duden R, and Rubinsztein DC (2002): “*Aggregate-prone proteins with polyglutamine and polyalanine expansions are degraded by autophagy*”. *Hum Mol Genet* **11**:1107-1117.
- Ravikumar B, Vacher C, Berger Z, Davies JE, Luo S, Oroz LG, Scaravilli F, Easton DF, Duden R, O'Kane CJ, and Rubinsztein DC (2004): “*Inhibition of mTOR induces autophagy and reduces toxicity of polyglutamine expansions in fly and mouse models of Huntington disease.*” *Nat Genet.* **36**:585-595.
- Rebec GV, Barton SJ, and Ennis MD (2002): “*Dysregulation of ascorbate release in the striatum of behaving mice expressing the Huntington's disease gene*”. *J Neurosci* **22**:RC202.
- Reddy PH, Williams M, Charles V, Garrett L, Pike-Buchanan L, Whetsell WO Jr, Miller G, and Tagle DA (1998): “*Behavioural abnormalities and selective neuronal loss in HD transgenic mice expressing mutated full-length HD cDNA*”. *Nat Genet* **20**:198-202.
- Reynolds GP, Dalton CF, Tillery CL, Mangiarini L, Davies SW, and Bates GP (1999): “*Brain neurotransmitter deficits in mice transgenic for the Huntington's disease mutation*”. *J Neurochem* **72**:17773-1776.
- Ribchester RR, Thomson D, Wood NI, Hinks T, Gillingwater TH, Wishart TM, Court FA, and Morton AJ (2004): “*Progressive abnormalities in skeletal muscle and neuromuscular junctions of transgenic mice expressing the Huntington's disease mutation*”. *Eur J Neurosci* **20**:3092-3114.
- Rigamonti D, Bauer JH, De-Fraja C, Conti L, Sipione S, Sciorati C, Clementi E, Hackam A, Hayden MR, Li Y, Cooper JK, Ross CA, Govoni S, Vincenz C, and Cattaneo E (2000): “*Wild-type huntingtin protects from apoptosis upstream of caspase-3*”. *J Neurosci* **20**:3705-3713.

- Rigamonti D, Sipione S, Goffredo D, Zuccato C, Fossale E, and Cattaneo E (2001): "*Huntingtin's neuroprotective activity occurs via inhibition of procaspase-9 processing*". *J Biol Chem* **276**:14545-14548.
- Ripley B, Overeem S, Fujiki N, Nevsimalova S, Uchino M, Yesavage J, Di Monte D, Dohi K, Melberg A, Lammers GJ, Nishida Y, Roelandse FW, Hungs M, Mignot E, and Nishino S. (2001): "*CSF hypocretin/orexin levels in narcolepsy and other neurological conditions*". *Neurology* **57**:2253-2258.
- Rosas HD, Koroshetz WJ, Chen YI, Skeuse C, Vangel M, Cudkowicz ME, Caplan K, Marek K, Seidman LJ, Makris N, Jenkins BG, and Goldstein JM (2003): "*Evidence for more widespread cerebral pathology in early HD: an MRI-based morphometric analysis*". *Neurology* **60**:1615-1620.
- Ross CA (2002): "*Polyglutamine pathogenesis: emergence of unifying mechanisms for Huntington's disease and related disorders*". *Neuron* **35**:819-822.
- Sakurai T, Amemiya A, Ishii M, Matsuzaki I, Chemelli RM, Tanaka H, Williams SC, Richardson JA, Kozlowski GP, Wilson S, Arch JR, Buckingham RE, Haynes AC, Carr SA, Annan RS, McNulty DE, Liu WS, Terrett JA, Elshourbagy NA, Bergsma DJ, and Yanagisawa M (1998): "*Orexins and orexin receptors: a family of hypothalamic neuropeptides and G protein-coupled receptors that regulate feeding behavior*". *Cell* **92**:573-585.
- Sanberg PR, Fibiger HC, and Mark RF (1981): "*Body weight and dietary factors in Huntington's disease patients compared with matched controls*". *Med J Aust* **1**:407-409.
- Sanchez I, Xu CJ, Juo P, Kakizaka A, Blenis J, and Yuan J (1999): "*Caspase-8 is required for cell death induced by expanded polyglutamine repeats*". *Neuron* **22**:623-633.
- Santamaria A, Perez-Severiano F, Rodriguez-Martinez E, Maldonado PD, Pedraza-Chaverri J, Rios C, and Segovia J (2001): "*Comparative analysis of superoxide dismutase activity between acute pharmacological models and a transgenic mouse model of Huntington's disease*". *Neurochem Res* **26**:419-424.
- Sapp E, Penney J, Young A, Aronin N, Vonsattel JP, and DiFiglia M (1999): "*Axonal transport of N-terminal huntingtin suggests early pathology of corticostriatal projections in Huntington disease*". *J Neuropathol Exp Neurol* **58**:165-173.
- Sathasivam K, Hobbs C, Turmaine M, Mangiarini L, Mahal A, Bertaux F, Wanker EE, Doherty P, Davies SW, and Bates GP (1999): "*Formation of polyglutamine inclusions in non-CNS tissue*". *Hum Mol Genet* **8**:813-822.

- Sawa A (2001): "*Mechanisms for neuronal cell death and dysfunction in Huntington's disease: pathological cross-talk between the nucleus and the mitochondria?*" *J Mol Med* **79**:375-381.
- Schiefer J, Alberty A, Dose T, Oliva S, Noth J, and Kosinski CM (2002): "*Huntington's disease transgenic mice are resistant to global cerebral ischemia*". *Neurosci Lett* **334**:99-102.
- Schilling G, Becher MW, Sharp AH, Jinnah HA, Duan K, Kotzuk JA, Slunt HH, Ratovitski T, Cooper JK, Jenkins NA, Copeland NG, Price DL, Ross CA, and Borchelt DR (1999): "*Intranuclear inclusions and neuritic aggregates in transgenic mice expressing a mutant N-terminal fragment of huntingtin*". *Hum Mol Genet* **8**:397-407.
- Schmued LC, Albertson C, and Slikker Jr. W (1997): "*Fluoro-Jade: a novel fluorochrome for the sensitive and reliable histochemical localization of neuronal degeneration*". *Brain Res* **751**:37-46.
- Shelbourne PF, Killeen N, Hevner RF, Johnston HM, Tecott L, Lewandoski M, Ennis M, Ramirez L, Li Z, Iannicola C, Littman DR, and Myers RM (1999): "*A Huntington's disease CAG expansion at the murine Hdh locus is unstable and associated with behavioural abnormalities in mice*". *Hum Mol Genet* **8**:763-774.
- Shi Y (2004): "*Beyond skin color: emerging roles of melanin-concentrating hormone in energy homeostasis and other physiological functions*." *Peptides* **25**:1605-1611.
- Shibata M, Lu T, Furuya T, Degtarev A, Mizushima N, Yoshimori T, MacDonald M, Yankner B, and Yuan J (2006): "*Regulation of intracellular accumulation of mutant Huntingtin by Beclin 1*." *J Biol Chem* **281**:14474-1485.
- Shimada M, Tritos NA, Lowell BB, Flier JS, and Maratos-Flier E (1998): "*Mice lacking melanin-concentrating hormone are hypophagic and lean*". *Nature* **396**:670-674.
- Shingo T, Sorokan ST, Shimazaki T, and Weiss S (2001): "*Erythropoietin regulates the in vitro and in vivo production of neuronal progenitors by mammalian forebrain neural stem cells*". *J Neurosci* **21**:9733-9743.
- Siegel JM (1999): "*Narcolepsy: a key role for hypocretins (orexins)*". *Cell* **98**:409-412.
- Sieradzan KA, and Mann DM (2001): "*The selective vulnerability of nerve cells in Huntington's disease*". *Neuropathol Appl Neurobiol* **27**:1-21.
- Siren AL, Fratelli M, Brines M, Goemans C, Casagrande S, Lewczuk P, Keenan S, Gleiter C, Pasquali C, Capobianco A, Mennini T, Heumann R, Cerami A, Ehrenreich H, and Ghezzi P (2001): "*Erythropoietin prevents neuronal apoptosis after cerebral ischemia and metabolic stress*". *Proc Natl Acad Sci*

- USA **98**:4044-4049.
- Slow EJ, Graham RK, Osmand AP, Devon RS, Lu G, Deng Y, Pearson J, Vaid K, Bissada N, Wetzel R, Leavitt BR, and Hayden MR (2005): "*Absence of behavioral abnormalities and neurodegeneration in vivo despite widespread neuronal huntingtin inclusions*". Proc Natl Acad Sci USA **102**:11402–11407.
- Slow EJ, van Raamsdonk J, Rogers D, Coleman SH, Graham RK, Deng Y, Oh R, Bissada N, Hossain SM, Yang YZ, Li XJ, Simpson EM, Gutekunst CA, Leavitt BR, and Hayden MR (2003): "*Selective striatal neuronal loss in a YAC128 mouse model of Huntington disease*". Hum Mol Genet **12**:1555-1567.
- Smith R, Brundin P, and Li JY (2005): "*Synaptic dysfunction in Huntington's disease: a new perspective*". Cell Mol Life Sci **62**:1901-1912.
- Spektor BS, Miller DW, Hollingsworth ZR, Kaneko YA, Solano SM, Johnson JM, Penney JB Jr, Young AB, and Luthi-Carter R (2002): "*Differential D1 and D2 receptor-mediated effects on immediate early gene induction in a transgenic mouse model of Huntington's disease*". Brain Res Mol Brain Res **102**:118-128.
- Spires TL, Grote HE, Varshney NK, Cordery PM, van Dellen A, Blakemore C, and Hannan AJ (2004): "*Environmental enrichment rescues protein deficits in a mouse model of Huntington's disease, indicating a possible disease mechanism*". J Neurosci **24**:2270-2276.
- Springborg JB, Sonne B, Frederiksen HJ, Foldager N, Poulsen L, Klausen T, Jorgensen OS, and Olsen NV (2003): "*Erythropoietin in the cerebrospinal fluid of patients with aneurysmal subarachnoid hemorrhage originates from the brain*". Brain Res **984**:143-148.
- Stack EC, Kubilus JK, Smith K, Cormier K, Del Signore SJ, Guelin E, Ryu H, Hersch SM, and Ferrante RJ (2005): "*Chronology of behavioral symptoms and neuropathological sequela in R6/2 Huntington's disease transgenic mice*." J Comp Neurol **490**:354-370.
- Steininger TL, Kilduff TS, Behan M, Benca RM, and Landry CF (2004): "*Comparison of hypocretin/orexin and melanin-concentrating hormone neurons and axonal projections in the embryonic and postnatal rat brain*." J Chem Neuroanat **27**:165-181.
- Stott K, Blackburn JM, Butler PJ, and Perutz M (1995): "*Incorporation of glutamine repeats makes protein oligomerize: implications for neurodegenerative diseases*". Proc Natl Acad Sci USA **92**:6509-6513.
- Sugars KL, and Rubinsztein DC (2003): "*Transcriptional abnormalities in Huntington disease*". Trends Genet **19**:233-238.
- Sulzer D, and Zecca L (2000): "*Intraneuronal dopamine-quinone synthesis: a*

- review*". Neurotox Res **1**:181-195.
- Sun B, Fan W, Balciunas A, Cooper JK, Bitan G, Steavenson S, Denis PE, Young Y, Adler B, Daugherty L, Manoukian R, Elliott G, Shen W, Talvenheimo J, Teplow DB, Haniu M, Haldankar R, Wypych J, Ross CA, Citron M, and Richards WG (2002): "*Polyglutamine repeat length-dependent proteolysis of huntingtin*". Neurobiol Dis **11**:111-122.
- Sun Y, Savanenin A, Reddy PH, and Liu YF (2001): "*Polyglutamine-expanded huntingtin promotes sensitization of N-methyl-D-aspartate receptors via post-synaptic density 95*". J Biol Chem **276**:24713-24718.
- Suzuki M, Desmond TJ, Albin RL, and Frey KA (2001): "*Vesicular neurotransmitter transporters in Huntington's disease: initial observations and comparison with traditional synaptic markers*". Synapse **41**:329-336.
- Tabrizi SJ, Cleeter MW, Xuereb J, Taanman JW, Cooper JM, and Schapira AH (1999): "*Biochemical abnormalities and excitotoxicity in Huntington's disease brain*". Ann Neurol **45**:25-32.
- Tabrizi SJ, Workman J, Hart PE, Mangiarini L, Mahal A, Bates G, Cooper JM, and Schapira AH (2000): "*Mitochondrial dysfunction and free radical damage in the Huntington R6/2 transgenic mouse*". Ann Neurol **47**:80-86.
- Taheri S, Zeitzer JM, and Mignot E (2002): "*The role of hypocretins (orexins) in sleep regulation and narcolepsy*". Annu Rev Neurosci **25**:283-313.
- Tang TS, Tu H, Chan EY, Maximov A, Wang Z, Wellington CL, Hayden MR, and Bezprozvanny I (2003): "*Huntingtin and huntingtin-associated protein 1 influence neuronal calcium signaling mediated by inositol-(1,4,5) triphosphate receptor type 1*", Neuron **39**:227-239.
- Tattersfield AS, Croon RJ, Liu YW, Kells AP, Faull RL, and Connor B (2004): "*Neurogenesis in the striatum of the quinolinic acid lesion model of Huntington's disease*". Neuroscience **127**:319-332.
- Temple S (2001): "*Stem cell plasticity--building the brain of our dreams*". Nat Rev Neurosci **2**:513-520.
- The Huntington's Disease Collaborative Research Group (1993): "*A novel gene containing a trinucleotide repeat that is expanded and unstable on Huntington's disease chromosomes*". Cell **72**:971-983.
- Thomas LB, Gates DJ, Richfield EK, O'Brien TF, Schweitzer JB, and Steindler DA (1995): "*DNA end labeling (TUNEL) in Huntington's disease and other neuropathological conditions*". Exp Neurol **133**:265-272.
- Tobin AJ, and Signer ER (2000): "*Huntington's disease: the challenge for cell biologists*". Trends Cell Biol **10**:531-536.
- Tomasevic G, Kamme F, and Wieloch T (1998): "*Changes in proliferating cell nuclear antigen, a protein involved in DNA repair, in vulnerable hippocampal neurons following global cerebral ischemia*". Brain Res Mol

- Brain Res **60**:168-176.
- Tsai PT, Ohab JJ, Kertesz N, Groszer M, Matter C, Gao J, Liu X, Wu H, and Carmichael ST (2006): "A critical role of erythropoietin receptor in neurogenesis and post-stroke recovery". *J Neurosci* **26**:1269-1274.
- Turmaine M, Raza A, Mahal A, Mangiarini L, Bates GP, and Davies SW (2000): "Nonapoptotic neurodegeneration in a transgenic mouse model of Huntington's disease". *Proc Natl Acad Sci USA* **97**:8093-8097.
- van Dellen A, Blakemore C, Deacon R, York D, and Hannan AJ (2000a): "Delaying the onset of Huntington's in mice". *Nature* **404**:721-722.
- van Dellen A, Welch J, Dixon RM, Cordery P, York D, Styles P, Blakemore C, and Hannan AJ (2000b): "N-Acetylaspartate and DARPP-32 levels decrease in the corpus striatum of Huntington's disease mice". *Neuroreport* **11**:3751-3757.
- van Praag H, Schinder AF, Christie BR, Toni N, Palmer TD, and Gage FH (2002): "Functional neurogenesis in the adult hippocampus". *Nature* **415**:1030-1034.
- Van Raamsdonk JM, Murphy Z, Slow EJ, Leavitt BR, and Hayden MR (2005a): "Selective degeneration and nuclear localization of mutant huntingtin in the YAC128 mouse model of Huntington disease". *Hum Mol Genet* **14**:3823-3835.
- Van Raamsdonk JM, Pearson J, Slow EJ, Hossain SM, Leavitt BR, and Hayden MR (2005b): "Cognitive dysfunction precedes neuropathology and motor abnormalities in the YAC128 mouse model of Huntington's disease". *J Neurosci* **25**:4169-4180.
- Vetter JM, Jehle T, Heinemeyer J, Franz P, Behrens PF, Jackisch R, Landwehrmeyer GB, and Feuerstein TJ (2003): "Mice transgenic for exon 1 of Huntington's disease: properties of cholinergic and dopaminergic pre-synaptic function in the striatum". *J Neurochem* **85**:1054-1063.
- von Hörsten S, Schmitt I, Nguyen HP, Holzmann C, Schmidt T, Walther T, Bader M, Pabst R, Kobbe P, Krotova J, Stiller D, Kask A, Vaarmann A, Rathke-Hartlieb S, Schulz JB, Grasshoff U, Bauer I, Vieira-Saecker AM, Paul M, Jones L, Lindenberg KS, Landwehrmeyer B, Bauer A, Li XJ, and Riess O (2003): "Transgenic rat model of Huntington's disease". *Hum Mol Genet* **12**:617-624.
- Vonsattel JP, and DiFiglia M (1998): "Huntington disease", *J Neuropathol Exp Neurol* **57**:369-384.
- Vonsattel JP, Myers RH, Stevens TJ, Ferrante RJ, Bird ED, and Richardson EP Jr. (1985): "Neuropathological classification of Huntington's disease". *J Neuropathol Exp Neurol* **44**:559-577.
- Waelter S, Boeddrich A, Lurz R, Scherzinger E, Lueder G, Lehrach H, and

-
- Wanker EE (2001): "Accumulation of mutant huntingtin fragments in aggresome-like inclusion bodies as a result of insufficient protein degradation". *Mol Biol Cell* **12**:1393-1407.
- Walling HW, Baldassare JJ, and Westfall TC (1998): "Molecular aspects of Huntington's disease". *J Neurosci Res* **54**:301-308.
- Wang L, Zhang Z, Wang Y, Zhang R, and Chopp M (2004): "Treatment of stroke with erythropoietin enhances neurogenesis and angiogenesis and improves neurological function in rats". *Stroke* **35**:1732-1737.
- Wang X, Zhu C, Wang X, Gerwien JG, Schrattenholz A, Sandberg M, Leist M, and Blomgren K (2004): "The nonerythropoietic asialoerythropoietin protects against neonatal hypoxia-ischemia as potently as erythropoietin". *J Neurochem* **91**:900-910.
- Weeks RA, Piccini P, Harding AE, and Brooks DJ (1996): "Striatal D1 and D2 dopamine receptor loss in asymptomatic mutation carriers of Huntington's disease". *Ann Neurol* **40**:49-54.
- Wiese C, Rolletschek A, Kania G, Blyszczuk P, Tarasov KV, Tarasova Y, Wersto RP, Boheler KR, and Wobus AM (2004): "Nestin expression--a property of multi-lineage progenitor cells?" *Cell Mol Life Sci* **61**:2510-2522.
- Willie JT, Chemelli RM, Sinton CM, Tokita S, Williams SC, Kisanuki YY, Marcus JN, Lee C, Elmquist JK, Kohlmeier KA, Leonard CS, Richardson JA, Hammer RE, and Yanagisawa M. (2003): "Distinct narcolepsy syndromes in Orexin receptor-2 and Orexin null mice: molecular genetic dissection of Non-REM and REM sleep regulatory processes". *Neuron* **38**:715-730.
- Wytenbach A, Carmichael J, Swartz J, Furlong RA, Narain Y, Rankin J, and Rubinsztein DC (2000): "Effects of heat shock, heat shock protein 40 (HDJ-2), and proteasome inhibition on protein aggregation in cellular models of Huntington's disease". *Proc Natl Acad Sci USA* **97**:2898-2903.
- Yamamoto A, Lucas JJ, and Hen R (2000): "Reversal of neuropathology and motor dysfunction in a conditional model of Huntington's disease". *Cell* **101**:57-66.
- Yohrling GJ4th, Jiang GC, DeJohn MM, Miller DW, Young AB, Vrana KE, and Cha JH (2003): "Analysis of cellular, transgenic and human models of Huntington's disease reveals tyrosine hydroxylase alterations and substantia nigra neuropathology". *Brain Res Mol Brain Res* **119**:28-36.
- Young AB (2003): "Huntingtin in health and disease". *J Clin Invest* **111**:299-302.
- Yu X, Shacka JJ, Eells JB, Suarez-Quian C, Przygodzki RM, Beleslin-Cokic B, Lin CS, Nikodem VM, Hempstead B, Flanders KC, Costantini F, and

- Noguchi CT (2002): “*Erythropoietin receptor signalling is required for normal brain development*”. *Development* **129**:505-516.
- Yu ZX, Li SH, Evans J, Pillarisetti A, Li H, and Li XJ (2003): “*Mutant huntingtin causes context-dependent neurodegeneration in mice with Huntington's disease*”. *J Neurosci* **23**:2193-2202.
- Yu ZX, Li SH, Nguyen HP, and Li XJ (2002): “*Huntingtin inclusions do not deplete polyglutamine-containing transcription factors in HD mice*”. *Hum Mol Genet* **11**:905-914.
- Zeitlin S, Liu JP, Chapman DL, Papaioannou VE, and Efstratiadis A (1995): “*Increased apoptosis and early embryonic lethality in mice nullizygous for the Huntington's disease gene homologue*”. *Nat Genet* **11**:155-163.
- Zeron MM, Hansson O, Chen N, Wellington CL, Leavitt BR, Brundin P, Hayden MR, and Raymond LA (2002): “*Increased sensitivity to N-methyl-D-aspartate receptor-mediated excitotoxicity in a mouse model of Huntington's disease*”. *Neuron* **33**:849-860.
- Zhao M, Momma S, Delfani K, Carlen M, Cassidy RM, Johansson CB, Brismar H, Shupliakov O, Frisen J, and Janson AM (2003): “*Evidence for neurogenesis in the adult mammalian substantia nigra*”. *Proc Natl Acad Sci USA* **100**:7925-7930.
- Zhuang X, Oosting RS, Jones SR, Gainetdinov RR, Miller GW, Caron MG, and Hen R (2001): “*Hyperactivity and impaired response habituation in hyperdopaminergic mice*”. *Proc Natl Acad Sci USA* **98**:1982-1987.
- Zoghbi HY, and Orr HT (2000): “*Glutamine repeats and neurodegeneration*”. *Rev Neurosci* **23**:217-247.
- Zuccato C, Ciammola A, Rigamonti D, Leavitt BR, Goffredo D, Conti L, MacDonald ME, Friedlander RM, Silani V, Hayden MR, Timmusk T, Sipione S, and Cattaneo E (2001): “*Loss of huntingtin-mediated BDNF gene transcription in Huntington's disease*”. *Science* **293**:493-498.
- Zuccato C, Tartari M, Crotti A, Goffredo D, Valenza M, Conti L, Cataudella T, Leavitt BR, Hayden MR, Timmusk T, Rigamonti D, and Cattaneo E (2003): “*Huntingtin interacts with REST/NRSF to modulate the transcription of NRSE-controlled neuronal genes*”. *Nat Genet* **35**:76-83.
- Zucker B, Luthi-Carter R, Kama JA, Dunah AW, Stern EA, Fox JH, Standaert DG, Young AB, and Augood SJ (2005): “*Transcriptional dysregulation in striatal projection- and interneurons in a mouse model of Huntington's disease: neuronal selectivity and potential neuroprotective role of HAP1*”. *Hum Mol Genet* **14**:179-189.